The Fire Performance of Timber-Concrete Composite Floors

By

James William O'Neill

Supervised by Prof. Andrew Buchanan

Supervisory Committee:

Dr David Carradine, Associate Prof. Rajesh Dhakal,

Associate Prof. Massimo Fragiacomo and Associate Prof. Peter Moss

A thesis submitted in partial fulfillment of the requirements for the degree of Master of Engineering in Fire Engineering

Department of Civil and Natural Resources Engineering
University of Canterbury
Private Bag 4800
Christchurch, New Zealand

December 2009

Abstract

Timber-concrete composite floors are a combination of timber joists and concrete topping, creating a flooring system to best utilise the advantages each material has to offer. Timber is used as the main tensile load bearing material due to its high strength-to-weight ratio, while concrete is used in floor slabs for its advantages in stiffness and acoustic separation. The strength of the system is dependent on the connection between timber and concrete, thus the connection must be strong, stiff, and economical to manufacture, to ensure that the flooring system is economically viable.

This research investigated the fire performance and failure behaviour of timber-concrete composite floor systems currently under development in New Zealand, resulting in a calculation method for evaluating the fire resistance of these floors. Furnace tests were performed on two full-size floor specimens at the Building Research Association of New Zealand (BRANZ). Both floor specimens were 4 m long and 3 m wide, consisting of 65 mm concrete topping on plywood formwork, connected to double LVL floor joists. They were tested over a 4 m span, subjected to a nominal design live load of 2.5 kPa. Both floors were subjected to the ISO 834 test fire for over 60 minutes. Two separate connection types were tested; concrete notches cut into the timber beams with an incorporated shear key, and metal toothed plates pressed between the double beams.

It was found that the reduction in section size of the timber beams due to the fire governed the failure mode of the floors. Due to the composite action achieved by the connections, the floor units were able to withstand prolonged exposure to the test fire, well exceeding one hour. The test data and visual observations aided in the development of a numerical model for evaluating the fire resistance of the floors. This was developed in a spreadsheet that is able to predict the expected fire resistance of these floors, taking into account some major time dependent variable properties that can have an effect on the overall performance. Load-span tables have been produced to give the estimated fire resistance of floors with differing floor dimensions, span lengths and applied loads.

Acknowledgements

Firstly I would like to thank my supervisors Professor Andy Buchanan, Dr David Carradine, Associate Professor Rajesh Dhakal, Associate Professor Massimo Fragiacomo and Associate Professor Peter Moss for their guidance and continued support during this research. Each brought a different set of opinions and expertise to the table that ultimately allowed for a more complete and thorough thesis to be presented. I would also like to acknowledge the large contribution Dr Carradine made to this research in terms of specimen construction and technical aid, without which this research would not have been possible.

I would also like to thank the Structural Timber Innovation Company for fully funding the research and providing me with the opportunity to carry out research in an area of my own interest. Their contribution to this and other similar projects has been greatly appreciated by all those involved.

I owe a very special thanks to the technical staff at the University of Canterbury for their help in preparation for the full scale testing and in carrying out the small scale testing. In particular I would like to thank Alan Poynter for his time and expertise, Bob Wilsea-Smith, Grant Dunlop and John Kooloos.

Thanks to Paul Bano-Chapman and the fire technicians at BRANZ who aided in the setup of the full scale furnace tests, and whose input into the specimen construction and testing was valuable and very much appreciated.

Thanks to Antony Cook from MiTek for the supply of the steel plates and to Westlake Timber for the use of their press which allowed for this connection type to be tested.

I would like to acknowledge the team at Carter Holt Harvey Woodproducts for their time and aid in supplying materials for the testing. I would also like to acknowledge Firth for their free supply of concrete for the full scale testing.

I would like to acknowledge the NZ Fire Service Commission for their financial support of myself during my Masters course, it is very much appreciated.

Special thanks to David Yeoh for his assistance during this thesis and previous work in this topic area, as his contribution to this field of study has proved extremely helpful in aiding my own efforts.

Finally, a special thanks to my family for their support throughout my University study, and in particular my parents, whose guidance has been the most valuable contribution of all.

Table of Contents

List of Figures

List of Tables

1.0 Introduction

1.1 Background

New Zealand has vast reserves of renewable forests, mainly Radiata Pine, and much of this timber is used in the residential sector for construction of new housing. However, very little of it is used in the commercial sector for large buildings and most of the wood harvested is exported to other countries.

At the University of Canterbury in New Zealand, research in timber engineering has been ongoing in a variety of fields for many years. Some of the major subject areas studied in the past have been seismic design, composite floors, fire safety and sustainability. In 2008 the Structural Timber Innovation Company Ltd was established as a research consortium to implement structural timber solutions into the commercial sector of the construction industry, with a focus on large multi-storey timber buildings. Although much timber research has been undertaken in the past at the University, the establishment of STIC has provided a major opportunity for old and new timber technologies to be combined and implemented in the modern commercial environment in the form of large buildings. The STIC initiative is discussed in detail in Section 1.2 below.

With the issue of sustainability becoming increasing prevalent on the agendas of major corporations and governments worldwide, timber as a structural material is fast becoming the most viable alternative to other materials such as concrete and steel. The ever increasing population of the planet is putting a strain on the limited natural resources available, and the most logical primary building material of the future must be a completely renewable one. Timber fills this void as both a completely renewable and environmentally friendly material which can provide a means of constructing the majority of the small and medium sized buildings of the future. The goal of many research centres around the world is to provide new and innovative timber products and systems to enable much larger timber structures to be built, and this ideal forms the basis of this research.

1.2 STIC Initiative

STIC is co-funded by the New Zealand government, major companies in the construction industry and research organisations for the purpose of aiding in timber research and promoting the use of timber products in the commercial sector of the construction industry. Part of the overall vision of STIC is "the development of innovative large-span timber buildings for a wide range of uses in New Zealand, Australia and other export markets. Primary applications include commercial, educational, industrial, recreational and residential buildings" (STIC, 2009). Engineered timber components such as glulam (glue laminated timber) and LVL (laminated veneer lumber) form the backbone of the systems that these large-span buildings will consist of.

The main objectives of STIC are:

- To create a step change in New Zealand's wood manufacturing and construction industries. It will enhance the international competitiveness of the wood manufacturing sector and will develop innovative solutions for construction of timber buildings world-wide.
- To target sustainable construction, developing new building solutions which greatly reduce environmental impacts. It will develop a wide range of new high-value structural products, and will add value to lower grade wood products that are part of the total construction package.
- To develop, commercialise and facilitate new structural timber solutions for New Zealand and Australia followed by the United States and other export markets.
- To produce comprehensive design guides for designers, regulators, manufacturers and builders. Delivery of the new building systems will be supported by strong relationships with fabricators and construction companies in local and international markets. Buildings will be constructed from prefabricated components, including beams, columns, frames, floors, walls, partitions and cladding panels, manufactured from sawn timber, glulam, LVL, and wood-based panel products, sometimes in composite construction with steel and concrete components.

The major portion of financial support for the research described in this thesis has been provided by STIC.

1.3 Objectives

The first major objective of this research is to investigate the failure behaviour of timber-concrete composite floors when exposed to fire. This includes not only observing the failure mechanism of the floor as a whole but obtaining information on the separate components of the system; such as the charring behaviour of the timber beams, the spalling behaviour of the concrete and any unforeseen effects of other parts of the system that may impact the performance of the floor.

The second major objective of this research is to develop a basic spreadsheet analysis tool that is able to predict the expected fire resistance of these types of floors, taking into account any time dependent variable properties that may arise as a result of the full scale testing, for instance a variable charring rate, a reduced section size or loss of composite action of the floor that may result from prolonged exposure to the fire.

1.4 Method

The first objective was achieved through the full scale furnace testing of two timber-concrete composite floors. Secondary small scale timber testing was undertaken to determine the mechanical properties of the timber at elevated temperatures, and if other connection issues may arise as a result of the heating of the timber. The test data and visual

observations obtained from both forms of testing aided in the development of the spreadsheet.

1.5 Outline of Thesis

A literature review follows in Section 2.0 which details some of the work done by other researchers around the world on similar floor systems, focussing on the structural performance in both ambient and fire conditions. A review of fire safety in timber buildings is also included. Section 3.0 details the full scale testing performed, and Section 4.0 shows the results obtained, including a full discussion on many of the issues that are pertinent. Similarly, Section 5.0 covers the small scale testing and results. Section 6.0 gives a background to the spreadsheet analysis and how it was developed and calibrated, and discusses the fire design methods which underpin the analysis. A set of tables showing the output of the spreadsheet for generic floor sizes is also included in this section. Conclusions and recommendations for further research follow in Section 7.0.

2.0 Literature Review

Despite being present in the construction industry for many decades in some countries, the widespread use of timber-concrete composite floors systems has not occurred in the modern day building environment. This is due in part to unresolved issues with regards to the fire safety of these systems. This literature review covers the topic of fire safety in timber buildings, and considers the current restrictions on timber buildings for different parts of the world. This section also details some of the different timber-concrete composite floor systems that have been studied from around the world, and some of the fire testing that has been conducted in recent years on these floors.

2.1 Fire Safety in Timber Buildings

One of the most prevalent questions that arise with regards to timber buildings worldwide is the question of fire safety. A timber structure can be designed to be as economical, as structurally sound and as aesthetically pleasing as concrete and steel counterparts, but without addressing the issue of fire safety these facts hold little weight when a decision is made on what material to build with. The general perception of the public is that timber is combustible, therefore it is considered to be more dangerous to use than steel or concrete. This is also compounded by the fact that timber has been used as a fossil fuel since the dawn of civilised humanity, and with the advent of the skyscraper, timber has fallen along the wayside when designing for large structures. However, timber has also been used as a primary means for shelter for thousands of years. Modern day structural timber solutions such as laminated veneer lumber and glulam can withstand much greater loads over longer spans, thus enabling modern timber buildings to be constructed much higher and larger than was possible 50 years ago.

Although large multi-storey timber structures are not found commonplace around the world, the fire safety of timber buildings has been addressed in the past. There are readily accessible standard methods of test and design standards for timber systems all over the world, such as Eurocode 5 (2004) and NZS 3603 (1993) that specify certain requirements that must be met for a timber system to provide adequate fire safety for a set period of time. However, due to a perception of timber being dangerous in terms of fire safety, there has been a strong resistance to using it as a primary building material for fears of collapse in a major fire. This has become most notable in recent years with the introduction of high performance engineered wood products such as glulam and LVL, as the use of these materials is extremely limited in many parts of the world.

Many countries have regulations and standards restricting the use of timber in buildings over a certain height or floor area, therefore it is paramount that the performance of the timber system with respect to fires is demonstrated to ensure the future use of this material for larger structures. An example of this is in Australia, where it is only permitted to build large multi-storey timber buildings up to three stories high depending on the specified

purpose of the building. Guidelines for the required structural performance of these buildings and many of the available timber products in the Australian market are detailed in the Australian Timber Manual (1995).

Some countries, such as New Zealand, have in recent years moved to a more performance based fire design environment as opposed to the generic prescriptive based design standards of the past. Performance based design allows more flexibility in designing fire safety strategies for buildings, as it is no longer a requirement to prove fire safety and fire protection to a pre-specified level for a building element. It instead requires that a certain level of fire safety is demonstrated by the entire system, in order to achieve a number of overall goals (generally based around ensuring the life safety of the building occupants). Clauses C1 to C4 of the New Zealand Building Code are a typical example of these types of goals, and are based around ensuring life safety by means of preventing the outbreak of fire, ensuring safe evacuation of building occupants, preventing the spread of fire and ensuring the structural stability of a building to prevent collapse.

This new way of thinking in fire safety shows great promise for large multi-storey timber buildings, as the fire safety of many timber systems can be easily demonstrated. As the major issue restricting the widespread use of timber is fire safety, a performance based approach will aid in changing the current perception of timber in the construction industry, and in the general public.

2.2 Timber-Concrete Composite Floors

Timber-concrete composite structures are not a new technology, and arose in Europe in the early twentieth century as a means of strengthening existing timber floors by the addition of a concrete slab. Due to the many advantages they possess over traditional timber floors, they are now being used in new construction (Lukaszewska et al., 2007, 2008, 2009). This is currently under investigation in many parts of the world such as the United States (Fragiacomo et al., 2007), Germany (Kuhlmann and Michelfelder 2006, Bathon et al., 2006), Switzerland (Frangi et al., 2009) and New Zealand (Buchanan, 2007, Buchanan et al., 2007, Yeoh et al., 2009, 2010). The performance of the flooring system depends mainly on the connection between the timber beams and the concrete slab, as a very stiff connection is required to ensure that sufficient composite action is achieved, resulting in a higher ultimate strength and smaller deflections. This is because the concrete slab acts mainly in compression while the timber member is subjected to bending and tension, therefore fully utilising the strengths of each respective material. As the connections become less stiff, the slip between the timber and concrete units increases which lowers the strength of the system and increases deflections. It should be noted that the connection between the timber and concrete is always deformable (Ceccotti, 2002) therefore the method of transformed sections cannot be used to analyse the system as the strain profile is not continuous. The strength and stiffness of the connection must be evaluated since both of these are required for the design of the composite beam.

There are many different types of composite flooring design, the main two categories being either solid timber slab type designs or beam type designs. Each main type has its advantages and disadvantages with respect to constructability, cost, strength and aesthetics.

Beam type designs consist of timber beams (either sawn timber, glulam or LVL) being used as floor joists, upon which a solid membrane (usually a plywood sheathing or steel deck) is fixed and a concrete slab is cast above. The forms of connections between the timber and concrete are extremely varied, some of which are glued, non-glued, and notched connections (Buchanan, 2007). Glued connections consist of a form of steel reinforcement (rebars, punched metal plates, steel lattices) which is glued into the timber members and continues out into the concrete slab. Non-glued connections can consist of screws partially screwed into pre-drilled holes in the timber, a punched steel profile screwed into the timber, inclined steel bars driven into tight holes, or shear studs screwed into the timber member. Notched connections consist of a notch cut out of the timber member which the concrete is cast into, and a stud can be incorporated in the notch for better performance. A number of these different types of connections have been investigated by Ceccotti (2002), Lukaszewska et al. (2007, 2008) and Yeoh (2009).

Solid timber slab type designs are generally composed of a solid timber decking from nailed timber planks with a concrete slab cast directly on top. Slab type floors generally utilise a grooved connection, the concrete is cast into grooves or trenches in the top of the timber decking which allows a large shear area of concrete to timber to be utilised, resulting in a very stiff and complete composite connection. Kuhlmann and Michelfelder (2006) have conducted extensive research on the strength and stiffness of grooved timber slabs. Some advantages of this design of floor are that they are quick to manufacture and can utilise lower quality timber, and the overall depth of the floor system is smaller than beam type floors. However, due to the completely solid nature of the floors there is no provision for allowing services to run parallel through the floors hence this must be exterior to the floor. In addition to this, a much greater quantity of timber is required to construct the system hence addition costs can be incurred in terms of on-site labour and transportation of materials.

The type of composite floor under study is a semi-prefabricated system comprising of "M" panels that are built with laminated veneer lumber beams and sheathed in a thick plywood interlayer, which acts as a permanent formwork for the concrete. The plywood interlayer has holes cut into it to accommodate the form of connection being used between the beams and the concrete slab. These panels are prefabricated off-site then transported to site and craned into position. The steel reinforcement can then be constructed and the concrete slab cast in-situ, the floor being propped if required. This system is shown in Figure 2.1.

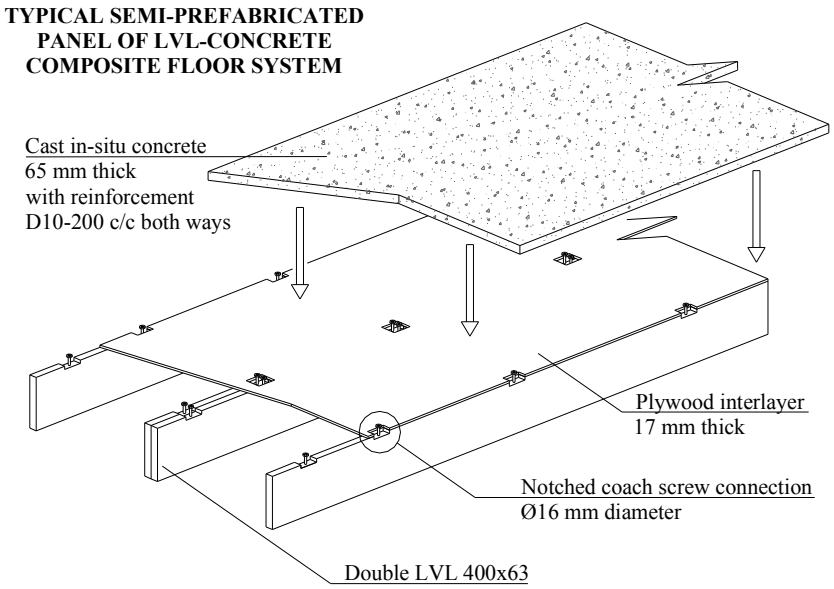

Figure 2.1: The Composite Floor System Under Study (Yeoh, 2009)

2.3 Fire Testing of Timber-Concrete Composite Floors

With the development of any new structural system, it is important to assess the fire safety of the system to ensure it can be used safely for its intended purpose. This is vital for timber systems, as a fire safety assessment can be a deciding factor in determining its success or failure in the international market. Many countries have strict regulations and guidelines regarding the use of timber materials, hence it is important to have conducted fire safety tests on the system to ensure it can meet a required level of fire safety.

Considerable research has been conducted on determining the ambient temperature characteristics of these types of floor systems in recent years, however the behaviour of these systems under fire conditions has attracted less attention due to the specialisation of the field. The fire resistance of timber-concrete composite elements is mainly influenced by the timber and the connectors (Frangi and Fontana, 1999). Their study looked at two separate systems, firstly a solid timber decking composed of nailed planks or glue laminated beams, this had grooves cut into the top of the decking to act as the connection system with threaded bars glued into predrilled holes along these grooves, and a concrete layer cast on top. The second system was a sawn timber beam system consisting of inclined self-drilling screws for the connection system implanted into a concrete slab cast on a plywood sheathing. Both of these floors are shown in Figure 2.2.

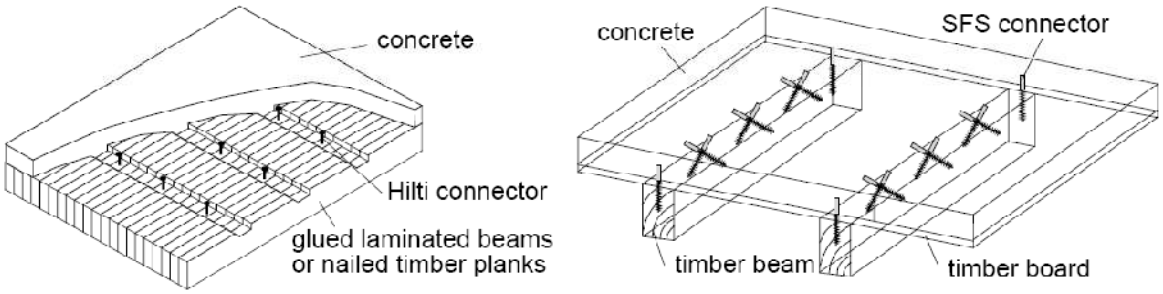

Figure 2.2: The Solid Timber Deck and Timber Beam Systems Under Study in Zurich (Frangi and Fontana, 1998)

Two full scale furnace tests were conducted and both systems exceeded 60 minutes of ISO fire exposure without structural collapse. From their research it is apparent that the effects of the fire on the timber such as heating and reducing overall section size act to weaken both the timber section and the connection between timber and concrete. The form of connection is also important, as the integrity of the connection during the fire is governed by the behaviour of its weakest element, which can sometimes be difficult to predict. For instance Frangi and Fontana (1999) found that the performance of their screw connectors was a linear function of the temperature of the surrounding timber, however their glued dowels exhibited no loss of strength until the glue temperature reached 50 °C, then performed very poorly at elevated glue temperatures.

A simplified design method developed by Frangi and Fontana (2001) for timber-concrete composite floors based on the effective cross section method from Eurocode 5 (2004) gave good results when compared with full scale fire tests. Although these systems have major differences to the one under investigation in terms of the connection type, timber type and major floor element geometries, it provides an insight into ways in which the issue of fire resistance for these systems can be addressed.

Although research into the fire performance of some timber-concrete composite structures has been conducted, the differing types of structures available in terms of material composition and design mean that different aspects of these systems will govern failure in fires. It is therefore important to identify what differences are present between tested and untested systems to determine what degree of scrutiny is required when researching the fire performance of a new system. This generally applies to beam type floors, as the fire performance of solid timber slab floors can generally be simplified down to the charring rate of the timber decking due to the one dimensional surface presented to the fire, as was found by Frangi and Fontana (1998) when they fire tested a solid timber slab floor.

For the timber-concrete composite floors under study in this research, it is clear that although the beam type system is similar to other floors previously fire tested, the connection types utilised in the system have not been tested extensively in fires and hence their actual fire performance is unknown. These connections may govern the failure of the

floors in fires, and the best way to determine the fire performance of a complex system such as this is with full scale tests.

2.4 Fire Testing of Laminated Veneer Lumber

The advent of high performance engineered wood materials such as LVL raises the question of how these new materials perform in fires. The fire behaviour of sawn timber has been well documented in the past, however questions pertaining to the physical composition of LVL (layers of wood glued together), the charring behaviour and the load bearing properties of the material are all vital when the material is subjected to fire conditions. It is important that the fire behaviour of any new material is understood before fire testing of systems utilising the material take place, as this information may be vital in dictating the failure mode of the system in a fire.

Recent research conducted by Lane (2005) has looked into the ignition, charring and structural performance of LVL. In terms of the glue lines in LVL affecting the charring rates, Lane found in a number of un-instrumented char tests that there was relatively no difference between charring for different grain orientations. These results suggest that the presence of the glue lines do not influence the burning behaviour of the material.

Lane also conducted cone calorimeter tests on LVL samples, and furnace tests on LVL members. This furnace testing consisted of subjecting LVL members to the standard ISO 834 fire (1975) in a pilot furnace, and also in a full scale furnace under loaded conditions. From this research he was able to specify a charring rate for New Zealand manufactured Radiata Pine LVL of 0.72 mm/min. From the testing conducted there were no obvious defects found in the design of the LVL material that reduced the performance of the material in fire conditions.

3.0 Full Scale Testing

3.1 Objectives

The primary objective of the full scale testing was to investigate the failure behaviour of timber-concrete composite floors when exposed to fire, which encompassed a wide range of information that was required to be collected from different parts of the floor system. Specifically, the failure mode of the floors was an important part of this as it would identify the critical component of the floor that governs the design for fire safety, whether it was a failure in the beams, the concrete slab or the connections between the two. Other important areas of interest were the charring behaviour of the timber beams, the spalling behaviour of the concrete, the fire damage about the connections and the performance of the plywood sheathing.

It was essential to conduct full scale experiments, as when a number of components of different materials are combined in a system, unanticipated and unforeseen behaviours and effects may result from the combination and interaction of these components when subjected to a fire under loaded conditions. These effects will not become evident from small scale tests conducted on each different component separate from the system. This is very important in relation to fires, where the nature of both the fire and the system behaviour can be difficult to predict with previously untested products.

A secondary objective of the full scale testing was to use the data obtained from the experiments to calibrate and develop the spreadsheet analysis tool for these floors, thus allowing the design tool to predict the fire resistance of the floors for a wide range of floor sizes and spans under different loading conditions.

3.2 Background

The specimen construction and testing was carried out at the Building Research Association of New Zealand (BRANZ), located in Porirua, New Zealand. The fire testing facilities at BRANZ are extensive, and include a full scale furnace, a smaller pilot furnace, an ISO room and a cone calorimeter.

The design fire used in the tests was the ISO 834 standard test fire (ISO 834, 1975). This was used as it is one of the most commonly used standard test fires around the world, hence using this fire type aids in the comparison of test results with other similar full scale tests. The ISO 834 design fire curve is shown in Figure 3.1 below.

The full scale furnace has an interior span of approximately 3 m by 4 m, and can accommodate varying depths depending on how many steel loading frames are stacked on top of the furnace. The floor units were designed to span along the 4 m length, simply supported on top of one loading frame on the furnace. The furnace is fuelled by diesel injection burners and a gas extraction system to allow the pressure and temperature inside

the furnace to be monitored and controlled (see Figure 3.3 and Figure 3.2). It is lined in ceramic fire bricks and has a number of thermocouples and pressure gauges about the interior to monitor the temperature and pressure, allowing the operator to manage the diesel inflow and produce the desired design fire. The primary use of the furnace is for testing floors and walls, and due to the large 25 tonne crane housed in the warehouse the furnace can easily be picked up and inverted for either use. It can also be used to test structural elements, smoke vents and extraction fans, large doorways or glazed areas. Due to the versatility of the crane, unloaded or loaded tests are possible without any significant risk of damaging the equipment.

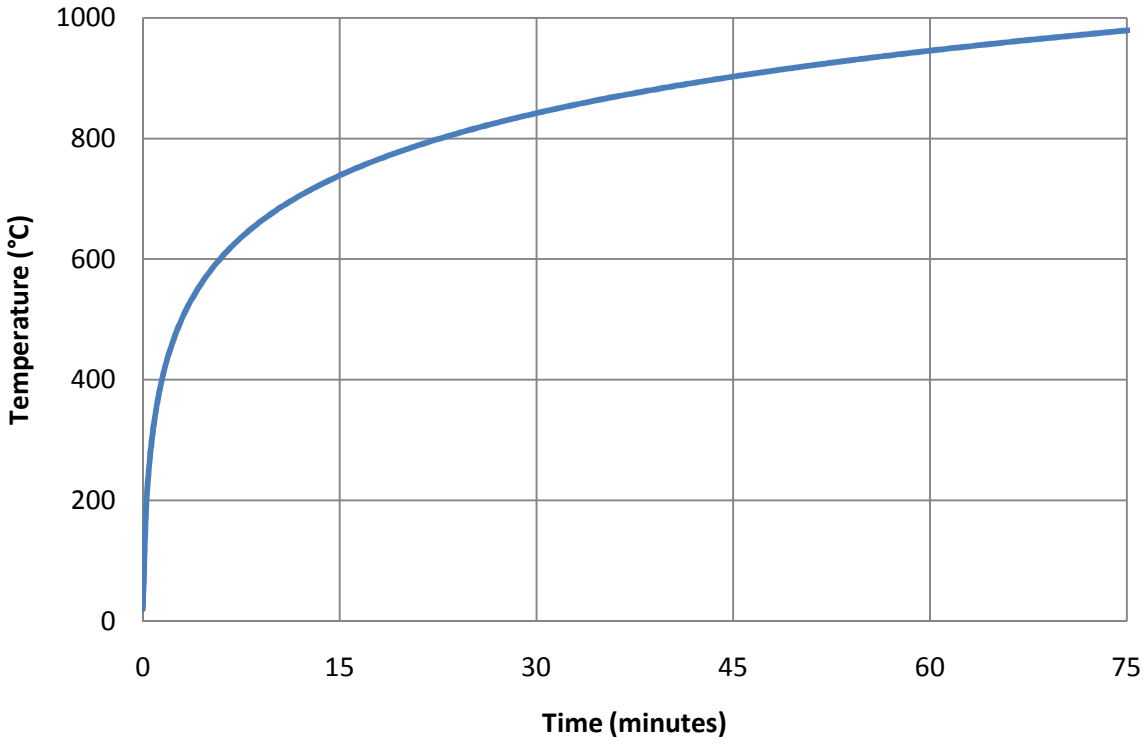

Figure 3.1: ISO 834 Design Fire Curve Used in the Furnace Testing

Figure 3.3: Inside the Full Scale Furnace at BRANZ

Figure 3.2: The Furnace Diesel Injection System

3.3 Materials

The floor joists utilised laminated veneer lumber (LVL) as the timber material which is composed of thin radiata pine wood veneers, glued together in a staggered formation which eliminated the effects of knots or imperfections in the wood and produces a high performance timber product. It is because of this low variability and high strength that LVL is a reliable engineering material (Buchanan, 2007), and is therefore ideal for use in the construction of these floors that may be required to span long distances and require large section sizes. The specific recipe used in this instance is Carter Holt Harvey's Truform LVL, and characteristic values for this are given in Table 3.1. The full specifications for Truform LVL are available in the product specifications on the manufacturer's website (Truform Brochure, 2008).

Table 3.1: LVL Material Properties for CHH Truform LVL

Characteristic Stresses (MPa)		
Bending	f'_b	48
Tension parallel to grain	f'_t	33
Compression Parallel to Grain	f'_c	45
Shear in Beams	f'_s	5.3
Compression Perpendicular to Grain	f'_p	12
Shear at Joint Details	f'_{si}	5.3
Elastic Moduli (MPa)		
Modulus of Elasticity	E	10700
Modulus of Rigidity	G	660

The concrete used was a standard 30 MPa mix design. Due to too little concrete being sent to site on the first delivery, a second mix was sent to pour one side of the remaining slabs. Although this was not ideal for testing purposes the construction method used in building the floors accommodated this well, as is discussed in further detail in Section 3.4.

Three cylinders were cast for each mix to monitor the strength of the concrete and were tested in accordance with NZS 3112: Part 2: 1986. The results of these tests can be found in Table 3.2.

Table 3.2: Concrete Test Results

Test	Age (days)	Mass in air (g)	Mass in water (g)	Length (mm)	Diam. 1 (mm)	Diam. 2 (mm)	Failure Load (kN)	Density (kg/m^3)	Strength (MPa)
A	28	3630	2060	200	99.3	100	278	2320	35.6
B	28	3620	2060	200	98.8	100	267	2320	34.3
C	28	3620	2050	200	100	99.7	271	2310	34.5
D	28	3630	2060	200	99.0	100	184	2320	23.6
E	28	3620	2060	200	98.8	100	184	2320	23.7
F	28	3620	2060	200	98.9	100	184	2320	23.7

The bulk of the concrete slabs had an average compressive strength of 34.8 MPa after 28 days, although one side of the smaller 300 mm beam slabs was only 23.7 MPa after 28 days. The impact of this on the testing is discussed in the following sections.

The bolts used in the notched connections were 16 mm diameter, 200 mm long coach screws supplied by Blacks Fasteners, shown in Figure 3.4. These were incorporated into the design as previous work conducted by Yeoh (2009) and O'Neill (2007) found that the addition of the mechanical fastener allowed for a ductile failure of the notch as opposed to a brittle failure, and also increased the ultimate strength of the connection significantly (up to 50 %).

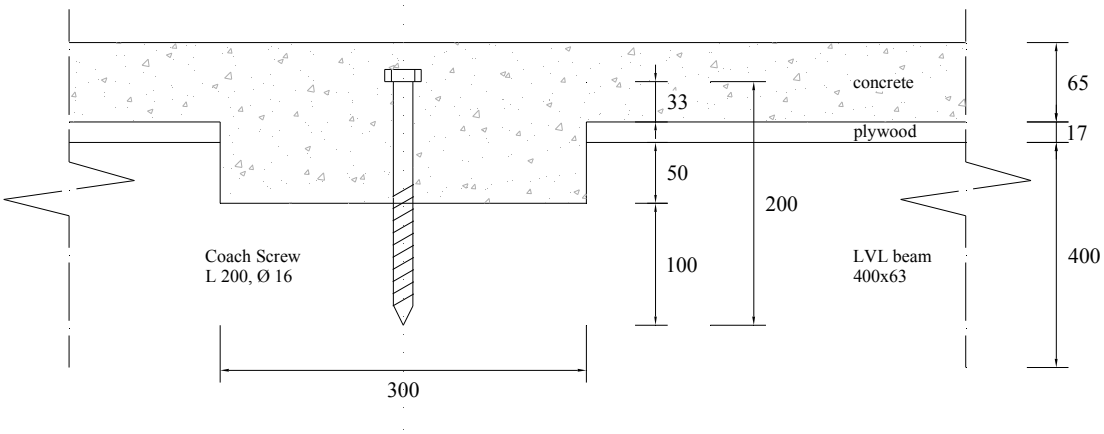

Figure 3.4: Design Detail of the Notched Connection

The second type of connection used in the testing was a toothed steel plate solution manufactured by MiTek. The exact dimensions of these plates are shown in Figure 3.5, and they were of 2 mm thickness and punched from mild steel. The plates were designed to protrude into the concrete slab, having the reinforcement bars threaded through the holes

and the concrete cast through them thus fully tying the connectors into the slab structure, primarily for means of earthquake resistance.

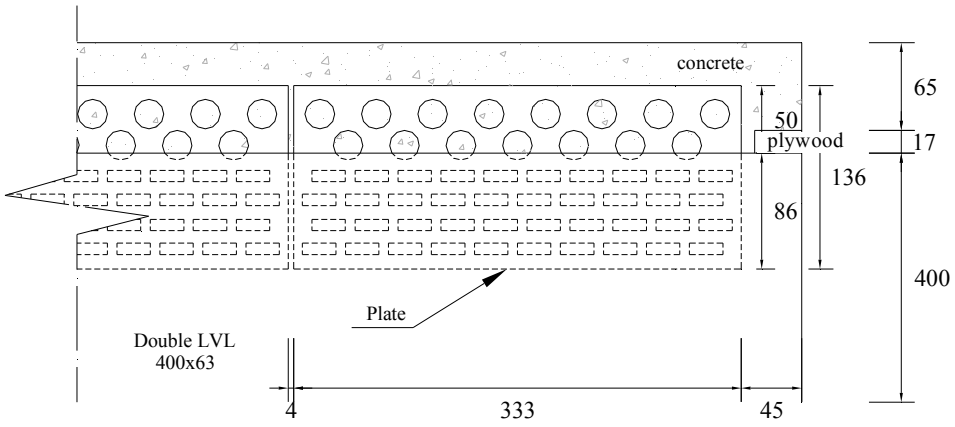

Figure 3.5: Design Detail of the Plate Connection

A number of short and long term tests on these connection types (including extensive push-out testing) are detailed in the research conducted by Yeoh (2009).

3.4 Specimen Details

The full scale testing involved two floor units tested under scaled loads, the dimensions of each floor unit being identical apart from the beam depth and design load. A 300 mm deep LVL beam floor was designed with a span of 5 m, and a 400 mm deep LVL beam floor was designed with a span of 7 m. Although smaller and larger sizes of beams are available, and the floor spans can be designed up to 11 m, the floor designs tested were limited by the loading capabilities of the full scale furnace at BRANZ. These beam sizes were also chosen as they would reflect what is expected to be most commonly used in the industry. A modification on the usual number of connections also had to be made to accommodate the 4 m span of the furnace, having only four notches or eight plates per beam, as opposed to the usual six notches or twelve plates. The general design of the timber-concrete composite floors used in the testing was based on the semi-prefabricated system under development at the University of Canterbury. Each floor unit consisted of two 4.6 m long double Laminated Veneer Lumber beams (four beams in total) spaced 1200 mm apart, one double beam utilising concrete filled notches to obtain composite action and the other utilising toothed steel plates which protrude into the concrete slab.

The double beams were fixed together using type 17 self-drilling screws in a staggered fashion at 300 mm centres, 75 mm from the edges of the beams as shown in Figure 3.6. The type 17 screws were 100 mm long composed of mild steel (300 MPa) and had a shank diameter of 5 mm (see Figure 3.7). Other forms of fixings are available to fasten the beams together, such as bolts and washers or completely gluing the beams, however the screw

option was chosen as it is fast, simple and was assumed to be a common method employed in the industry for constructing these floor systems.

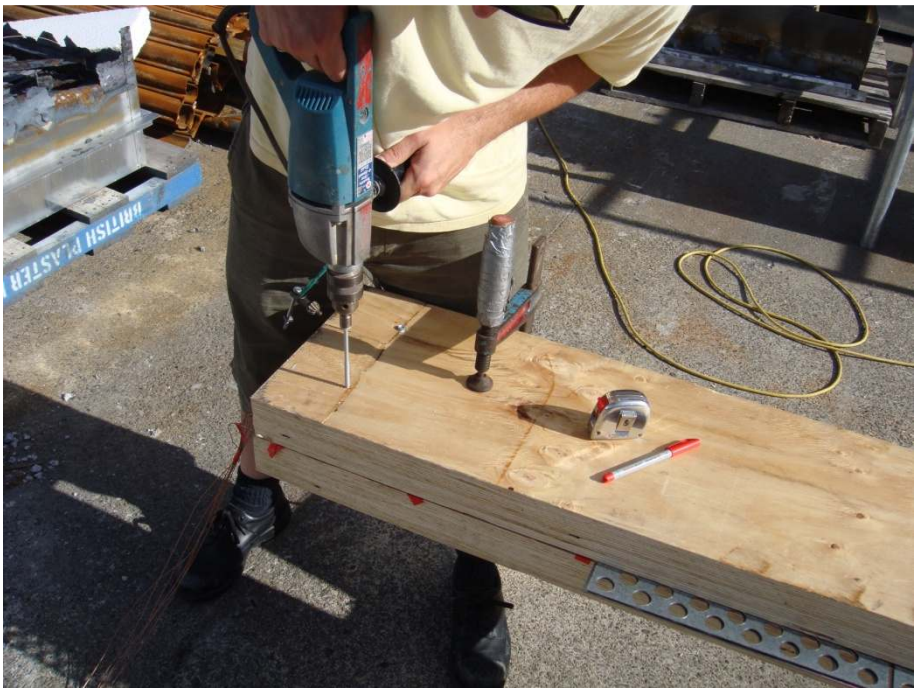

Figure 3.6: Fastening the Double Beams Together

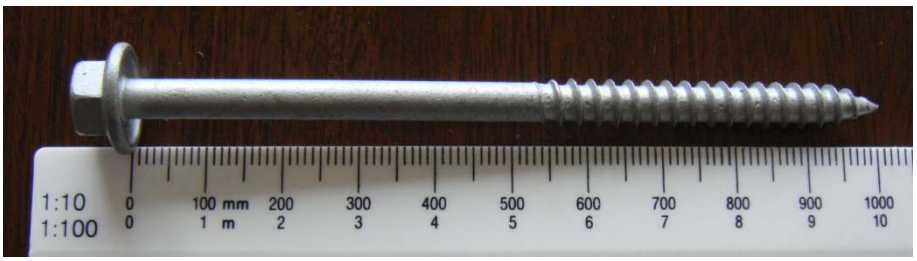

Figure 3.7: A Typical Type 17 Screw used to Fasten the Beams Together

Two different connection types were used in each test specimen. The first connection type tested was the result of previous short and long term testing by Yeoh (2009) and O'Neill (2007), and was a 50 mm deep by 300 mm long rectangular notch cut into each beam. A 16 mm coach screw was installed 100 mm into the centre of this notch, and concrete was cast about it. Figure 3.8 shows a typical notch connection ready for concrete to be cast into it. The second connection type tested was a toothed steel plate pressed between the double beams. This required a truss press to perform the installation and was carried out at Westlake Timber in Christchurch, shown in Figure 3.9 below.

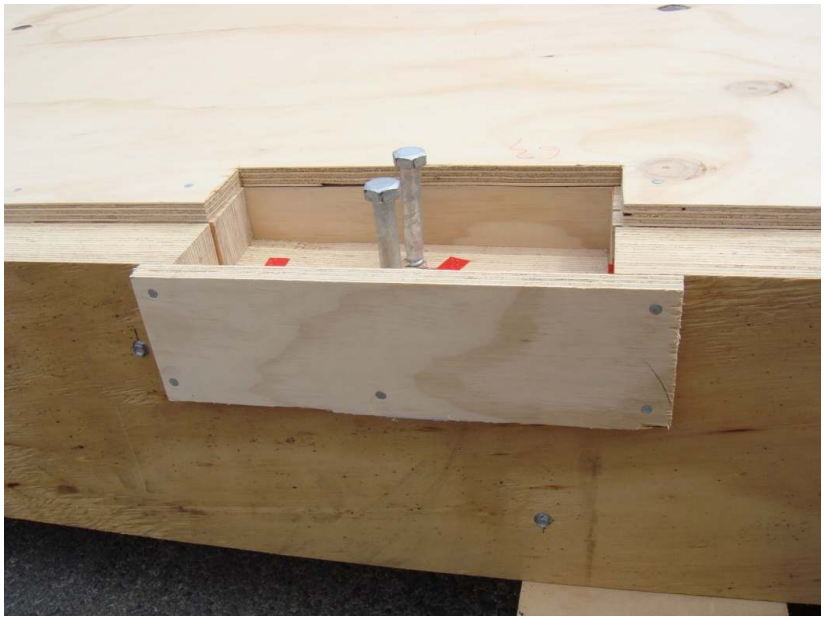

Figure 3.8: A Typical Notched Connection

Figure 3.9: Pressing the Steel Plates at Westlake Timber

In order to span the timber floors across the top of the steel loading frame on the furnace each floor specimen needed to be bounded by dummy walls that would contain the fire for the expected duration of the testing. This was to ensure the pressure and temperature inside the furnace could be properly controlled and that hot smoky gases and flames would not escape the enclosed furnace compartment, thereby invalidating the testing. These walls were constructed from 50 mm by 50 mm sawn timber sticks which were spaced nominally at 600 mm centres along the sides of the specimen, as shown in Figure 3.10. A plywood

backing was nailed to the back of the wall which protruded 82 mm above the top plate of the wall. This allowed for the plywood sheathing of the floor to be nailed down onto the walls about the edges of the specimen, thus leaving 65 mm for the topping concrete to be poured and levelled to at a later date. The inside of the walls were lined with two layers of 13 mm Winstones Fyreline Gib Board (a fire rated gypsum plasterboard product) which would conservatively achieve a minimum of 60 minutes fire protection. These were installed in a staggered fashion with overlapping joints, fastened at 200 mm centres with approved screws and stopped with an intumescent filler along the joins, which can be seen in Figure 3.11.

Figure 3.10: Walls to Bound the Underside of the Test Specimens

Figure 3.11: Gib Board Lining on the Underside of Test Specimens

A 17 mm thick plywood sheathing was nailed to the top of the beams providing permanent formwork for the concrete topping. The plywood had holes cut into it to accommodate the connection systems. The processes of preparing the connections and cutting the plywood sheathing were labour intensive and time consuming, and as such the majority of the cost of installing these systems would be incurred at this stage. However, the solution of preparing these portions in shop and installing a prefabricated panel ensures quality control and reduces time spent on site. Furthermore, the time saved when installing these lightweight components results in significant cost savings of manual labour, crane hire, transport costs and site workability and should outweigh the initial construction expenditures.

A 65 mm thick 30 MPa concrete topping was cast in the forms, filling the notched connections and through the steel plate connections. The forms were painted with one coat of acrylic paint in order to reduce moisture absorption by the timber and ensure the concrete did not crack. The completed test specimens before concrete casting are shown in Figure 3.12. The steel mesh used was a standard 6 mm thick mild steel mesh welded at 200 mm centres. Although the floor design for earthquake resistance requires much larger steel bars to be tied at a smaller spacing, a simple welded mesh was used in the fire tests as it was not expected that the full tensile strength of these bars would be developed. The most

critical aspect of the reinforcement was assumed to be the cover depth, as when the fire reaches the steel the high thermal conductivity and small dimensions of the material ensures that the temperature increases rapidly and thus the strength decreases rapidly.

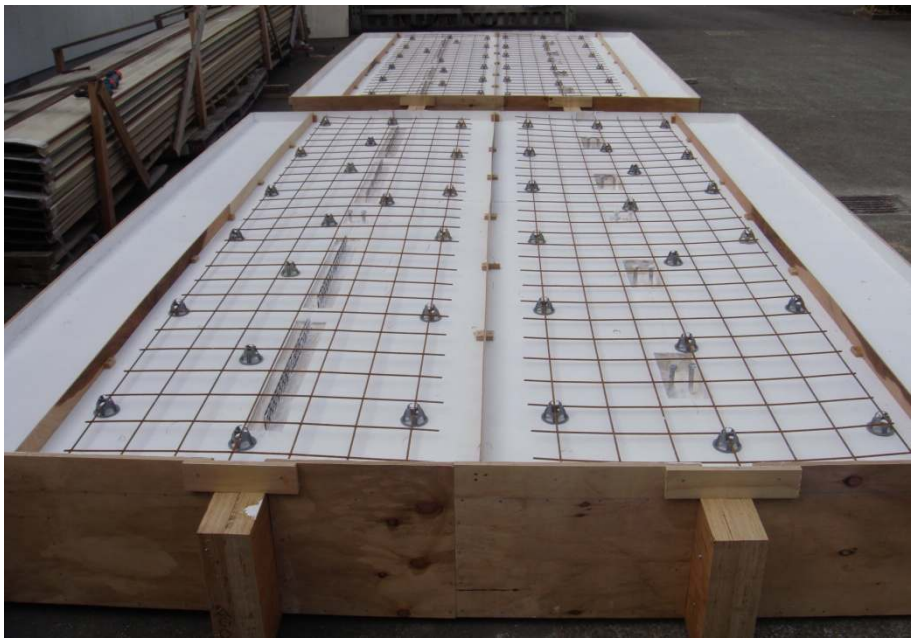

Figure 3.12: Completed Floor Specimens before Concrete Casting

In order to test two different connection types, the concrete slab was separated via thin plywood strips which were spaced at 1200 mm centres over the beams (see Figure 3.12). This left a 300 mm width of dummy concrete along the edges of each specimen which did not have any steel mesh cast into it as it served no structural purpose; it was only present to form a complete seal across the top of the furnace. This would eliminate any load sharing between the separate double beams once the plywood sheathing had burned through and the concrete was exposed, thus allowing each side of the floor to be loaded and tested independently of the other.

During different stages of the construction process thermocouples were placed in critical areas to allow for temperature data to be recorded at points of interest. The set of thermocouples to measure the temperature distribution through the beams were installed sandwiched between the double beams. These were placed in a staggered fashion at 50 mm depths throughout the beams. A cross section of this can be seen in Figure 3.13. To ensure that the data recorded from the thermocouples was accurate, they were continued along the same thermal plane for at least 300 mm. Thermocouples were also installed in the concrete, the connections, the various composite interfaces and on the steel mesh, seen in Figure 3.13 and Figure 3.14. The data recorded for every thermocouple used and those inside the furnace can be found in Appendix B: Full Scale Testing Thermocouple Measurements.

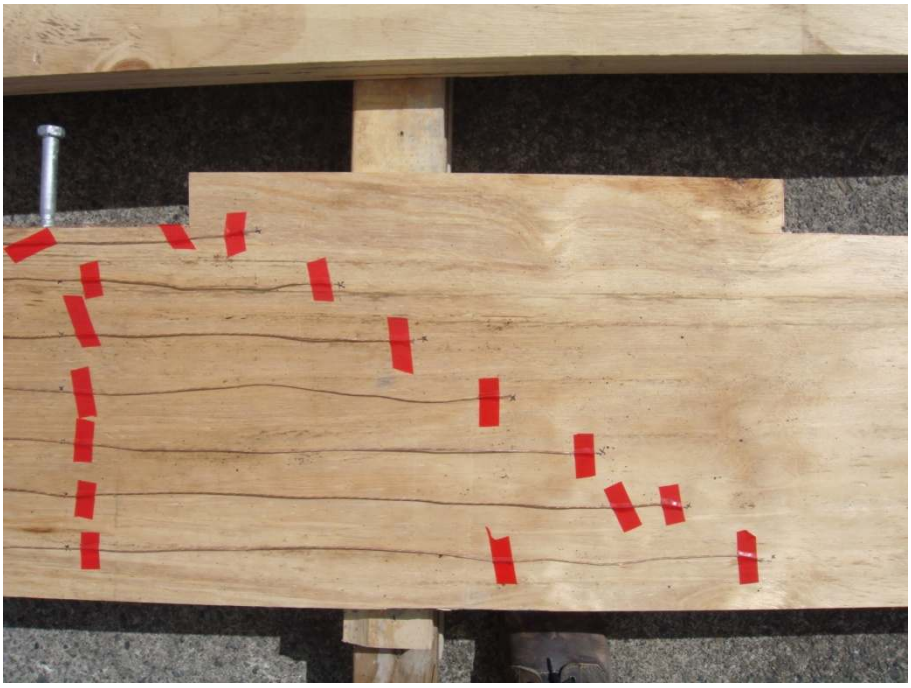

Figure 3.13: Thermocouple Placement Throughout the Beams

Figure 3.14: Thermocouples at Different Locations in the Notched Connection

3.5 Design of Test Floors

As fire conditions cannot be scaled or manipulated in the conventional manner that many other external conditions and loads can be for experimental testing, attempting to simulate the likely fire performance of a large structural system can be difficult. Due to their combustibility, timber beams cannot be scaled down in size as their fire behaviour is dependent on the actual cross-section present. This required that the loads on the floor units be scaled up in such a way that similar stresses were induced in the load bearing members of the floor and the same bending moment at the midspan of the floors was obtained. The design loads of the test specimens were based primarily on a live load of 2.5 kPa and a dead load of the self weight of the floor only with no additional superimposed dead load.

The member span and hence total scaled load was further restricted by the load capabilities of the full scale furnace, in that the largest loading that could be physically achieved was approximately 3.5 kPa. In order to achieve the desired loads within the above constraints the 300 mm deep LVL beam floor was designed with a span of 5 m, and the 400 mm deep LVL beam floor was designed with a span of 7 m. This resulted in the final scaled and factored loads for these beams to be 1.56 kPa and 3.06 kPa respectively.

To accommodate the smaller span of the furnace, the generic number of connections was reduced from the usual six notches or twelve plates per beam to four notches or eight plates. This was incorporated into the full scale design of the floors, and when scaled down the number or size of the connections was not changed, only the relative connection spacing along the beams. This was because the increase in load to achieve the same bending moment at the midspan induced a much larger shear force in the floor than was present in the unscaled design. However, since each connection was designed to resist a shear force given by the integral of the shear flow along the length of the beam, and the area of the shear force diagrams were the same for both designs, the connection is subjected to approximately the same force as in the design. Therefore retaining the same number and size of connections for both designs ensured that the test behaviour would closely represent actual full size floor behaviour. The full set of design drawings for the test specimens are shown in Appendix A: Floor Design.

3.6 Experimental Procedure

The test specimens were subjected to the ISO 834 design fire (1975). This was monitored and controlled by one of the fire technicians operating the diesel inflow equipment for the duration of the testing, allowing the temperature and pressure inside the furnace to be adjusted continuously to most accurately mimic the design fire curve.

The loading rig used in the testing consisted of a large steel frame that was supported on the edges of the rectangular loading frame holding the test specimen. The rig had two

beams with 5 barrels along each beam, and the barrels had three feet to spread the load over the slab area. This was ideal for the floor testing as each line of barrels corresponded to the centreline of the beams to be loaded. The barrels could be filled with water and steel weights could be added to the top of the barrels to obtain loads up to approximately 3 kPa. Each barrel had a steel hanger which allowed them to load a floor until its vertical displacement was such that the hanger would catch on the rig beam and support the weight of the barrels. This prevented the barrels from falling into the furnace upon failure of a loaded test. Figure 3.15 shows the loading rig before the first test.

Figure 3.15: The Loading Rig

For the first furnace test of the 300 mm beam floor, the barrels were three-quarter filled with water to attain the 1.56 kPa design load required. For the second test (on the 400 mm beam floor design) the barrels were completely filled with water and steel weights were placed on top of the barrels to attain the 3.06 kPa design load. In addition to the thermocouple measurements being taken, six potentiometers (refer to Figure 3.15) were fixed to the loading rig and drawn down to the slab surface to measure the vertical displacement of the floors. These were approximately in line with the centrelines of the beams and spaced at third points across the floors.

Once the testing was terminated the loading rig was required to be removed and set down before the test specimen and loading frame could be removed. This was a period of only a few minutes but because the timber kept burning after the fire in the furnace was extinguished it was critical that this time was minimised in order to obtain accurate charring rate measurements after testing. This involved craning the specimen and loading frame in the air and immediately soaking the underside of the floors to extinguish the fire. After this

the entire specimen was doused with fire hoses on the ground for a time to cool it down sufficiently for it to be moved and dissected (see Figure 3.16 and Figure 3.17).

Figure 3.16: Lifting the Test Specimen off the Furnace

Figure 3.17: Dousing the Test Specimen with Fire Hoses

4.0 Full Scale Testing Results

4.1 General Observations

The first floor specimen tested on the 7th April 2009 was the smaller 300 mm beam floor, which was tested to destruction. This lasted approximately 75 minutes under the ISO 834 design fire and 1.56 kPa applied load. The side with notched connections was the first to fail, and the testing was terminated immediately at this point due to a large amount of flames spewing out of the furnace and the loss of control of the test conditions. Fortunately the damage to the furnace interior was mainly superficial, and due to the fire bricks requiring renewal the damage was easily repaired for testing the next day as new materials were on hand. After enough cross section was lost in the timber beams the concrete slab could not support the loads transferred to it, resulting in catastrophic failure. Visible in Figure 4.1 is the spalling damage to the underside of the concrete, the extent of the char damage to the beams and some charred plywood remains.

Figure 4.1: The Underside of the Failed 300 mm Beam Floor

The second floor was the larger 400 mm beam floor and was tested on the 8th April 2009. The test was stopped shortly after 60 minutes to assess the damage after that time and provide insight into how the beams were charring before complete destruction. The initial and remaining timber section sizes are shown in Table 4.1, and photos of the floors turned

upside down after the testing and with sections removed can be seen in Figure 4.2, Figure 4.3 and Figure 4.4. Measurements represented in the tables were taken from intermediate regions in the beams (seen in Figure 4.2), as the char depth was extremely uniform across the beams and between both beam types in each test (plates and notches).

Table 4.1: Residual Double Beam Section Sizes Before and After Furnace Testing

Test Specimen	Size Before Furnace Testing		Size After Furnace Testing		Burning Time (min)
	Width (mm)	Depth (mm)	Width (mm)	Depth (mm)	
300 mm	126	300	44	130	75
400 mm	126	400	52	255	60

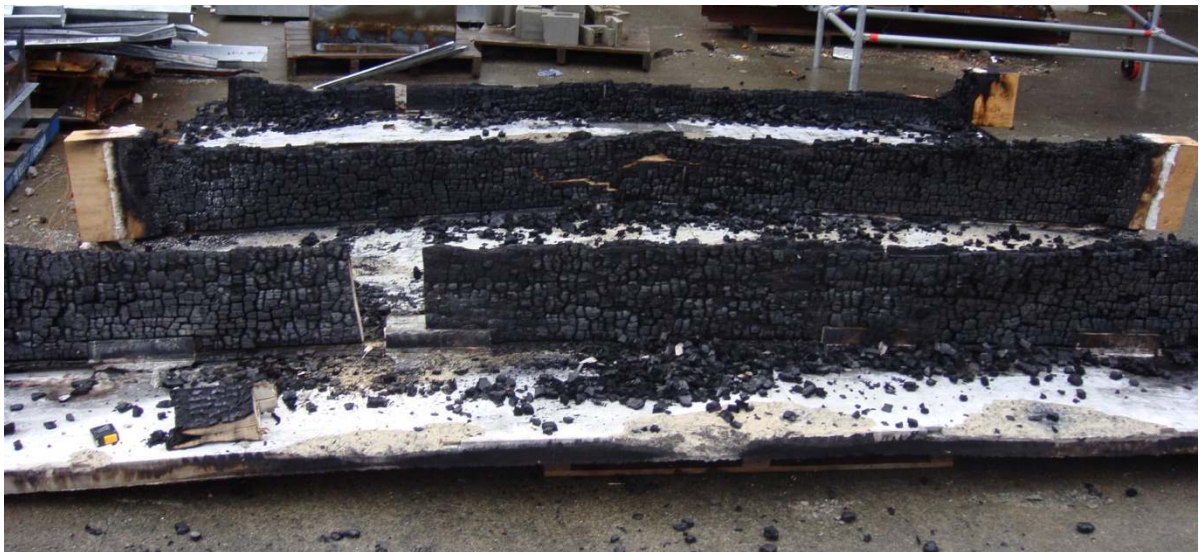

Figure 4.2: Upside Down Charred Floor Units After Testing

Figure 4.3: 300 mm Floor Residual Remains After 75 minutes of Fire Exposure

Figure 4.4: 400 mm Floor Residual Remains After 60 minutes of Fire Exposure

The reduction in section size of the timber beams due to the fire governed the failure mode of the floors, as observed by the BRANZ technical staff, student and supervisors present during the testing. The smaller 300 mm floor underwent an average section size reduction of 65 % of its width and 57 % of its depth. This corresponds to a total cross sectional area reduction of 85 %. This massive reduction in area would not have been possible with standard simply supported timber beams, but due to the composite action achieved by the connections, the floor units were able to withstand prolonged exposure to the test fire exceeding an hour in both cases as the remaining load was transferred to the other part of the system, namely the concrete slab. Previous testing in the full scale furnace by Lane (2005) of a large LVL section (305 mm wide by 400 mm deep) subjected to a central point load of 30 kN lasted approximately 37 minutes under exposure to the ISO 834 fire (1975). Comparing the smaller composite floors tested with this test they had a beam cross section of under a third, a load of approximately half (including concrete weight), and lasted 75 minutes before failure. This result emphasised the advantages in strength and reliability that these timber-concrete composite systems hold over standard timber floors, in that the fire resistance is greatly increased when composite action is utilised.

The larger 400 mm floor test was terminated at 60 minutes and as seen in Table 4.1 the beams underwent an average section size reduction of 59 % of its width and 36 % of its depth at this time. This corresponds to a total cross sectional area reduction of 74 % after an hour, which indicated that although the applied load was double that of the smaller test specimen, the burning behaviour was similar and the larger floor did not fail prematurely. The calculated average charring rates for each floor are shown in Table 4.2.

Table 4.2: Calculated Average Charring Rates for the Tested Floors

Test Specimen	Side Charring Rate (mm/min)	Bottom Charring Rate (mm/min)	Overall Charring Rate (mm/min)
300 mm	0.55	2.27	1.12
400 mm	0.62	2.42	1.22
Both Floors Average	0.58	2.35	1.17

The charring rate for the 400 mm floor beams above was slightly higher than the 300 mm floor from both directions. This was most likely attributed to a deeper layer of char providing better insulation on the smaller floor beams, as deeper layers of char will reduce the charring rate of the timber (the smaller floor was removed after 75 minutes of exposure, the larger floor after 60 minutes). The deeper floor beams also exhibited separation at the midline to a much greater degree than the smaller beams, allowing further charring to penetrate the bottom surface. This separation phenomenon is discussed in detail in Section 4.4.

A sketch of both beams with initial and final cross section sizes are shown in Figure 4.5. This is a pictorial description of Table 4.1 to allow a better understanding of the physical remains after furnace testing. The massive reduction in section size is clearly visible, most notably on the smaller 300 mm deep beam which was tested to destruction.

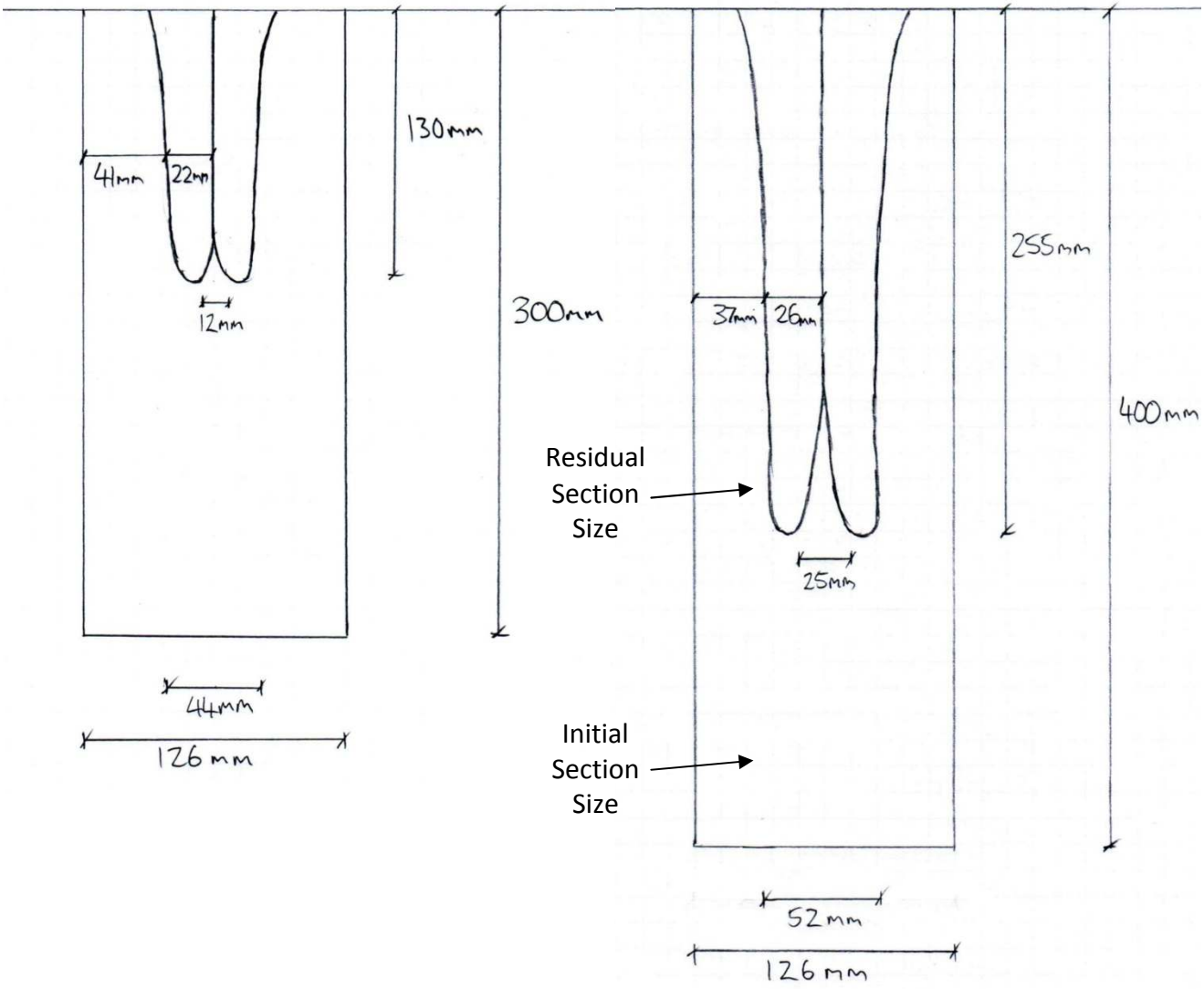

Figure 4.5: Sketches of the Initial and Residual Remains of Both Beam Cross Sections After Furnace Testing

4.2 Vertical Displacement

The average displacement measurements of the potentiometers on the top of the slab can be seen in Figure 4.6 and Figure 4.7. The separate measurements for each floor can be found in Appendix C: Full Scale Testing Displacement Measurements.

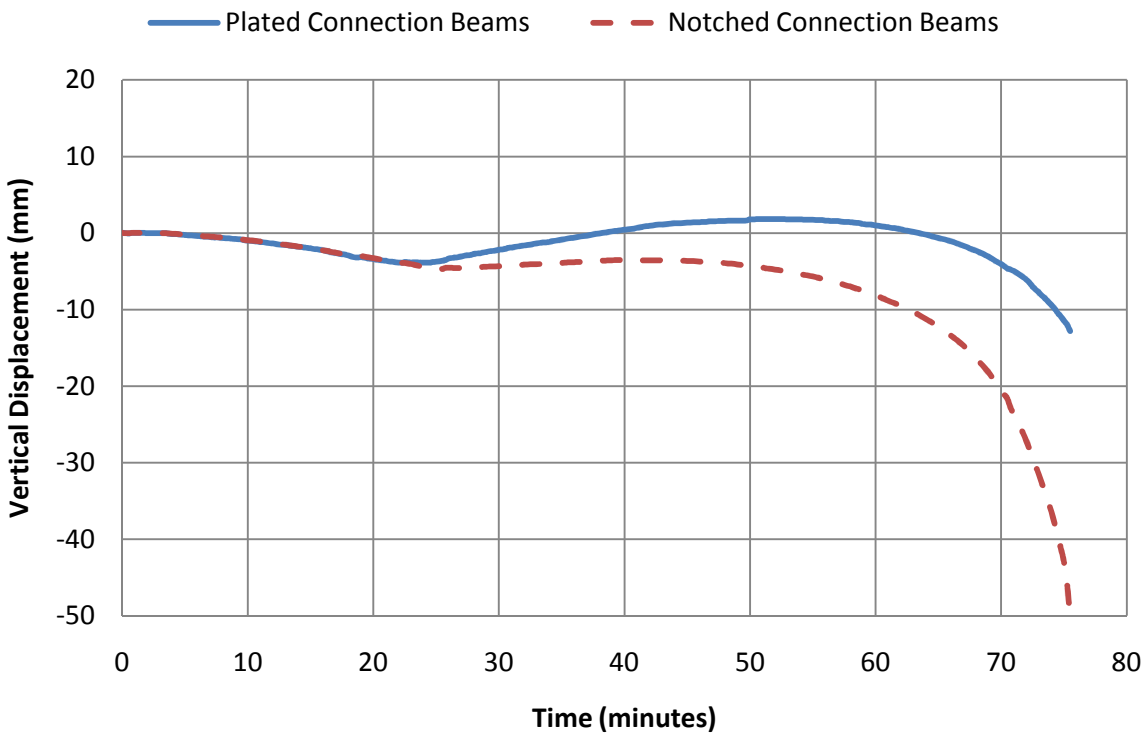

Figure 4.6: Displacement Results of the 300 mm Floor

From these measurements it is clear the 300 mm floor sections sagged for the first 23 minutes of testing due to the applied load and reduction in timber beam cross section. However, it can be seen for both sides of the floor that the vertical displacement begins to decrease back towards the initial rest position. The time this behaviour begins is concurrent with the almost complete burning through of the plywood sheathing, and is due to the heating of the underside of the concrete slab. Calculating the approximate time in which it the plywood burns through, using an average charring rate value for timber of 0.65 mm/min specified by NZS 3603 (1993):

$$\frac{Plywood\ Thickness}{Charring\ Rate} = Burn\ Time$$

$$\frac{17\ mm}{0.65\ mm/min} = 26.2\ min$$

This calculation correlates well with the measured values shown in Figure 4.6, as a faster initial charring of the plywood and thermal transference through the thin plywood layer would act to reduce the time until slab heating. Higher charring rates for different timber material types such as 0.72 mm/min for LVL suggested by Lane (2005) give even closer results.

As a significant thermal gradient was introduced across the depth of the concrete, the bottom of the slab expanded due to the increase in temperature. This behaviour was

restrained by the beam however due to the composite connections, therefore a thermal bowing action was induced in the floor that tended to hog the entire specimen. This thermal bowing aided in resisting the gravity loads imposed on the floors, and was essentially the same thrust force that can be developed via axial restraint (Buchanan, 2002). This behaviour was more apparent in the side of the floor with plated connections, as the reduction in slip modulus due to fire exposure was much less than for the notched connections as the plates were well insulated from the fire. The notched connections underwent a larger reduction in slip modulus due to the charring of the timber and loss of bearing area for the concrete to timber interface. Therefore the effect of the slab elongation was more significant for the plated connections than for the notches, resulting in less floor displacement, a more marked thrust force being developed and better fire resistance overall.

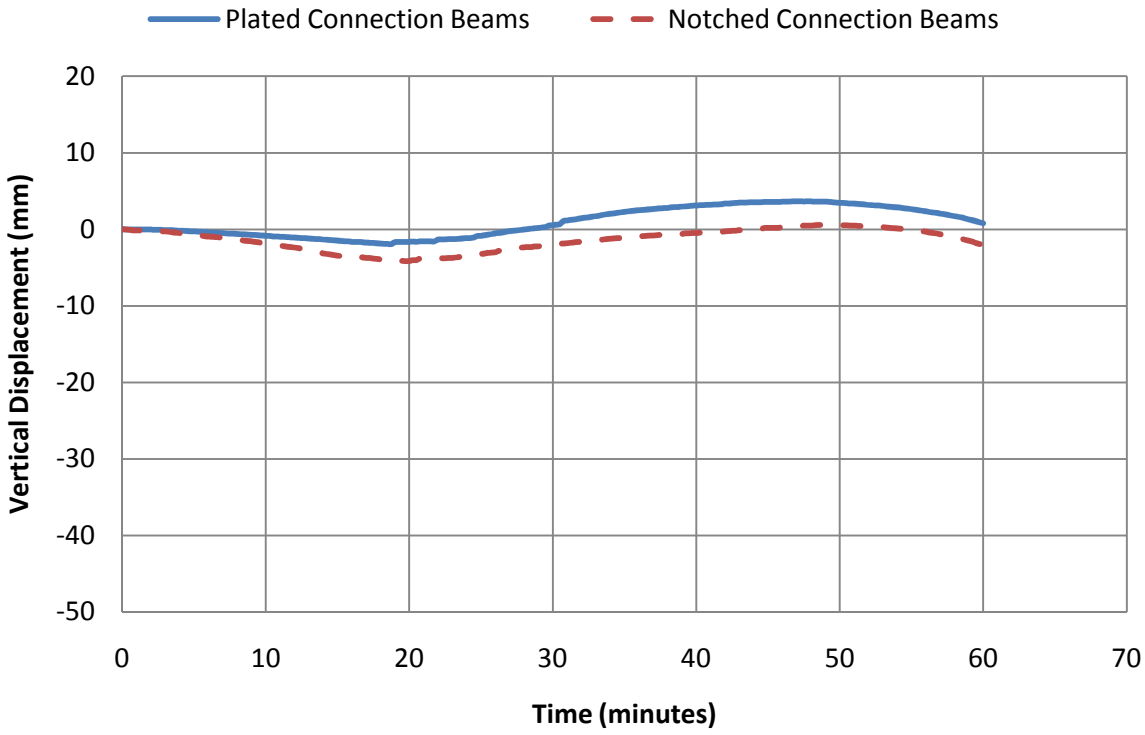

Figure 4.7: Displacement Results of the 400 mm Floor

As seen above for both floors tested, the displacement up to structural failure was less than 1/20 of the span (200 mm) and the rate of increase of displacement was also low. This was a promising result as many structural requirements specify deflections of less than 1/20 of the span or a limiting rate of deflection when deflection is 1/30 of the span (Buchanan, 2002). It should also be noted that for the larger floor the displacement measurements diverged at approximately 5 minutes. This was most likely attributed to the loads being much larger on this floor (see Section 3.5), and coupled with a fast initial charring of the plywood it is very likely that the plywood fractured at this time allowing each side of the floor specimen to separate. The data shows that the hogging action began sooner than for the smaller floor

and was more significant for the notched beams. This was most likely due to the thermal bowing induced having a larger eccentricity about the top of the slab as the initial displacement was lower and the composite section deeper, hence the bowing force generated was larger.

4.3 Concrete Slab Temperature

Figure 4.8 shows the average temperature measured on top of the slab for both floor units. The full data set for each thermocouple is recorded in Appendix B: Full Scale Testing Thermocouple Measurements.

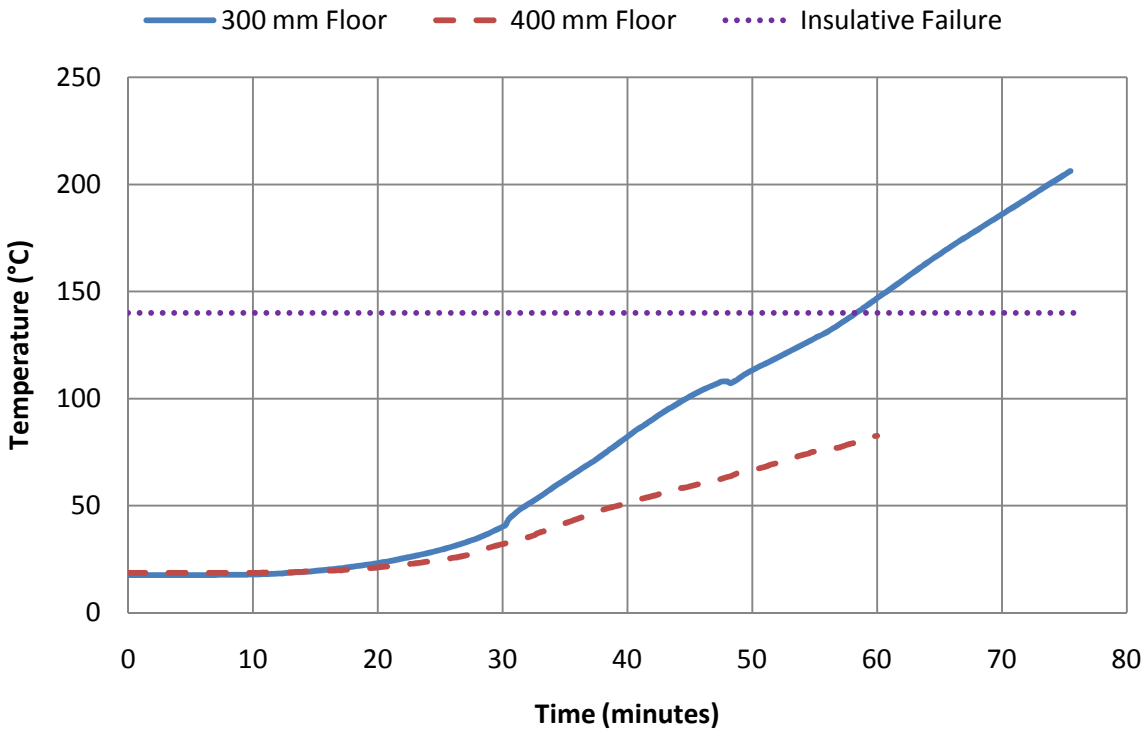

Figure 4.8: Average Top of Slab Temperatures for Both Tests

These temperatures were measured by thermocouples at five separate points across the top of the separated slabs spaced in a pattern representing an X, resulting in ten thermocouples used for each test. Due to the thickness of the slab being only 65 mm on average, and the average spall depth being 15 mm to 20 mm, the top surface of the concrete slab began to rise in temperature after 20 minutes into the testing. This indicated a potential issue with the small relative thickness of the slab, as in general to meet most insulative criteria requirements the average temperature increase on the top of the slab should be lower than 140 °C (Buchanan, 2002). As discussed in Section 3.3 the concrete mix was not consistent across both specimens tested. The 300 mm beam floor unit had a lower grade concrete slab cast above the beam with the notched connections. It was this side of the floor unit that failed at 75 minutes, hence it is highly likely that the poor performance

exhibited by this floor when considering displacement (Figure 4.6) can be partially attributed to weaker concrete, and partially to the connection stiffness. As seen in Figure 4.6, the beams with plate connections had less displacement at the failure time of 75 minutes but were degrading rapidly and it is estimated they would not have lasted much longer. This is also the reason for the discrepancy between the two tests as the thermocouples on the lower grade concrete slab gave much higher temperature readings than on the higher grade concrete slab. This is because the lower grade concrete had much more water in its composition, and upon application of heat to the underside of the slab the spalling was much more frequent and penetrated deeper into the slab. Spalling most often occurs when the water vapour is driven off from the cement paste during heating, with high pore pressures creating effective tensile stresses in excess of the tensile strength of the concrete (Buchanan, 2001). The combination of high stresses, a small slab thickness and in this case, a wetter lower quality concrete mix all contributed to more prolific spalling and hence greater thermal transference to the top of the slab. This effect however is mitigated over time by the drying out of the concrete slabs in a building during its operational use, and considering the time it took for the smaller floor to exceed 140 °C with a low quality concrete mix, the likelihood of a properly constructed dry slab exceeding this temperature before structural collapse is low.

4.4 Timber Charring Effects

The charring rate on the sides of the LVL beams was found to be 0.58 mm/min on average (see Table 4.2), lower than reported values of 0.72 mm/min based on research conducted by Lane (2005) on similar New Zealand produced LVL at the BRANZ facilities. This was most likely due to the double-tee configuration of the floor beams such that convection of flames and hot gases throughout the space was slightly impeded, and the nearest beam was spaced away far enough that re-radiation off this surface was not significant. It should also be noted that heat flow within the furnace was not entirely uniform across the floor unit, in that the action of pumping of the fuel into the compartment via the sides of the furnace and extracting the hot gases through the bottom at the centre of the compartment tended to induce hotter burning in the central region of the furnace. This was observed on the residual beam sections after furnace testing, as the char damage was more prevalent on the side of the beam facing the centre of the furnace. It was also reflected in the spall patterns on the underside of the concrete, as it was much more prevalent in the middle of the floor units compared with the edges. Major spalling began approximately 25 minutes into each test indicating that the plywood sheathing had completely burned through by this time, this is also apparent from Figure 4.6 and Figure 4.7 as discussed above.

The charring rate on the underside of the beams was very high, being on average four times as large as the charring rate from either side of the beams. This can be seen in the results presented in Table 4.2. This may also be partly due to the uneven heating inside the furnace and the configuration of the beams in floor units, as previously discussed, however the

difference in side and bottom charring rates was much too significant to be attributed to these factors alone. The majority of this charring most likely occurred in the latter stages of burning once the residual section had been reduced to such a size that the central area of the timber beams had increased above the initial ambient temperature, thus increasing the rate heating and burning of the remaining section. This means that slender beam members are obviously much more susceptible to structural failure earlier in fires as the core heating would be more rapid than a larger timber member. An inherent advantage of structural timber members is that much more redundancy can be designed into the members without a major increase in material costs, when compared to other structural materials such as steel and concrete. Larger beam member sizes (especially width wise) in the case of timber-concrete composite floors serve to drastically increase the expected fire resistance.

Another important observation was the separation of the double beams after significant burning, that is each beam tended to splay outwards which induced extra charring on the insides of the beam sections and exposed the connections to further fire damage (refer to Figure 4.9). This phenomenon was primarily caused by the uneven drying of the timber beams and the loss of integrity of the fixing around the fasteners holding the beams together, and would have had a greater impact on the floor performance in the latter stages of the testing when the residual section was smaller and closer to failure. On closer inspection of the beam remains, the glue lines of the timber were curved outwards, indicating that the beams were warping outwards and thus the timber was exposed to burning up through the centreline opening. This behaviour reduced the tensile strength of the beams as it reduced the neutral axis depth and also rotated the grain of the laminates, reducing the average mechanical properties of the section (as LVL exhibits its best characteristic properties parallel and not perpendicular to the laminates). The influence of the beam warping on the overall strength is questionable however, since at this stage of burning the cross section has reduced to such a degree that it is the major governing factor of the remaining fire resistance of the floors. It may be more prevalent in deeper section sizes (see Figure 4.3 and Figure 4.4), depending on the number, type and spacing of any mechanical fasteners used to hold the beams together.

The section shown in Figure 4.9 was removed at one of the notched connections. The centre of the furnace was located to the left of the beams shown here, hence the greater fire damage on this side can be seen from the figure. The average opening size was 25 mm at the bottom of the beams, measured from the tip of the shorter beam as seen on the left of the Figure. Directly above this cross section shown is the timber-concrete interface at the notch, the timber is jagged and uneven here due to the sample being pried loose from the concrete, it is not damage from the fire.

Figure 4.9: Residual Section of the 400 mm Floor After 60 minutes Exposure

Possible ways of mitigating this effect may be to change the style of fixing as discussed in Section 3.4, with the least number of fixings giving the most splaying to a completely glued beam section producing the least separation. Further research into this phenomenon is required however before any conclusions are reached.

The configuration of the concrete slab above the connections also aided in reducing the impact of the fire about the connection regions, as the concrete acted as a heat sink which preserved more residual timber about the connections and further reduced the likelihood of a connection failure. This can be seen in Figure 4.9, where the increased width at the top of the timber is visually evident from the charred remains.

A sketch of the expected charring damage on a double beam identical to those tested is shown in Figure 4.10. A charring rate of 0.72 mm/min has been used for LVL (Lane, 2005). The reason why this published value is higher than the recorded charring rate in the full scale testing (from the sides) is possibly due to the double-tee configuration of the timber beams, in that Lane tested a single LVL member in the same furnace facilities at BRANZ.

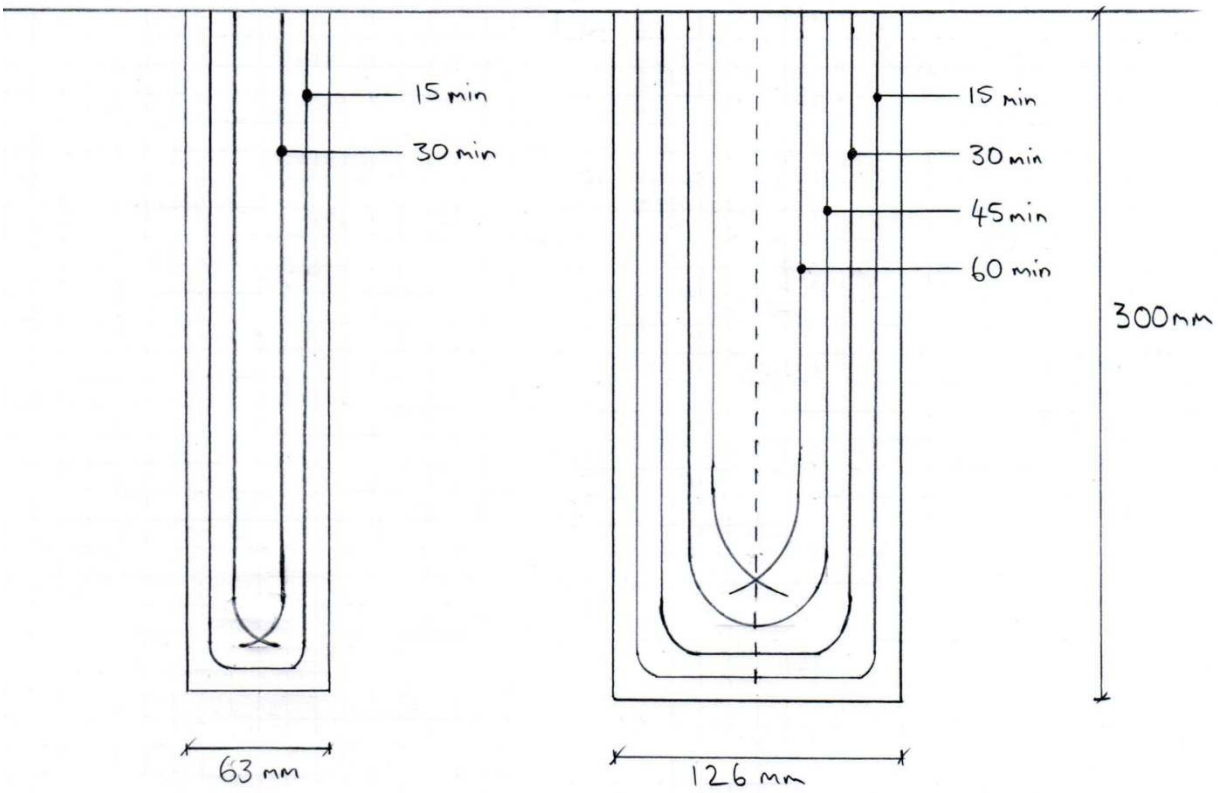

Figure 4.10: A Sketch of the Expected Charring Damage for Generic Single and Double LVL Beams

The important point to note in Figure 4.10 is that for one sided fire exposure the charring rate is approximately constant over the burning surface. However the corners of the beam are subjected to two sided exposure hence they char faster and a degree of corner rounding occurs. Generally the radius of corner rounding is approximated as equal to the char layer depth. It is when the beam becomes so thin that these radii cross over each other that the rate of charring on the underside of the member increases. This increase can be very high, accounting for the large average charring rate values on the underside of the beams seen in Table 4.1. This charring rate increase with decreasing member size has been well documented by Frangi and Fontana (2003) for solid timber beams. The comparison between charring of a single or double members is also evident from Figure 4.10, as a single unprotected joist would exhibit poor fire performance (failure in less than 30 minutes). Doubling the joists together is a simple and effective method of improving the fire resistance of any timber beam floor.

4.5 Steel Plate Temperatures

The plate connections can fail in a variety of ways, such as pull out of the teeth from the timber, shearing through the concrete, tearing across the plate, crushing of the timber or crushing of the concrete. The application of a fire to the system has the effect of heating the timber beams and making failure modes in the timber or steel much more likely as their

temperatures increase. An inherent benefit of this design of floor system is that the two beams surrounding the plates act as excellent insulation from the fire and prevent the temperature of the plates from rising rapidly. This was exhibited in the testing where a connection failure did not occur, and data recorded during the testing and observations of the charred remains showed that the timber surrounding the plates performed well in protecting them from the fire. There was no pull out of the plate teeth, no crushing of the timber and the overall temperature of both did not exceed 100 °C at 60 minutes. This can be seen in Figure 4.11 below, where the temperature curves of the plates from thermocouple readings are plotted together for both furnace tests.

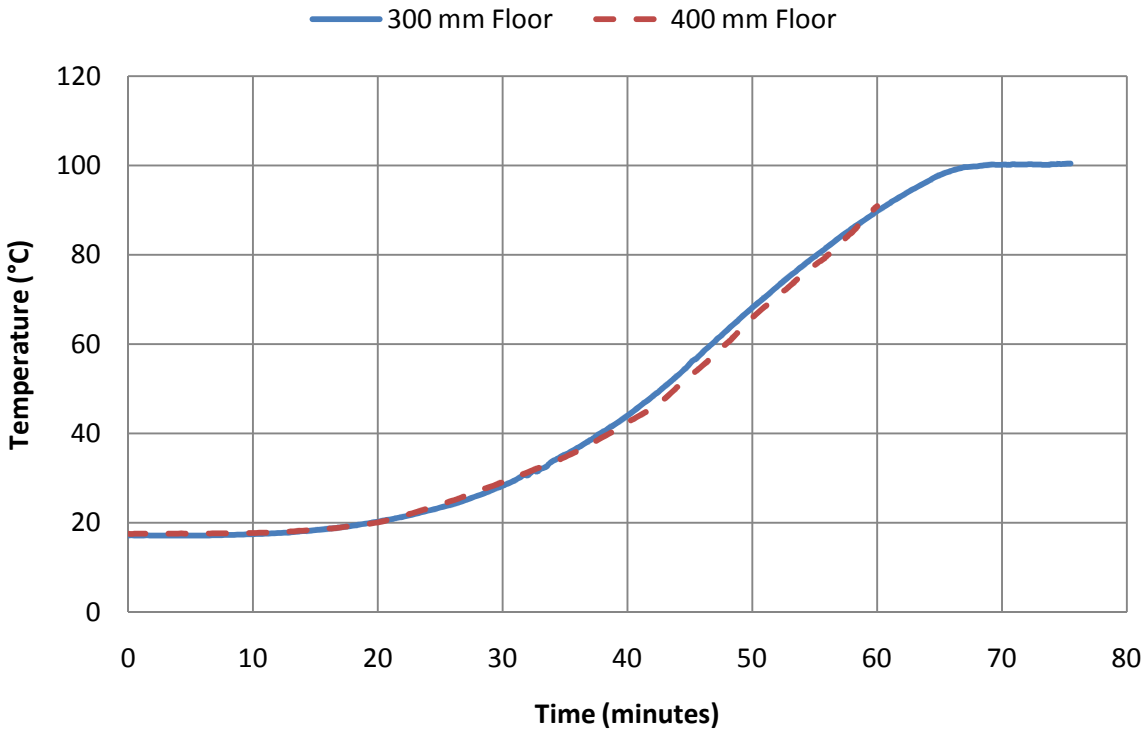

Figure 4.11: Plate Temperatures during the Furnace Tests

It should be noted however that the opening phenomenon exhibited by the double beams did expose the steel plates to hot gases and fire in the latter stages of the testing, and that further research into this is warranted to evaluate the extent to which it may contribute to a connection failure in future floor designs. This is not reflected in the results above however as the degree to which the beams separate near the plates must also be enough to allow an adequate current of heat to flow through it, and a few millimetres is generally not enough. Until the separation of the beams begins, the shallow depth that the plates are inset into the beams ensures that their heating is purely a function of the heating of the sides of the beams, and this is reflected in the relatively consistent values seen above.

5.0 Small Scale Testing

5.1 Objectives/Purpose

The objective of the small scale testing was to determine the failure strength and behaviour of the LVL at different temperatures. This was to determine whether the heating of the timber from the fire conditions would have a noticeable effect on the notched connections in the beams and cause a premature failure of the floor system.

The first failure mode of concern was a crushing failure of the timber at the timber to concrete interface in the notched connections as the timber section is heated and reduced by the fire. This would result in loss of composite action as the stiffness of the notches would decrease rapidly with the increasing displacement, eventually leading to failure in the timber beams.

The second failure mode of concern was a shear failure in the timber beam between two notch sites, causing a cascading failure throughout the beam of each connection as the extra load is transferred to them. This would effectively sever the composite beam into two parts parallel to the span of the beam, and cause a system failure as all composite action would be lost in a very short period of time.

5.2 Materials

The LVL used was supplied by the same manufacturer of the LVL for the large scale testing, and was produced from the same material as presented in Table 3.1.

Structural LVL is an engineered wood composite made from rotary peeled veneers (usually of 3 mm thickness), glued with a durable adhesive and laid up with parallel grain orientation to form long continuous sections (Buchanan, 2007). This results in low variability and thus in an extremely reliable engineering material. For general purpose LVL, the wood veneers of a higher grade cut from the better parts of the log are used on the outsides of the beams, and the lower quality veneers are used as the insides of the beams. This ensures the beam has the best possible mechanical properties while reducing any wastage of lower grade wood peels. The glue used in the Truform LVL material is a phenolic adhesive that complies with the requirements of AS/NZS 1328.1 (1998).

The species of wood used in the LVL was Radiata Pine, and although it is possible to use other species, they can pose manufacturing problems, and Pine has been proven in the past to be the most reliable and easiest to source in New Zealand.

5.3 Specimen Details

Two types of specimens were constructed to test each failure mode. The standard specification for the evaluation of structural composite lumber products (ASTM D 5456-06, 2007) refers to using the test methods in ASTM D 143-94 (2007) for assessing material

properties of LVL (and other structural composite lumber products). The first specimen was based on the guidelines in D 143-94 for testing specimens of clear wood in compression parallel to the grain.

This test was chosen as it approximately models the crushing action of the concrete on the timber interface in the beam notch.

Due to the width of the LVL being 63 mm in this case (as this is a generic beam width commonly produced), the test specimen size was scaled up by 25 % in each direction. This resulted in the 50 x 50 x 200 mm standard specimen size being converted to 63 x 63 x 250 mm for the LVL testing. Although using this size specimen was deviating from the standard test method, it was deemed to be more desirable than cutting a smaller specimen from the LVL as either a glue line or wood veneer would be sawn through, and the veneers are of varying grade from the outside to the inside as discussed in Section 5.2. This would undoubtedly provide an inaccurate representation of the beam cross section and produce questionable results.

The second specimen type for the shear testing was made solely for the purpose of checking for shear failures in the timber in this specific beam design with a notched connection, although no standard test method was applicable for this. Therefore the test specimen was designed to best simulate the actual shearing action of the beams within the limitations of the available testing loads and space, but was based on the guidelines presented in the shear parallel to grain section of ASTM D 143-94 (2007). This was a 400 mm wide and 150 mm deep T shaped block, with two 50 x 50 mm sections cut from the bottom corners to allow the composite action within the notch to be simulated on both sides of the sample, which is discussed in Section 5.4. Figure 5.1 shows the compression specimen on the top left and the large shear specimen at the bottom, and a third shear block cut to the exact specifications of the standard which was not tested at the time due to a lack of appropriate testing apparatus and time restraints.

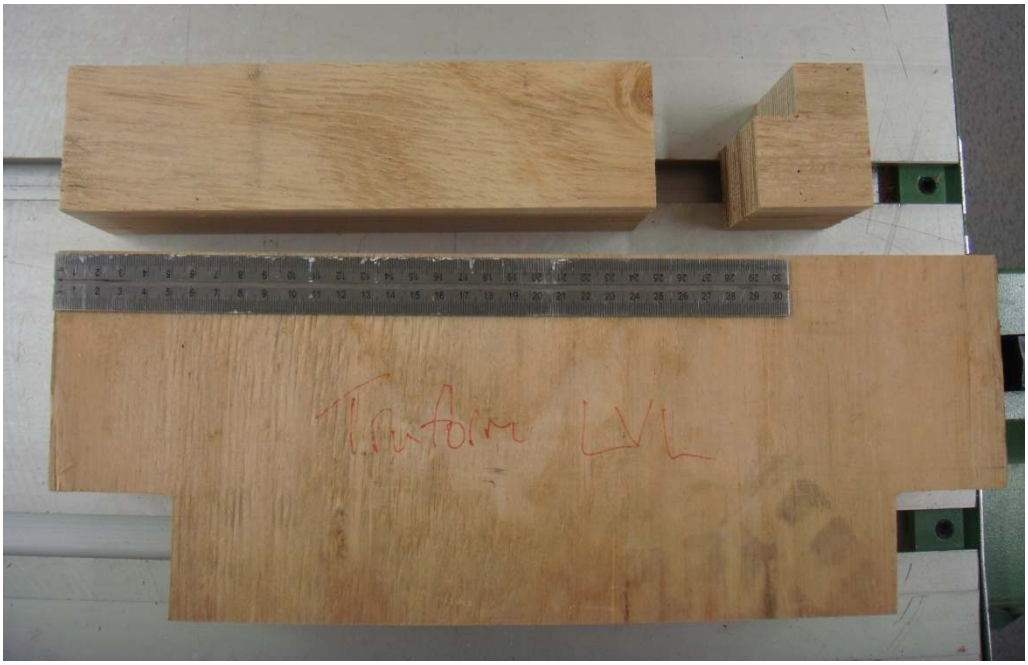

Figure 5.1: The Compression and Shear Specimens for Small Scale Testing

The test specimens were prepared in a wood workshop using a large circular table saw, a drop saw and a band saw. Care was taken to ensure each specimen was cut to the same size and that the cut surfaces were level and smooth. This was important for the compression blocks to have a flat loading surface but paramount for the shear blocks, as they needed to be supported on completely level surfaces or this could induce stress concentrations in the inside corners and force an early failure of the specimen. It is likely that some of the variability seen in the results may be attributed to the specimen construction.

5.4 Experimental Procedure

An Instron test frame was used to apply the loads required and ensure a stable testing assembly for the duration of the testing. The Instron could apply up to 250 kN of force onto a specimen situated on the level testing surface. Due to the previous intended use for the machine, the fixed loading rates increased in increments of 0.5 mm/minute although the calculated loading rates for compression and shearing tests were 0.75 and 0.60 mm/minute respectively (ASTM D 143-94, 2007). As per the requirements of the standard, the loading head was equipped with a spherical bearing to allow uniform distribution of load across the timber surface. The test apparatus with a shear specimen in place is shown in Figure 5.2.

Figure 5.2: The Instron Testing Apparatus and Datalogging Equipment

As seen in Figure 5.2, steel blocks were used as supports and spreaders across the shear test specimens. Small nails were implanted into the compression specimens at a gauge length of 200 mm and potentiometers attached to measure the displacement during testing and output a load-slip curve, allowing the stiffness of the specimens to be calculated. Although the Instron had a potentiometer on the ram, the results recorded from this potentiometer were not used as the timber specimens exhibited a slight amount of crushing as the load was initially applied, hence skewing the displacement readings from the ram potentiometer. The potentiometer setup for the compression testing is shown in Figure 5.3.

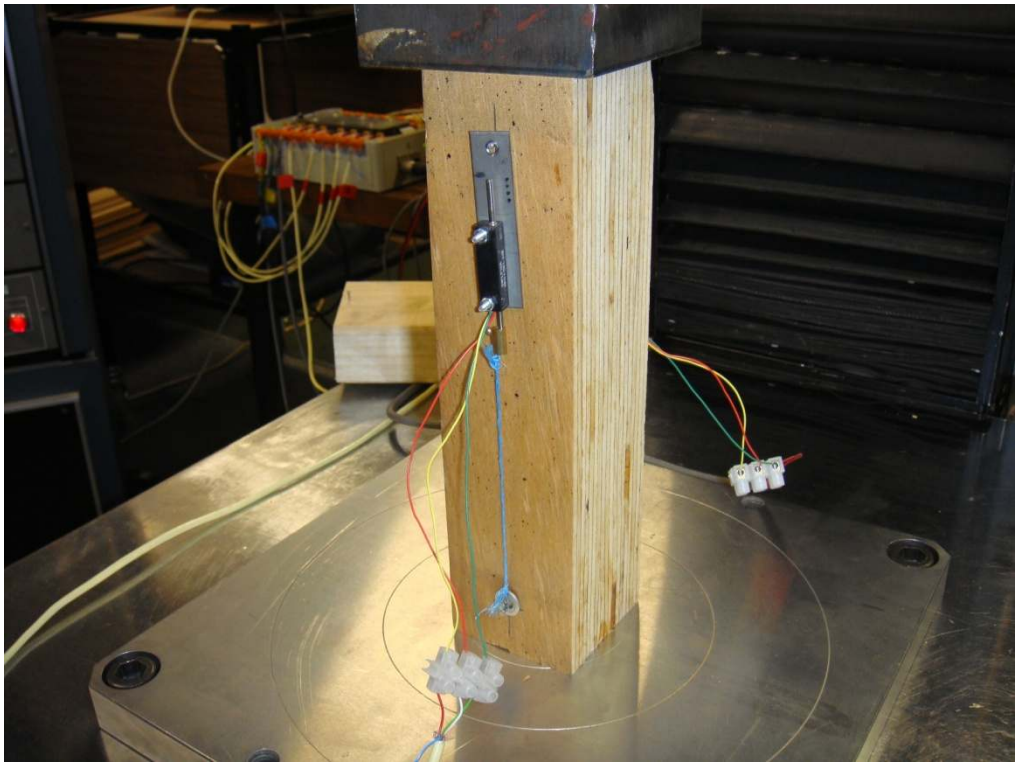

Figure 5.3: A Compression Specimen Ready to Test

Before testing, all test specimens were kept in a standard climate chamber for over a month to allow the timber to reach a moisture content of approximately 12 %.

The specimens were tested at temperatures of 20, 50, 100, 150 and 200 °C. This was due to the fact that at a temperature of about 200 °C wood begins to undergo rapid thermal decomposition (Frangi and Fontana, 1998), and previous attempts at temperatures higher than this had resulted in eventual combustion in the ovens. Each heated specimen was left in a pre-heated oven for a minimum of 4 hours, and due to the number of tests involved at each temperature some specimens were left in the oven for 8 hours before testing. A test specimen with a thermocouple embedded in the centre was heated in the oven at several different temperatures including 200 °C, and it was found the centre of the specimen was at the required temperature after 1.5 hours at the most. However to account for uneven oven temperatures and to be sure of even temperature distribution through the large centres of the shear blocks the specimens were left in the oven to heat for much longer.

It should be noted that during the testing process small amounts of heat would have been lost from the specimens in the time it took to transport and set up the specimens in the test apparatus. However, the cooling effect was minimised due to a short travel distance from oven to test apparatus and each specimen was wrapped in a heat resistant blanket and handled with insulated gloves during transportation and before testing.

As a check to determine the overall effect of moisture content on the timber, a small number of compression test specimens were completely dried in an oven for over a week at

102 °C to ensure they were completely dry. These were then tested at 20 and 50 °C in the same manner as those taken directly from the climate chamber to the ovens without pre-drying. These results are presented in Table 5.1. Immediately before testing a digital vernier caliper was used to measure the exact end dimensions of each specimen. These results can be found in Appendix F: Small Scale Test Specimen Dimensions.

The determination of the moisture content of some select samples of wood was carried out in accordance with ASTM D 143-94 (2007). The purpose of this was to check whether the timber specimens had been left for an adequate amount of time in the climate chamber to reach approximately 12 % moisture content, and also to check the moisture content of the specimens after heating in the oven at temperatures below 100 °C. To achieve this, the wood samples were cut from a selection of specimens both from the ovens and from the climate chamber, sized approximately 63 x 63 x 50 mm (larger slices for the shear blocks) and weighed immediately. These samples were then put in an oven for 3 days at 102 °C to drive out the moisture. The loss in mass as a percent of the oven dry mass was then calculated for each specimen. These results can be found in Section 5.5.

5.5 Results

In total, 23 compression tests and 20 shear tests were conducted at varying temperatures. The maximum values obtained during the compression testing are shown in Table 5.1.

Table 5.1: Compression Test Results

Temperature (°C)	Moisture Content (%)	Maximum Recorded Loads (kN)	Average Value (kN)
20	10.4	149, 150, 150, 151, 152, 153, 163	152
20 (Dried)	0	204, 226	215
50	10.1	138, 142, 145	142
50 (Dried)	0	202, 203, 203	203
100	N/A	122, 125, 130	126
150	N/A	130, 153, 154	146
200	N/A	173, 174, 175	174

The general trend seen in the compression testing was that of a "V" shaped strength curve as shown in Figure 5.4. As the wood specimens were heated towards 100 °C, their ductility increased with the presence of moisture and softening from elevated temperatures, thereby lowering the strength of the specimens. Once the specimens were heated beyond 100 °C however their strength began to increase as the moisture was completely driven off and the wood hardened under higher temperatures. As previously discussed, as the temperature

increased above 200 °C the wood would begin to thermally degrade and pyrolyse, hence testing was not undertaken beyond this point.

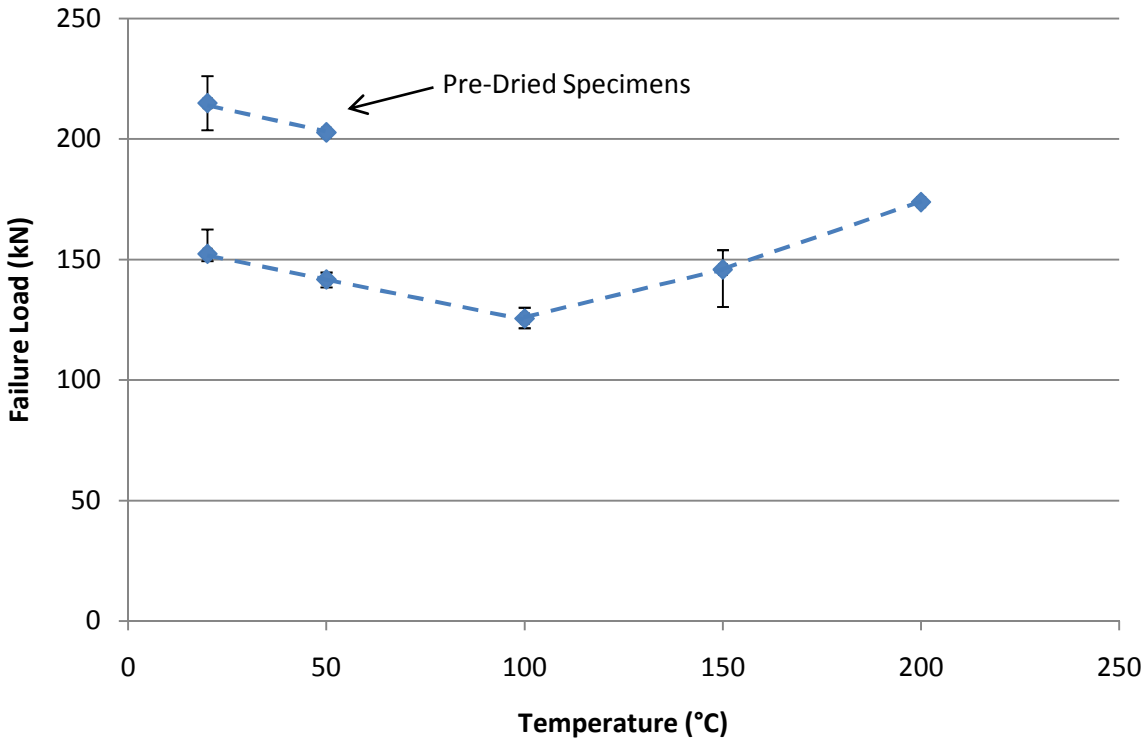

Figure 5.4: Compression Test Results Showing the Spread of Values Obtained

The two sets of higher valued data at 20 and 50 °C are the results for the pre-dried specimens. Due to the absence of moisture these recorded strength values were found to be much higher than the other wood specimens, as increasing moisture content serves to decrease the strength of clear wood specimens parallel to the grain (Green et al., 1999). Since LVL is similar to clear wood (devoid of defects), it was intuitively expected that this behaviour would be the same. These values still followed the "V" shaped strength curve, decreasing in strength towards 100 °C as the wood softened. Compression strength after 100 °C is commonly assumed to be a linear decay to zero strength at 300 °C, such as that derived by Konig and Walleij (2000), however in this instance it is clearly not the case. A lack of reported test results for these types of tests on wood at elevated temperatures has led to this assumption being generally accepted as reasonable among the international community, and further research is required on different types of wood and wood products to verify the results found in these tests and allow the validity of this approximation to be confirmed. The major failure types seen during the testing support the above results obtained. At lower temperatures the full compression strength was able to be achieved such that a crushing/yielding failure occurred in many of the specimens, as seen in Figure 5.5. However as the plasticity of the wood increased with increasing temperature to 100 °C early crushing failures became more common, an example of which is shown in Figure 5.6.

Figure 5.5: Typical Compression Specimen Tested at 20 °C (Note the angular shear plane)

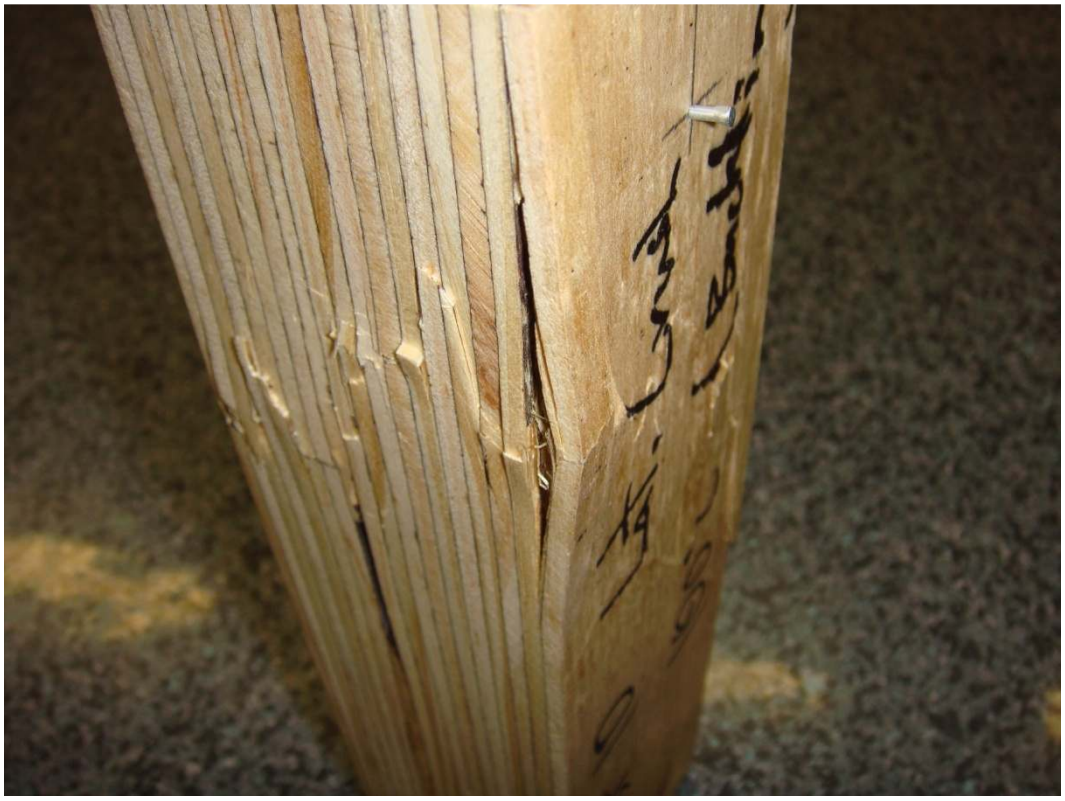

Figure 5.6: Typical Compression Specimen Tested at 100 °C (Note the localised crushing of individual veneers)

The pre-dried specimens and specimens heated over 100 °C exhibited extremely brittle failure behaviour, as the absence of any moisture ensured the failure mode be dictated by the propagation of a crack through the specimen, as seen in Figure 5.7. The fracture plane passed through a veneer, and was not down a glue line.

Figure 5.7: Compression Specimen Tested at 50 °C (Pre-dried)

The same "V" shaped strength pattern was reproduced by the values for the modulus of elasticity. This was calculated using the measurements recorded by the potentiometers attached to the sides of the specimens. Table 5.2 gives the average values calculated for each temperature, and a full table of the exact results can be found in Appendix H: Small Scale Testing Modulus of Elasticity Calculations.

Table 5.2: Calculated Average Modulus of Elasticity Results

Temperature (°C)	20	20 (Dried)	50	50 (Dried)	100	150	200
Average E (GPa)	11.7	12.9	9.8	12.0	8.0	9.9	12.5

The modulus of elasticity was calculated over the elastic region for each test which was approximately 95 % of the maximum load obtained during testing. The displacement from rest was recorded in the datalogger with a sampling rate of 5 times per second, enabling the corresponding change in length of the specimen to be found in the datafile for each

specimen. Since the end dimensions and gauge length were also known for each specimen, this allowed E to be calculated. Figure 5.8 shows the reproduction of the trend seen in the compression testing, with the drier specimens exhibiting much stiffer behaviour and more brittle failure modes.

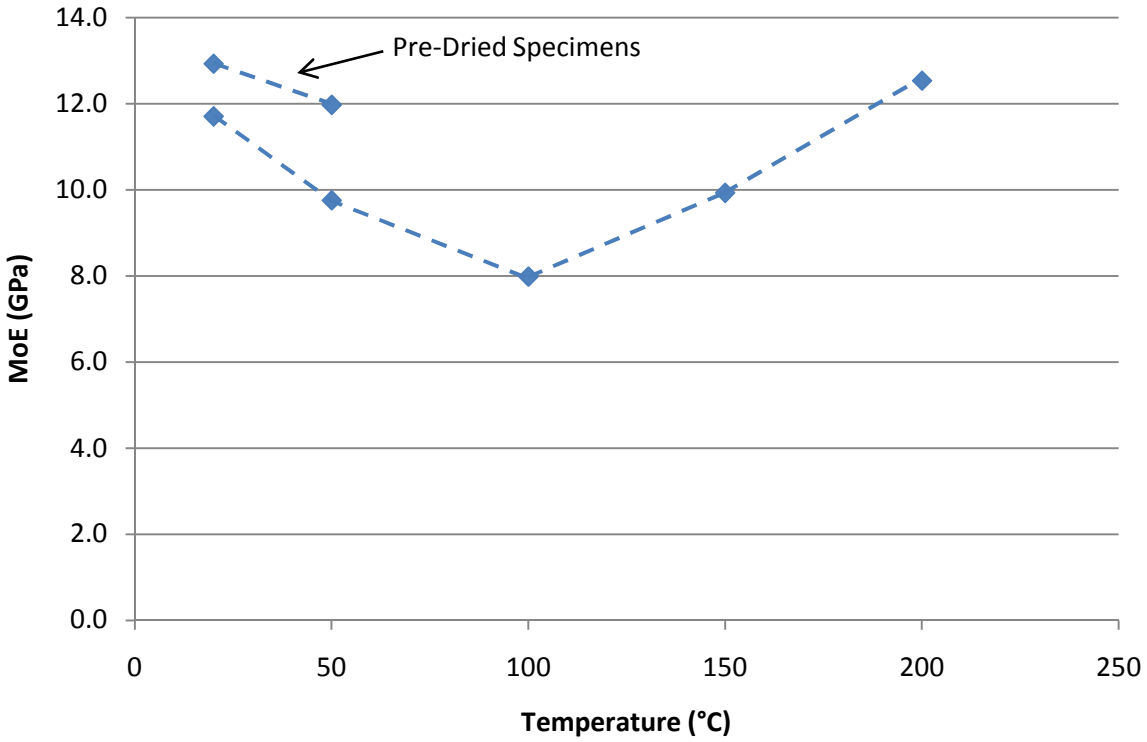

Figure 5.8: Plotted Average Modulus of Elasticity Results

The maximum values obtained in the shear testing are shown in Table 5.3. It can be seen from the results that relatively consistent values were obtained throughout most of the temperature range tested. However, the tests conducted for the temperature of 20 and 150 °C produced a large amount of variance. As discussed in Section 5.3, this may be attributed to the specimen construction in that extremely precise craftsmanship is required when preparing such large specimens, and uneven cuts can induce premature failure for these types of test. This variance can also be seen in graphical form in Figure 5.9.

Table 5.3: Shear Test Results

Temperature (°C)	Maximum Recorded Loads (kN)	Average Value (kN)
20	60, 68, 71, 78, 83, 84, 98	78
50	68, 74, 82	65
100	59, 61, 65	61
150	38, 49, 68, 73	57
200	55, 56, 57	56

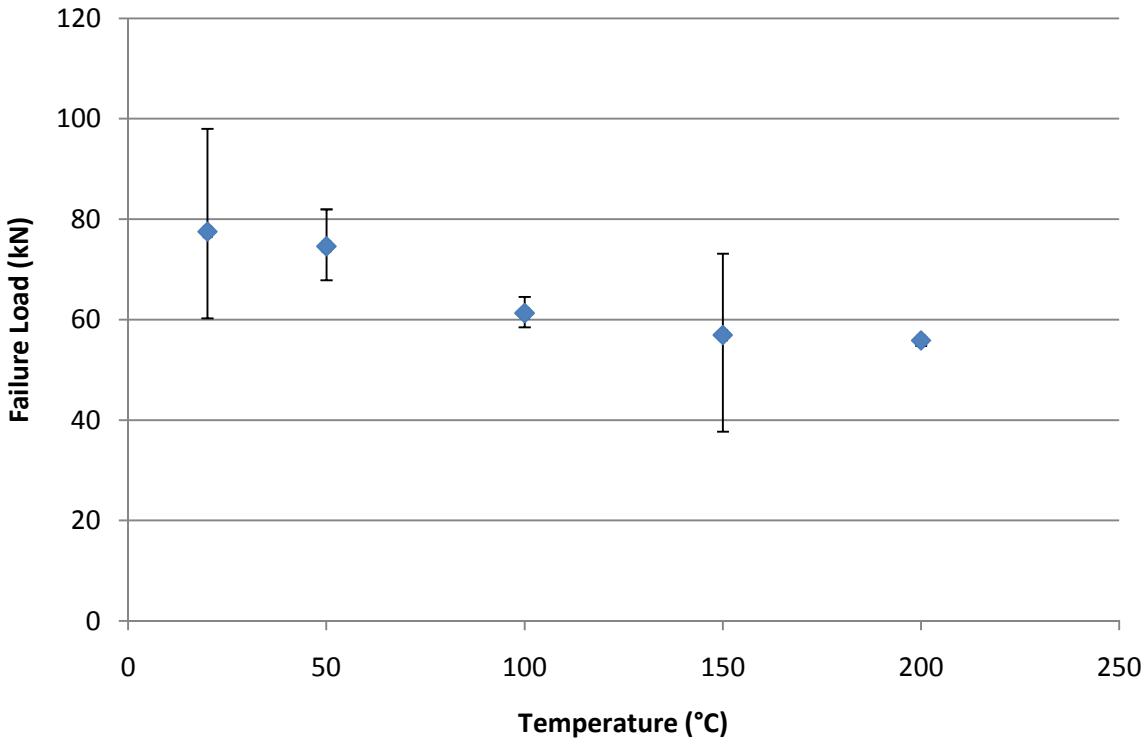

Figure 5.9: Shear Test Results Showing the Spread of Values Obtained

It can be seen from the results that a relatively steady decay trend is followed, with the shear strength of the specimens at 200 °C being roughly 75 % of the value of the specimens tested at 20 °C. Due to the large margin of error seen in some of these results, further research into improving the test method and conducting additional experiments is warranted before any conclusive arguments to the exact behaviour can be made. For the purposes of this research however the level of detail provided by these results was adequate, as it allowed an approximate idea of the effects of heat on this particular type of shear failure to be gained.

The failure mode was forced at either side of the specimen near the supports due to the nature of the test setup. Failure was always brittle, and an example of a broken specimen is shown in Figure 5.10.

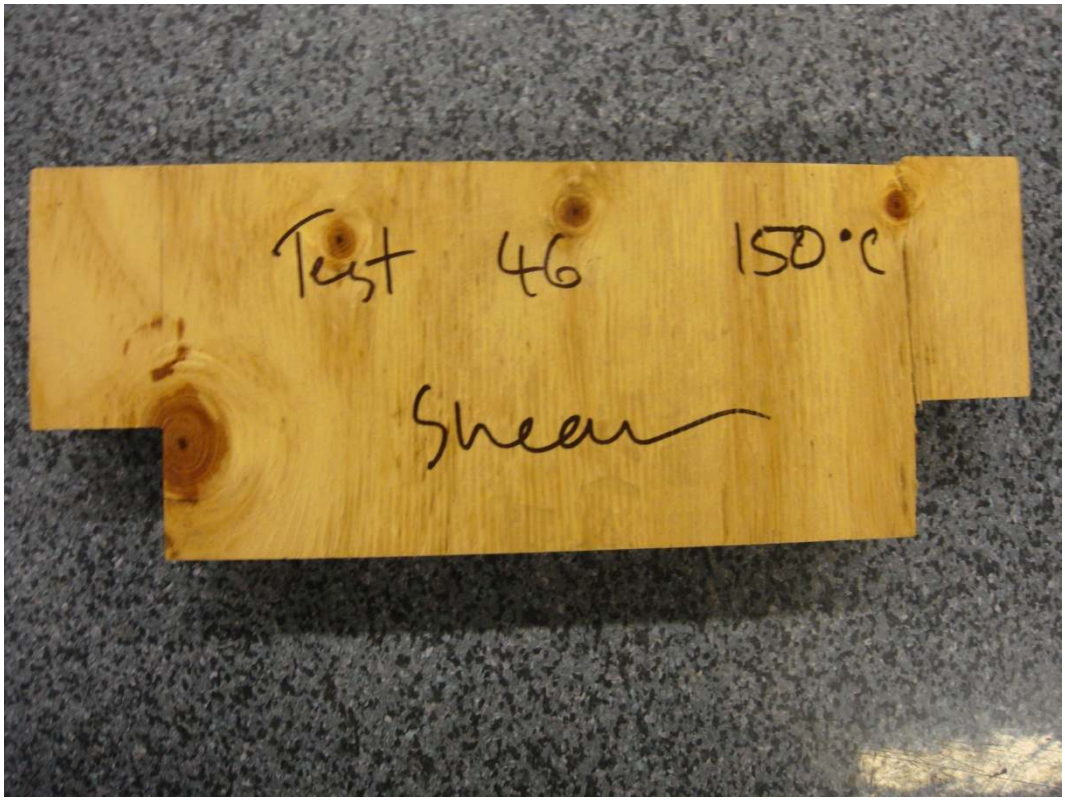

Figure 5.10: Shear Specimen Tested at 150 °C with Failure on the Right of the Picture

The full set of load displacement curves for each compression and shear test can be found in Appendix G: Small Scale Testing Load Displacement Measurements.

Due to the burning characteristics of the timber and the insulative properties of the char layer, the effects of reduced timber material properties due to elevated temperature in both shear and compression parallel to the grain had a very small impact on the overall performance of the floor units. This was shown by the very small residual section left behind in the full scale testing and the mode of failure, in that if reduced section properties were significant the floors would have failed at an earlier stage by shear or crushing at the connections in the timber beams.

It is important to note that in these small scale tests the entire section was heated through while simulating beam behaviour, and in the case of a real fire the temperature gradient across the section would be vastly different and most definitely not uniform. This emphasises the fact that reduced section properties are important to consider for smaller, more slender members than large heavy timber members. The behaviour of wood in fires is such that only a small heated layer of approximately 35 mm is affected by a fire below the char layer (Buchanan, 2002), and beyond this the temperature of the wood is at ambient conditions. This effectively nullifies the importance of reduced section properties of heat affected timber for these composite floors until the member section is so small that collapse is imminent due to the reduced cross sectional area of the timber members alone. This was found to be the case in the full scale testing, however it must be noted that the notch

connection spacings were designed beforehand with these types of failure in mind. A poor composite beam design with a small number of connectors spaced very closely together will undoubtedly reduce the shear capacity of the timber between the connections in the beam, and increase the effect reduced section properties have on the collapse behaviour of the floor, most likely making the reductions in mechanical properties of the timber shown above much more significant.

The effect of reduced timber properties would also be more significant in cases of direct heating to the timber members in the absence of a fire, such as hot pipes or mechanical devices directly impinging on the members and heating the wood. However, this situation is unlikely as this type of activity should not go unnoticed by building occupants and would not be allowed by inspections during building construction.

Although it was not studied as part of this research, reduced tensile strength due to elevated temperature may also have a significant impact on the fire performance of timber-concrete composite floors. A number of researchers testing the tensile strength of wood parallel to the grain at elevated temperatures have found a trend of decreasing strength with increasing temperature (Buchanan, 2002). Due to the nature of timber-concrete composite floors utilising the timber section mainly in tension and the concrete slab mainly in compression, the likelihood of a tensile failure of the timber in these floors in a fire may be much more significant than for traditional timber floors, and further investigation into the tensile strength of LVL at elevated temperatures is warranted.

With the above points in mind, in fire conditions the structural integrity of the large timber members used in these floors are not governed by reduced timber properties but rather by the reduced section size of the member and by other effects such as increased charring rates and beam splaying.

6.0 Spreadsheet Analysis

6.1 Background

As part of the work undertaken by Yeoh (2009) at the University of Canterbury, a spreadsheet design tool was developed to analyse the behaviour of the semi-prefabricated composite floor system in terms of short and long term loading. This analysis however was lacking in the ability to evaluate the floors in fire conditions, and a simple yet robust spreadsheet tool was required to perform this task as an addition to the current research. The design tool developed during this research was aimed to meet these requirements, but also to be useable as a standalone tool for estimating expected fire resistance of the composite floor system.

The spreadsheet design tool has been developed as a tool to aid in the understanding of how certain timber-concrete composite systems can perform in fires, and to provide a fast method of estimating the expected fire resistance time of a floor under user defined load conditions and floor geometries. The calculation methods used in the spreadsheet are discussed in detail in Section 6.2, and a view of the layout is shown in Appendix J: Spreadsheet Design.

6.2 Development and Calibration

The design equations used for evaluating the strength of the composite floor in the spreadsheet was based on the method presented in Chapter 25 of the Timber Design Guide (Buchanan, 2007). Due to the modular nature of the semi-prefabricated system, the most likely method of construction is to be craned in place and simply supported for their lifetime, hence the spreadsheet currently only takes into account a simply-supported floor. However, as the spreadsheet has been written to be relatively user friendly, modifications to allow the evaluation of different forms of support conditions can be easily made without a breakdown of the spreadsheet coding. Provided that all floor dimensions, material properties and connection properties are known, the major design method used to calculate the strength of the composite floors is as follows:

The load combinations for the floor system under fire are calculated in accordance with AS/NZS 1170 (2002) for fire conditions:

$$w = 1.0G + 0.4Q$$

Where:

w	=	ultimate limit state load (kN/m)
G	=	sum of the superimposed dead load and the self weight of the floor (kN/m)
Q	=	live load (kN/m)

The design bending moment at midspan, shear force at the supports and shear force at the span/4 from the supports are then calculated:

$$M^* = \frac{wL^2}{8}$$

$$V^* = \frac{wL}{2}$$

$$V^*_{L/4} = \frac{wL}{4}$$

Where:
- M^* = design bending moment at midspan (kNm)
- V^* = design shear force at the supports (kN)
- $V^*_{L/4}$ = design shear force at L/4 from the supports (kN)
- L = span of the floor (m)

The timber strength capacity at midspan is also found for tension and bending:

$$\phi N_R = \phi k_1 k_8 f_t A_t$$

$$\phi M_R = \phi k_1 k_4 k_5 k_8 f_b Z$$

Where:
- ϕ = strength reduction factor
- N_R = timber tensile strength parallel to grain (kN)
- M_R = timber bending strength (kNm)
- k_1 = load duration factor
- k_4 = parallel support factor
- k_5 = grid system factor
- k_8 = stability factor
- f_t = characteristic tensile strength of the timber (MPa)
- A_t = area of the timber section (mm^2)
- f_b = characteristic bending strength of the timber (MPa)
- Z = section modulus of the timber section (mm^3)

The effective flexural stiffness of the composite is evaluated by first calculating the concrete gamma coefficient (Eurocode 5, 1995) to calculate the slip between the composites:

$$\gamma_c = \frac{1}{1 + \frac{\pi^2 E_c A_c s_{ef}}{K_{SLS} L^2}}$$

Where:
- γ_c = concrete gamma coefficient
- E_c = modulus of elasticity of the concrete (MPa)
- A_c = tributary area of the concrete slab (mm^2)

s_{ef} = effective spacing of the connections (mm)
K_{SLS} = connection stiffness for serviceability limit state (kN)

Calculating the a_c and a_t distances:

$$a_c = \frac{E_t A_t H}{\gamma_c E_c A_c + E_t A_t}$$

$$a_t = H - a_c$$

Where:
a_c = lever arm between compression force and neutral axis (mm)
E_t = modulus of elasticity of the timber (MPa)
H = distance between the force couple (mm)
a_t = lever arm between tension force and neutral axis (mm)

And finding the effective flexural stiffness:

$$(EI)_{ef} = E_c I_c + E_t I_t + \gamma_c E_c A_c a_c^2 + E_t A_t a_t^2$$

Where:
$(EI)_{ef}$ = effective flexural stiffness (Nmm^2)
I_c = second moment of area of the concrete slab (mm^4)
I_t = second moment of area of the timber section (mm^4)

The timber stress due to the axial force can now be calculated:

$$\sigma_t = \frac{E_t a_t M^*}{(EI)_{ef}}$$

Where:
σ_t = timber stress due to the axial force (MPa)

Calculating the timber axial force, and the timber bending moment:

$$N_t^* = \sigma_t A_t$$

$$M_t^* = \frac{E_t I_t M^*}{(EI)_{ef}}$$

Where:
N_t^* = timber axial force (kN)
M_t^* = timber bending moment (kNm)

The combined bending and tension ratio of the composite floor can now be found:

$$\frac{N_t^*}{\phi N_R} + \frac{M_t^*}{\phi M_R} < 1.0$$

The floor is considered to fail once this ratio exceeds 1.0, in that the strength demand has exceeded the strength capacity.

To evaluate the shear strength of the floors, the timber design shear strength can be found:

$$\phi V_s = \phi k_1 k_8 f_s \frac{2A_t}{3}$$

Where: V_s = timber shear strength (kN)
f_s = characteristic shear strength of the timber (MPa)

If the design shear force at the supports exceeds the design strength, the floor is considered to fail in shear:

$$\phi V_s > V^*$$

The connection profile used in the spreadsheet is a 300 mm long by 50 mm deep connection with an incorporated 16 mm coach screw implanted in the centre. From previous work conducted at the University of Canterbury on the shear strength of connection types, the ultimate limit state and serviceability limit state strength and stiffness of this notch type has been found, therefore the design connection strength can be found.

$$\phi Q_d = \phi k_1 Q_K$$

Where: Q_d = design connection strength (kN)
Q_K = ultimate limit state connection strength (kN)

The shear force in the connection at maximum shear, and at the span/4 from the supports is then calculated:

$$F_{max} = \frac{\gamma_c E_c A_c a_c s_{min}}{(EI)_{ef}} V_{max}$$

$$F_{L/4} = \frac{\gamma_c E_c A_c a_c s_{max}}{(EI)_{ef}} V_{L/4}$$

Where: F_{max} = shear force in the connection at maximum shear (kN)
$F_{L/4}$ = shear force in the connection at L/4 from the supports (kN)
s_{min} = minimum spacing of the connections (mm)
s_{max} = maximum spacing of the connections (mm)

A failure in the connection is assumed to occur when the shear forces exceed the design shear strength:

$$\phi Q_d > F_{max}$$

$$\phi Q_d > F_{L/4}$$

It should be noted that strength reduction factors for the connection design strength and for the other strength evaluations are different. These can also change depending on the situation, as in fire conditions the strength reduction factor is specified by NZS 3603 (1993) as 1.0 for shear and bending, whereas it would be 0.9 for LVL in normal conditions.

To incorporate the effects of fire conditions into the spreadsheet the major portion of the calculations are set to run in a quasi steady state analysis. That is, the mechanical properties of the floor are evaluated iteratively over a number of equal time intervals (in this case each minute) during which time the effects of the fire reduce the residual beam size based on an initial charring rate and subsequent charring relationship. This relationship was derived from that recorded during the full scale testing to incorporate the effects of increased beam bottom surface charring during the latter stages of burning (as discussed in Section 4.4). The default charring rate is set at 0.55 mm/min, which was recorded during the large scale tests, and this is increased by a specified factor once the beam width reduces past a lower limit of 31 mm beam thickness remaining per side (62 mm thickness total). As previously mentioned, the spreadsheet has been calibrated via these factors to output the expected fire resistance time and subsequent residual beam size for any floor dimension, based on the results of the two floor units tested in the full scale testing. Similar calculation methods for a single iteration of the spreadsheet are demonstrated in the Fire Engineering Design Guide (Buchanan, 2001), and Structural Design for Fire Safety (Buchanan, 2002).

To enable the steady state analysis to run instantaneously after all desired inputs were entered, a macro was written to run the calculations for a set number of timesteps (currently set at a default of 120 minutes) and to output the desired result of expected fire resistance time. This macro reviews the four failure criteria outlined above at each timestep, and outputs the time of first failure of any of these criteria to a specified cell at the beginning of the worksheet. The macro has been linked to a button at the start of the worksheet to ensure ease of use.

As found in Section 5.0, reduced section properties were not found to have much effect on the timber material and were not included in the spreadsheet calculations. It should be noted that some failure modes are not considered in the spreadsheet analysis, such as a bearing failure, because in fire conditions it was assumed that a this failure mode would not be critical due to the concrete slab reinforcement being tied into the supporting structure and adequate protection of the connections will be present. The floors are only checked for ultimate limit state in the short term as a fire event is short term, and the main focus is to determine whether structural failure will occur, hence service loadings do not apply.

In addition to the above analysis of the floor systems in fire, a preliminary cold design check with a revised load combination and set of load factors is also included at the beginning of the analysis to ensure the floor design will be acceptable in general conditions.

6.3 Spreadsheet Calculations

Table 6.1, Table 6.2 and Table 6.3 show the expected fire resistance time outputs of the spreadsheet design tool, encompassing a variety of load combinations, member spans and section sizes. Note that all sections are based on the double LVL "M Panel" configuration, and denote two beams of the specified size. These are all designed with four notched connections per beam, spaced a minimum of 650 mm from the beam ends and nominally throughout the length of the beam.

Table 6.1: Fire Resistance-Span Table for SDL = 0.5kPa, Q = 1.5 kPa

Fire Resistance Time (min) SDL = 0.5 kPa, Q = 1.5 kPa									
Beam Dimensions (mm)	**Span (m)**								
	4	**5**	**6**	**7**	**8**	**9**	**10**	**11**	**12**
200x45x2	40	38	-	-	-	-	-	-	-
240x45x2	44	42	-	-	-	-	-	-	-
300x45x2	49	47	41	-	-	-	-	-	-
360x45x2	-	51	45	41	-	-	-	-	-
400x45x2	-	-	48	44	40	36	-	-	-
450x45x2	-	-	-	47	43	40	37	-	-
600x45x2	-	-	-	-	53	49	46	44	41
200x63x2	71	69	64	-	-	-	-	-	-
240x63x2	75	73	67	-	-	-	-	-	-
300x63x2	80	78	72	67	-	-	-	-	-
360x63x2	-	83	77	72	68	-	-	-	-
400x63x2	-	-	80	75	71	68	-	-	-
450x63x2	-	-	-	79	75	71	68	-	-
600x63x2	-	-	-	-	84	81	78	75	72
200x90x2	117	115	110	-	-	-	-	-	-
240x90x2	120+	119	114	-	-	-	-	-	-
300x90x2	120+	120+	119	114	110	-	-	-	-
360x90x2	-	120+	120+	119	115	111	-	-	-
400x90x2	-	-	120+	120+	118	115	111	-	-
450x90x2	-	-	-	120+	120+	118	115	112	-
600x90x2	-	-	-	-	120+	120+	120+	120+	120+

Table 6.2: Fire Resistance-Span Table for SDL = 0.5kPa, Q = 2.0 kPa

Fire Resistance Time (min) SDL = 0.5 kPa, Q = 2.0 kPa									
Beam Dimensions (mm)	**Span (m)**								
	4	**5**	**6**	**7**	**8**	**9**	**10**	**11**	**12**
200x45x2	39	37	-	-	-	-	-	-	-
240x45x2	43	41	-	-	-	-	-	-	-
300x45x2	48	46	39	-	-	-	-	-	-
360x45x2	-	50	44	40	-	-	-	-	-
400x45x2	-	-	47	43	39	-	-	-	-
450x45x2	-	-	-	46	42	39		-	-
600x45x2	-	-	-	-	52	48	45	42	39
200x63x2	70	68	62	-	-	-	-	-	-
240x63x2	74	72	66	-	-	-	-	-	-
300x63x2	80	77	71	66	-	-	-	-	-
360x63x2	-	81	76	71	67	-	-	-	-
400x63x2	-	-	79	74	70	67	-	-	-
450x63x2	-	-	-	78	74	70	67	-	-
600x63x2	-	-	-	-	84	80	77	74	71
200x90x2	116	115	109	-	-	-	-	-	-
240x90x2	120+	119	112	-	-	-	-	-	-
300x90x2	120+	120+	118	113	-	-	-	-	-
360x90x2	-	120+	120+	118	114	-	-	-	-
400x90x2	-	-	120+	120+	117	114	-	-	-
450x90x2	-	-	-	120+	120+	117	114	-	-
600x90x2	-	-	-	-	120+	120+	120+	120+	118

Computing the results for the actual tested floors with live loads of 2.5 kPa and no superimposed dead loads, the spreadsheet design tool gives 79 minutes for the 300 mm deep floor and 76 minutes for the 400 mm deep floor. Comparing these results with the furnace test results, the 300 mm floor tested to destruction lasted 75 minutes and the 400 mm floor lasted over 60 minutes without failure (and with considerable cross sectional area remaining) before it was removed from the furnace. This shows a relatively good correlation between the actual test results and spreadsheet outputs, however more tests are warranted to improve the accuracy and reliability of the numbers obtained from the spreadsheet at this stage.

Table 6.3: Fire Resistance-Span Table for SDL = 1.0kPa, Q = 3.0 kPa

Fire Resistance Time (min) SDL = 1.0 kPa, Q = 3.0 kPa									
Beam Dimensions (mm)	**Span (m)**								
	4	**5**	**6**	**7**	**8**	**9**	**10**	**11**	**12**
200x45x2	37	-	-	-	-	-	-	-	-
240x45x2	40	36	-	-	-	-	-	-	-
300x45x2	46	41	35	-	-	-	-	-	-
360x45x2	51	45	40	-	-	-	-	-	-
400x45x2	-	48	43	39	-	-	-	-	-
450x45x2	-	-	47	42	-	-	-	-	-
600x45x2	-	-	-	52	48	45	-	-	-
200x63x2	68	64	-	-	-	-	-	-	-
240x63x2	72	67	-	-	-	-	-	-	-
300x63x2	77	72	67	-	-	-	-	-	-
360x63x2	82	77	72	-	-	-	-	-	-
400x63x2	-	80	75	70	-	-	-	-	-
450x63x2	-	-	78	74	70	-	-	-	-
600x63x2	-	-	-	83	80	76	-	-	-
200x90x2	114	111	-	-	-	-	-	-	-
240x90x2	118	114	-	-	-	-	-	-	-
300x90x2	120+	119	114	-	-	-	-	-	-
360x90x2	120+	120+	119	-	-	-	-	-	-
400x90x2	-	120+	120+	117	-	-	-	-	-
450x90x2	-	-	120+	120+	117	-	-	-	-
600x90x2	-	-	-	120+	120+	120+	-	-	-

The numbers presented in these tables are the result of the analysis and calibration based on theoretical formulae and a small number of full scale tests, and therefore they are only an estimation of what may be expected from such systems. It is extremely important that the user understands the many other factors which should be considered when designing for fire safety, such as the intended use of the space, the design fire appropriate to the space and evacuation considerations for occupants. This research has been primarily focussed on determining the structural fire performance of timber-concrete composite floors, however the design fire and furnace conditions used to represent an actual fire may not be severe enough to encompass every possible fire situation in the real world. It should be understood that the numbers presented here may be underestimating or overestimating the actual fire resistance time of these floor systems in different situations.

Furthermore, no reduction factors have been applied to the above tables. However, it is recommended that a reduction factor of 0.9 is used for all beams less than 63 mm wide (126 mm combined double beam width) or less than 300 mm deep. This is to account for the small sized member sections, as with a reduced section size and hence burning time, the fire resistance becomes more difficult to predict and factors such as beam opening, defects and construction errors all have a greater impact on the overall floor performance in fire.

Only one notched connection type has been tested and therefore used to produce the above tables. As previously discussed in Section 6.2, this can be easily modified in the spreadsheet to incorporate a range of notch dimensions and properties, however the resistance times in the tables are based on this notch alone. It was chosen as it is an optimised version of a number of connection types tested in previous research by Yeoh (2009), and represents an ideal standard notch size for these floors. It should be emphasised that care must be taken to ensure the floor units are properly designed in terms of the number and spacing of connections to allow the full strength of the floors to be developed and the above tables to be interpreted in their proper context.

6.4 Other Considerations

These calculations are also representative of fully unprotected floor systems, and as such any means of fire protection applied to the system, whether active or passive, will increase the expected fire resistance of the system in a fire.

It should be noted that due to the combustible nature of timber materials, it is a requirement that after the fire event the timber members are completely doused and the fire put out. Timber members will continue to burn and char after a fire if adequate oxygen is present, and if not put out this slow burning may cause the collapse of a floor system or other structure that was otherwise still standing after all other fuel sources in the room have been consumed by a fire. This should be kept in mind when considering the above tables, in that it is of paramount importance that fire fighter operations include the complete dousing of all burning timber members floors to stop the combustion process.

After proper cleaning, repair of the timber members should be a straightforward process, however it must be remembered that for any structural system such as a floor, the repaired sections must be fixed in place under the same loading conditions of the original design. The new timber members or repair work must be installed so that after the propping is removed the floor will return to the same position of rest as the original floor, under the required design loading.

7.0 Conclusions and Recommendations

7.1 Conclusions from Full Scale Testing

The first major objective of this research was to investigate the behaviour of timber-concrete composite floors when exposed to fire. From both large and small scale testing conducted, a number of key points can be made in relation to this objective:

- The charring of the timber members governed the failure of the floors. The floor tested to destruction consisted of double LVL beams 63 mm wide by 300 mm deep, and was loaded with 1.56 kPa. The floor failed after 75 minutes of ISO 834 fire exposure, and the residual timber section left behind was only 15 % the size of the original cross sectional area. The composite action achieved in the floor aided in increasing the actual fire resistance of the floor to a high degree when compared with similar tests on loaded LVL beam members in the same furnace.
- As a significant thermal gradient was introduced across the depth of the concrete slab, the bottom of the slab acted to expand due to the increase in temperature. This behaviour was restrained by the beam due to the composite connections, therefore a thrust force was induced in the floor that tended to hog the entire specimen. This thrust force aided in resisting the gravity loads imposed on the floors and reduced the vertical deflections of the floors for a significant part of the burning duration. This action served to prolong the fire resistance time of the floors.
- The thickness of the concrete slab and concrete mix quality used had a large impact on the insulation performance of the floor unit. A lower quality concrete mix used in one of the tests induced a greater amount of spalling, and due to the relatively thin slab used in the floors this resulted in the measured temperatures of the top of the slab increasing at a much greater rate than for the other floor tested. This issue however is easily resolved with the use of a concrete mix specified at 30 MPa, and will be mitigated over time as the slab dries out.
- The unanticipated separation of the double LVL members during the latter stages of burning induced a much faster rate of charring in the timber beams by way of exposing the central protected area to burning. This effect can be mitigated by different methods of fixing the double beams together however, such as gluing. A greatly increased charring rate for the underside of the beams was recorded in the latter stages of burning as the residual section size was reduced down to a small thickness and the heated regions from both sides of the double beams overlapped.
- The LVL beams with the steel plate connection system exhibited stiffer performance and lower deflections when compared with the notched connection beams during the full scale testing. This form of connection system required specialised pressing equipment to install which may incur a higher cost in terms of transport and equipment use, however the notched connection system was more labour intensive to produce.

7.2 Conclusions from the Small Scale Testing

- Results obtained in the small scale testing found that the heat affected timber lost compression strength with increasing temperature toward 100 °C as the wood softened and behaved in a more plastic manner. After this the strength increased towards 200 °C as the wood hardened.
- The same trend was followed for the stiffness calculations. Pre-dried wood samples exhibited much higher strength characteristics than the samples which were kept at a moisture content of 12 %.
- The results from the shear testing showed a steady linear decrease in strength to 200 °C.
- The effects of reduced timber material properties due to elevated temperature had a very small impact on the overall performance of the floor units.

7.3 Conclusions from the Spreadsheet Analysis

The second major objective of this research was to develop a basic spreadsheet analysis tool that was able to predict the expected fire resistance of these types of floors. This was successfully achieved and some of the features of this spreadsheet were:

- The incorporation of user defined time-dependent variables such as the charring rate.
- User defined floor geometry, material properties and loading conditions.
- An output of expected fire resistance utilising a macro to enable the user to determine exactly when the floor will fail and the failure criterion.

The spreadsheet was used to derive a number of resistance span tables for varying spans of these timber-concrete composite floor systems with regard to the varying section sizes available, and different combinations of live and superimposed dead loads. These tables were developed to be used as a general guide to expected fire resistance only, and care must be taken to understanding what differences are present between the floors tested in this study and a specific user's design. Some differences may include material types, connection spacings and dimensions, loading arrangements or the design fire severity. It is important that the user recognises that the numbers presented in this research may not represent some real fire scenarios.

7.4 Overall Conclusions

In conclusion this research has shown that the performance of unprotected timber-concrete composite floors when subjected to fire is excellent. A large degree of safety is possible without risking structural collapse, and this research should serve as a guideline to the expected performance . The benefits in aesthetics, sustainability and economical savings due to fast erection time will undoubtedly be a significant factor to their widespread use in the future. Further means of protection to these floors such as passive protection (fire rated suspended ceilings, gypsum plasterboard encasement) or active protection (sprinkler

systems) will only serve to further increase the reliability and longevity of these floors in fires.

7.5 Recommendations for Further Research

Although this research has provided an insight into the fire performance of timber-concrete composite floors, there is much that has not been considered in the timeframe available. There are many possible variations of timber-concrete composite floors and connection types available, only two of which were studied in this research. There are also a diverse number of different timber flooring systems, such as stressed skin floors and slab type systems, which each present a unique challenge in predicting the fire behaviour, all of which require a rigorous analysis in fire to ensure they are safe to use. Some areas warranting further investigation that have been uncovered as a result of this research are:

- The double beam splaying phenomenon uncovered in the full scale testing. Further research into the conditions that produce this beam splaying, what effect it has on the load bearing capacity of the beams and how it can be mitigated are all required. This would include both loaded and unloaded small scale furnace testing on portions of floors. This may also include a review of the available fastener options for fixing the beams together, and a cost analysis which weighs the overall performance achieved versus cost of each fastener type.
- The strength trends uncovered in the small scale testing, with increasing compression and shear strength of specimens tested at temperatures higher than 100 °C. The effects of heating LVL are not yet fully understood, and a lack of reported test results for these types of tests on wood at elevated temperatures has led to an assumption of linearly decreasing strength from 100 °C to zero strength at 300 °C being generally accepted among the international community. Further research is required on different types of wood and wood products to verify the results found in these tests and allow the validity of this approximation to be confirmed. Tensile testing at elevated temperatures would also be a valuable addition to determine whether this may have an influence on the collapse behaviour of timber-concrete composite floors in fires.
- The strength and stiffness reduction of the connections under fire conditions. Although some small scale tests were performed on small samples of LVL, push-out tests at normal temperatures and under fire conditions could be performed as they would provide a better understanding of this relationship.
- A more in-depth analysis of the timber-concrete composite floor system in terms of computer modelling. This could include finite element modelling or a modification of the current spreadsheet design tool to incorporate different floor systems, more connection types and different floor configurations. The current spreadsheet software has been solely based on the floor configuration in this research, and its flexibility to accurately predict fire performance for a large range of floor types and connection methods has not been adequately tested.

- Updating the spreadsheet design tool to properly model the charring of the timber, and to check more methods of failure. Currently the spreadsheet is calibrated on only the floors tested in this research, and further investigation into the charring behaviour of the timber is required to produce a more accurate representation of the charring behaviour of the beams. An analytical charring model should be developed, based on the results of furnace testing. Further design checks should also be included in the spreadsheet such as checking deflections and other modes of failure in the concrete.

Looking at the bigger picture of constructing large buildings in timber, the fire resistance of timber structures is mainly a problem of perception as opposed to factual information. Although fire testing and investigations of specific systems such as floors and walls are valuable, proving that these systems are safe in fires without addressing the larger issue of the perception of fire safety in timber buildings will not aid in their implementation. This requires a change in the perception of the public, who may or may not read and understand technical reports and research such as this. Therefore the most important requirement for further research in this field is the education of the public and the construction industry, so that the facts about timber buildings with regards to fire safety are understood and the myths surrounding timber buildings are dispelled. This is of the utmost importance if large timber buildings are to become an integral part of the construction industry in the future.

References

AS/NZS 1170 (2002) "Structural Design Actions, Part 0: General Principles." AS/NZS 1170.0: 2002 , Standards New Zealand.

AS/NZS 1328.1 (1998) "Glue Laminated Structural Timber, Part 1: Performance Requirements and Minimum Production Requirements." AS/NZS 1328.1: 1998, Standards New Zealand.

ASTM Standard D 143-94 (2007) "Standard Test Methods for Small Clear Specimens of Timber." ASTM International, West Conshohocken, Pennsylvania, USA.

ASTM Standard D 5456-06 (2007) "Standard Specification for Evaluation of Structural Composite Lumber Products." ASTM International, West Conshohocken, Pennsylvania, USA.

Bathon, L., Bletz, O., Schmidt, J. (2006) "Hurricane Proof Buildings-An Innovative Solution using Prefabricated Modular Wood-Concrete-Composite Elements." Proc. 9th World Conference on Timber Engineering, Portland, Oregon, USA.

Buchanan, A.H. (Ed.) (2001) "Fire Engineering Design Guide." Second edition. New Zealand Centre for Advanced Engineering, Christchurch, New Zealand.

Buchanan, A.H. (2002) "Structural Design for Fire Safety." John Wiley & Sons Ltd., West Sussex, England.

Buchanan, A.H. (2007) "Timber Design Guide." Third Edition. New Zealand Timber Industry Federation Inc., Wellington, New Zealand.

Buchanan, A., Deam, B., Fragiacomo, M., Pampanin, S., and Palermo, A. (2007) "Multi-Storey Prestressed Timber Buildings in New Zealand." Structural Engineering International, IABSE, Special Edition on Tall Timber Buildings, Volume 18, Issue 2, pp. 166-173.

Ceccotti, A. (2002) "Composite Concrete-Timber Structures." Prog. Struct. Engng Mater. 2002; 4:264-275.

EC5a (2004) "Eurocode 5: Design of Timber Structures, Part 1-1: General - Common Rules and Rules for Buildings." EN 1995-1-1: 2004, European Committee for Standardisation, Brussels, Belgium.

EC5b (2004) "Eurocode 5: Design of Timber Structures, Part 1-2: General - Structural Fire Design." EN 1995-1-2: 2004, European Committee for Standardisation, Brussels, Belgium.

Fragiacomo, M., Gutkowski, R.M., Balogh, J., Fast, R.S. (2007) "Long-Term Behavior of Wood-Concrete Composite Floor/Deck Systems with Shear Key Connection Detail." ASCE Journal of Struct. Engrg., Volume 133, Issue 9, pp. 1307-1315.

Frangi, A., Fontana, M. (1998) "Fire Behaviour of Timber-Concrete Composite Slabs." Proc. The 5th World Conference on Timber Engineering, Montreux, Switzerland, August 17-20, 1998.

Frangi, A., Fontana, M. (1999) "Fire Behaviour of Timber-Concrete Composite Slabs." Proc. The 6th International Symposium on Fire Safety Science, Poitiers, France, July 5-9, 1999.

Frangi, A., Fontana, M. (2001) "A Design Model for the Fire Resistance of Timber-Concrete Composite Slabs." Proc. Innovative Wooden Structures and Bridges, Lahti, Finland, August 29-31, 2001.

Frangi, A., Fontana, M. (2003) "Charring Rates and Temperature Profiles of Wood Sections." Fire and Materials, Volume 27, pp. 91-102.

Frangi, A., Knobloch, M., and Fontana, M. (2009) "Fire Design of Timber-Concrete Composite Slabs with Screwed Connections." ASCE Journal of Struct. Engrg., in print.

Green, D.W., Kretschmann, D.E., and Winandy, J.E. (1999) "Wood Handbook - Wood as an Engineered Material, Chapter 4: Mechanical Properties of Wood." USDA General Technical Report FPL-GTR-113, Department of Agriculture Forest Service, Madison, Wisconsin, United States of America.

ISO (1975) "Fire Resistance Tests - Elements of Building Construction." ISO 834: 1975, International Organisation for Standardisation.

Konig, J., Walleij, L. (2000) "Timber Frame Assemblies Exposed to Standard and Parametric Fires." Report No. I 0001001. Tratek, Swedish Institute for Wood Technology Research, Stockholm, Sweden.

Kuhlmann, U., Michelfelder, B. (2006) "Optimized Design of Grooves in Timber-Concrete Composite Slabs." Proc. The 9th World Conference on Timber Engineering WCTE 2006, Portland, Oregon, USA, CD.

Lane, W.P. (2005) "Ignition, Charring and Structural Performance of Laminated Veneer Lumber." Fire Engineering Research Report 05/3, School of Engineering, University of Canterbury.

Lukaszewska, E., Fragiacomo, M., Frangi, A. (2007) "Evaluation of the Slip Modulus for Ultimate Limit State Verifications of Timber-Concrete Composite Structures." Meeting forty of the Working Commission W18-Timber Structures, CIB, International Council for Research and Innovation, Bled (Slovenia), August 28-31, paper No. CIB-W18/40-7-5, 14 pp.

Lukaszewska, E., Johnsson, H., and Fragiacomo, M. (2008) “Performance of Connections for Prefabricated Timber-Concrete Composite Floors.” Materials and Structures, RILEM, Vol. 41 No. 9, pp. 1533-1550.

Lukaszewska, E., Fragiacomo, M., and Johnsson, H. (2010) “Laboratory Tests and Numerical Analyses of Prefabricated Timber-Concrete Composite Floors.” ASCE Journal of Struct. Engrg., in print.

New Zealand Building Code (2005) "Clauses C1, C2, C3, C4: Fire Safety." Department of Building and Housing, Wellington, New Zealand.

NZS 3112 (1986) "Specification for Methods of Test for Concrete, Part 2: Tests Relating to the Determination of Strength of Concrete." NZS 3112: Part 2: 1986, Standards New Zealand.

NZS 3603 (1993) "Timber Structures Standard." NZS 3603: 1993, Standards New Zealand.

O'Neill, J.W. (2007) "A Study of the Connections in Timber-Concrete Composite Systems." Project Report in Civil Engineering, University of Canterbury, Christchurch, New Zealand.

Structural Timber Innovation Company, STIC (2009) Summary Document. www.stic.co.nz. Accessed August, 2009.

Timber Manual (1995) "Multi-Residential Timber Framed Construction 3: Structural Engineering Guide for Class 2 and 3 Buildings up to 3 Storeys." National Association of Forest Industries Ltd, Deakin, Australian Capital Territory.

Truform Brochure (2008) Product Specifications, Carter Holt Harvey Woodproducts, Auckland, New Zealand. www.chhwoodproducts.co.nz. Accessed October, 2009.

Yeoh, D. (2009) "Behaviour and Design of Timber-Concrete Composite Floors under Short and Long-Term Loading." Doctorate Thesis in Civil Engineering, University of Canterbury, Christchurch, New Zealand, in preparation.

Yeoh, D., Fragiacomo, M., Buchanan, A., and Gerber, C. (2009) “A semi-prefabricated LVL-concrete composite floor system for the Australasian market.” Australian Journal of Structural Engineering, Special Issue on Timber, Vol. 9 No. 3, pp. 225-240.

Yeoh, D., Fragiacomo, M., De Franceschi, M., and Buchanan, A. (2010) “Experimental tests of notched and plate connectors for LVL-concrete composite beams.” Submitted for possible publication on Journal of Structural Engineering, ASCE.

List of Appendices

Appendix A: Floor Design

Plan 1

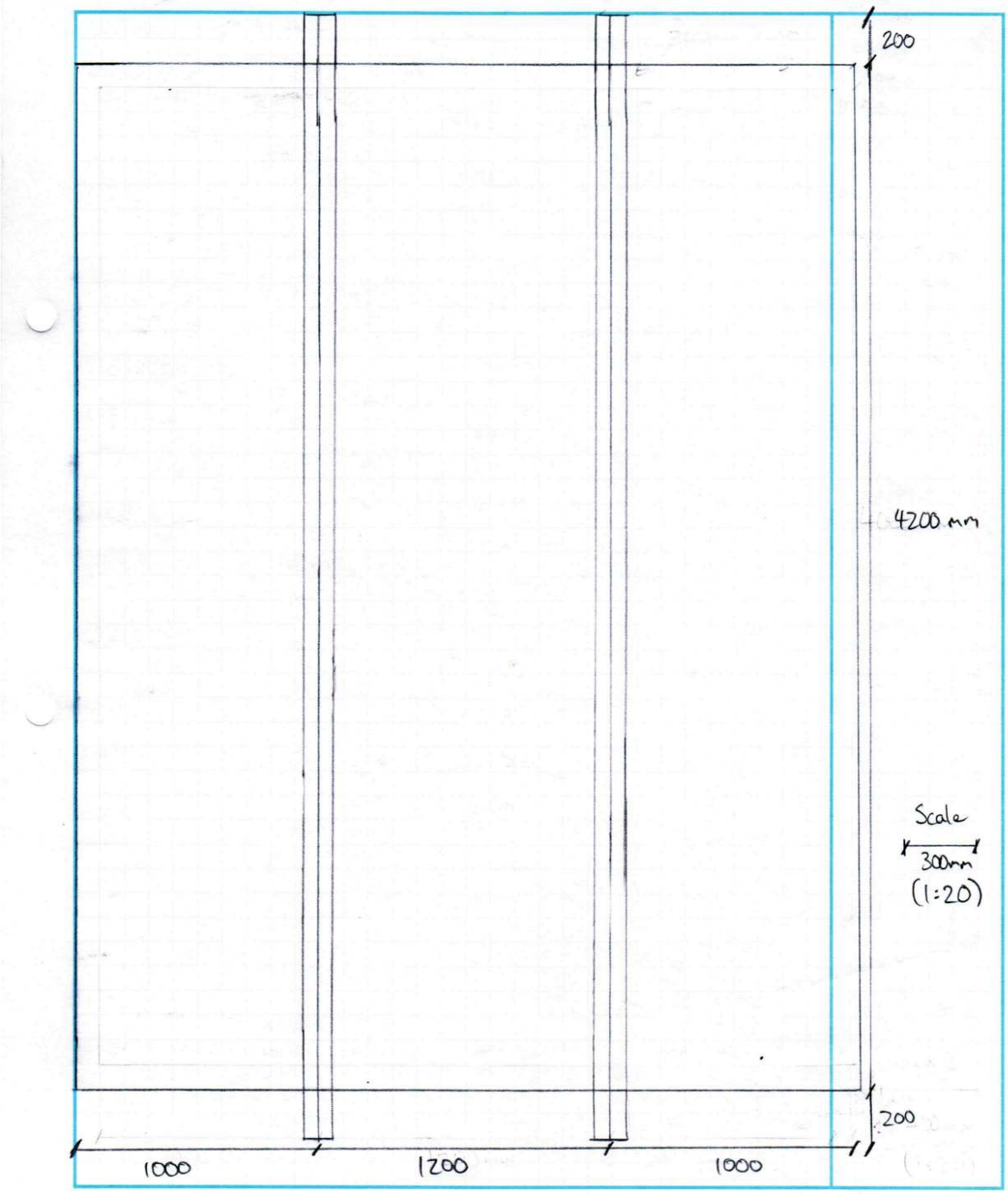

Elevation 1

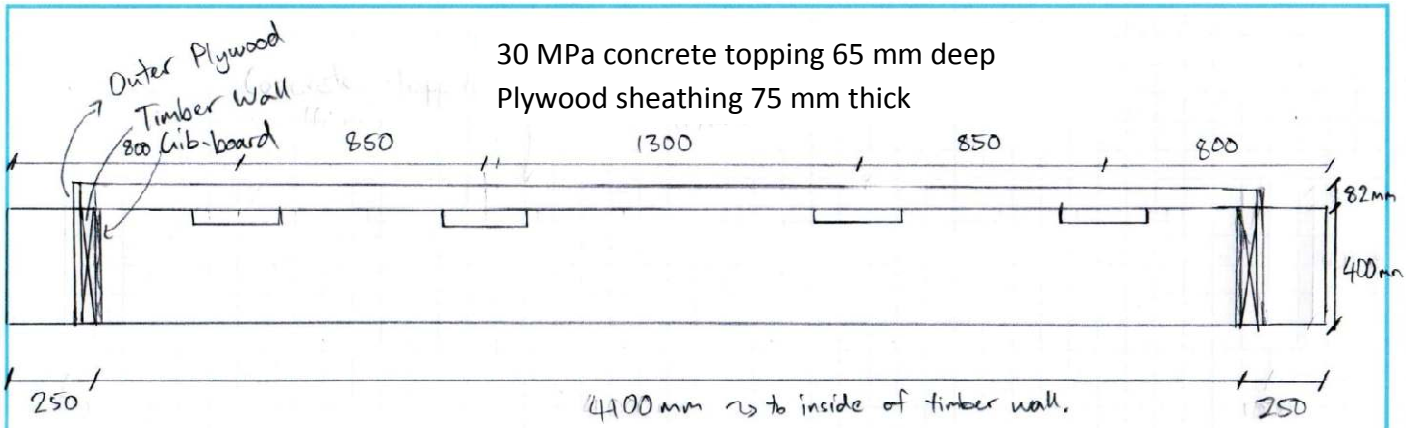

30 MPa concrete topping 65 mm deep
Plywood sheathing 75 mm thick

- LVL beam has four 300 mm long x 50 mm deep notches, holes must be cut in the plywood sheathing to allow concrete infilling.
- Allow 300 mm each end for bearing on the furnace frame for beams.
- Use plywood about the edges to create formwork for pouring the concrete topping. The inside of the walls are to be lined with fire-rated gypsum plasterboard, and the wall is 50 mm x 50 mm timber.
- Each notch incorporates a coach screw (see Elevation 2).
- The centre of each beam has a coach screw drilled in to prevent uplift of the concrete

Scale
400mm
(1:20)

- Coach screws must have pre-drilled holes 100 mm deep into the timber.
- Centre to centre spacings of the notches are as follows (4.6 m beam): 800 mm, 850 mm, 1300 mm, 850 mm, 800 mm.

Elevation 2

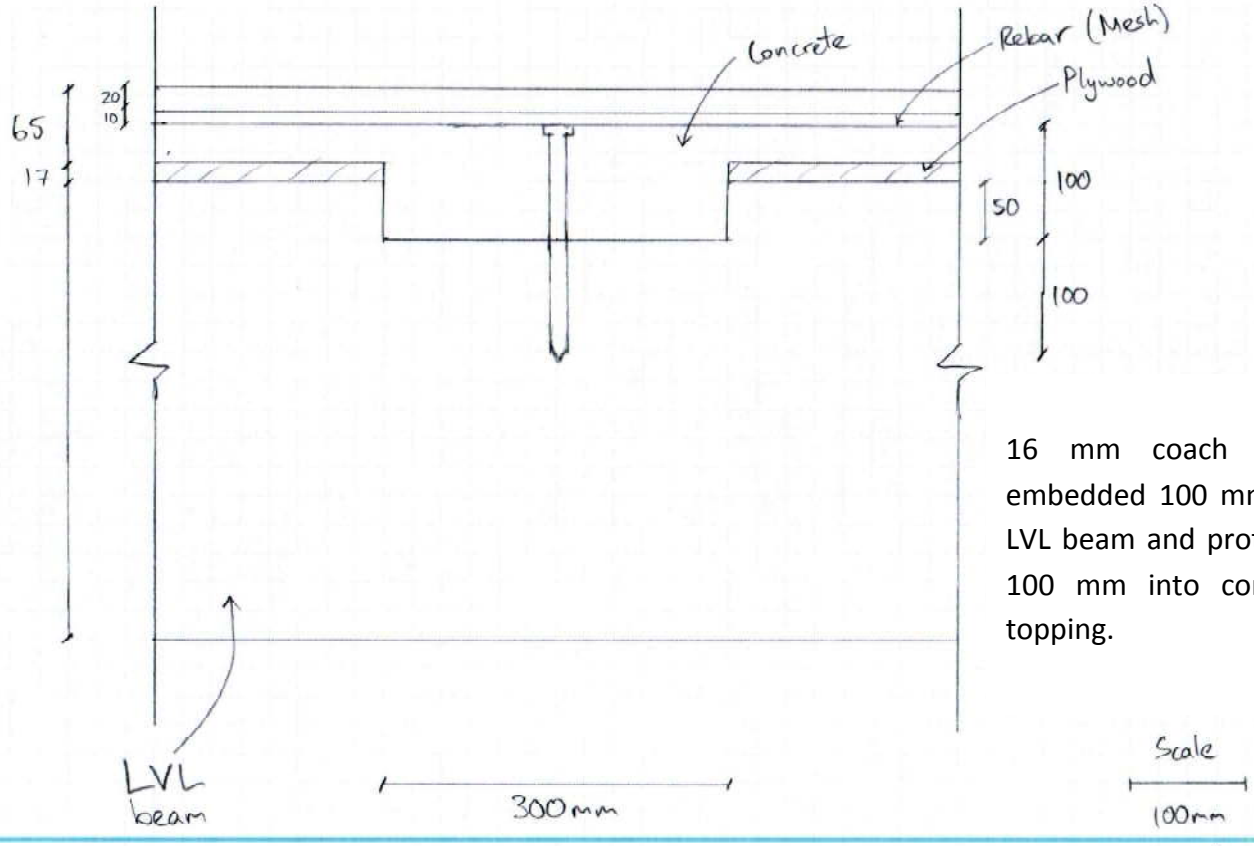

16 mm coach screw embedded 100 mm into LVL beam and protrudes 100 mm into concrete topping.

Note: During Construction a plywood plate will be nailed to the sides of the notches to ensure complete concrete formwork. Holes are cut through the plywood to allow the notch to be filled with the topping.

Section 1

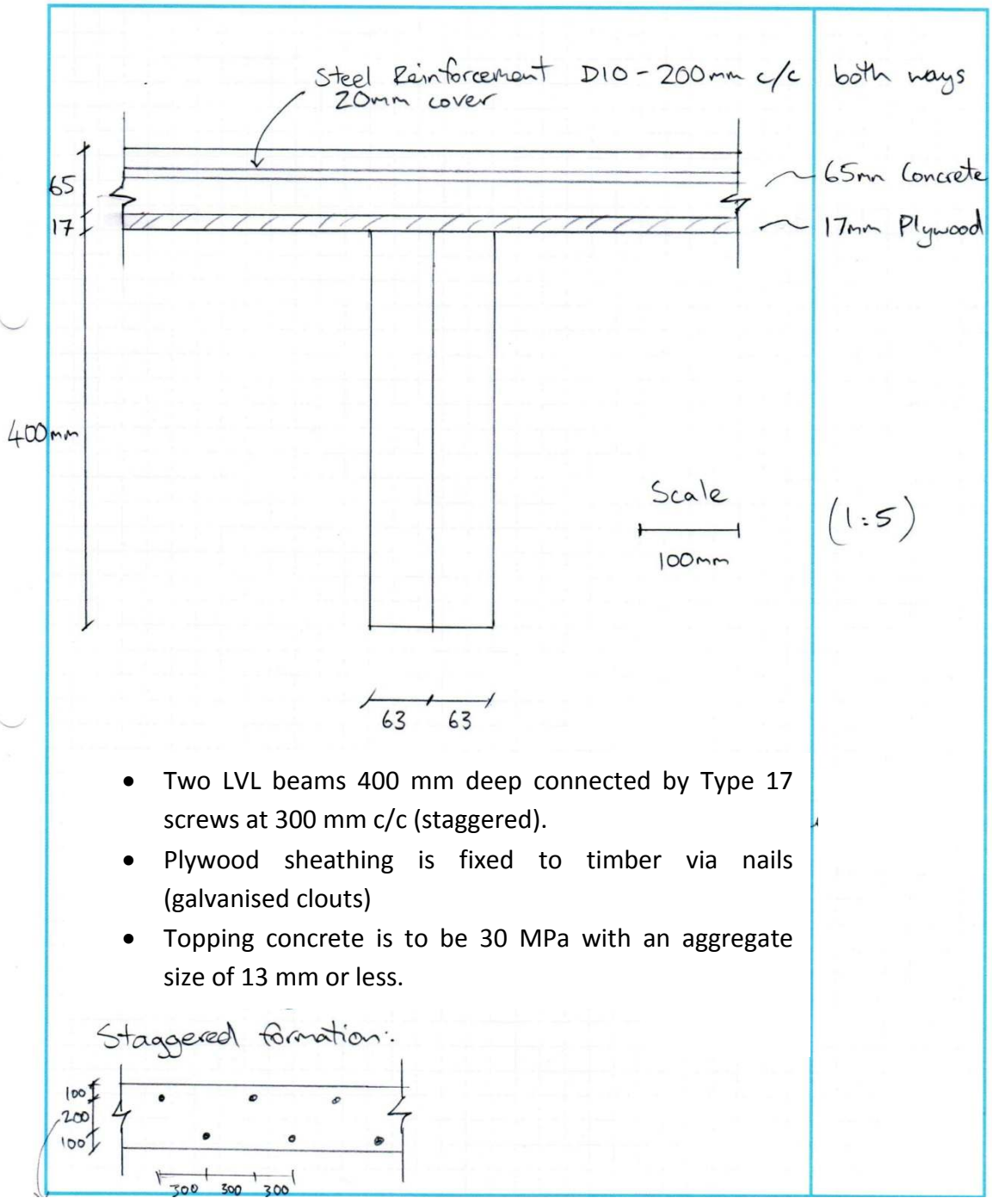

- Two LVL beams 400 mm deep connected by Type 17 screws at 300 mm c/c (staggered).
- Plywood sheathing is fixed to timber via nails (galvanised clouts)
- Topping concrete is to be 30 MPa with an aggregate size of 13 mm or less.

3-Dimensional View

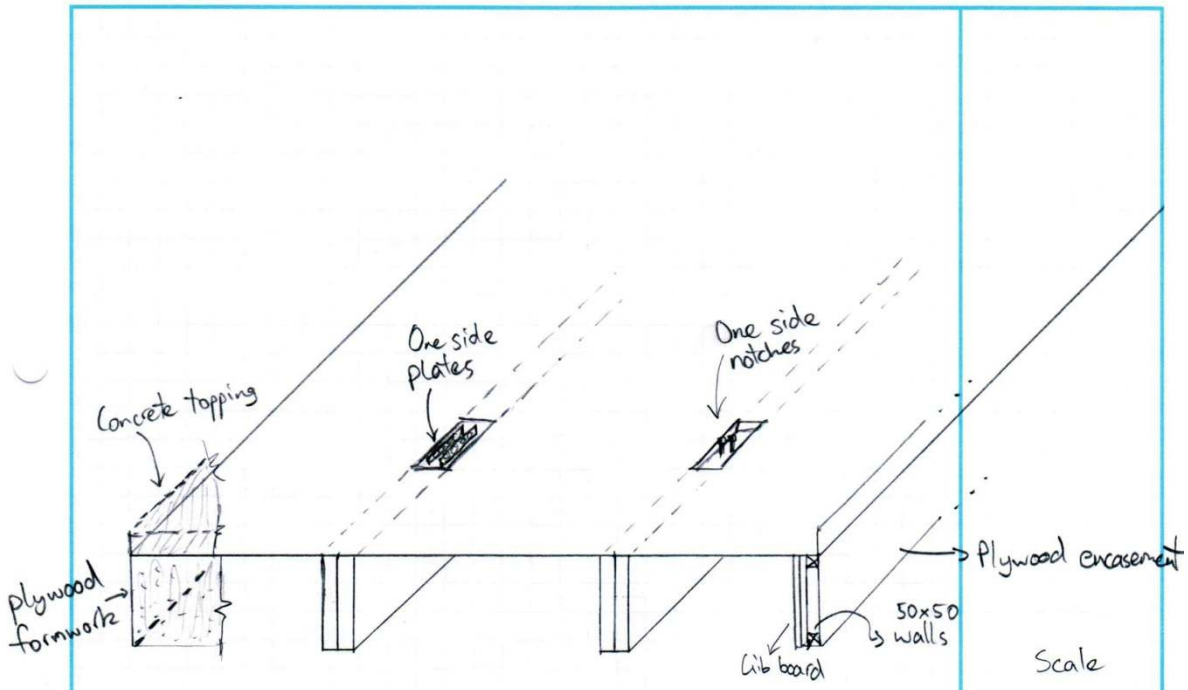

- Holes are cut into the plywood sheathing to expose the notches and plates.
- The double beams are spaced at 1200 mm c/c.
- An exterior plywood encasement will be built about the floor units to accommodate the fire-rated gypsum plasterboard sealing and to provide formwork.
- The encasement consists of walls made from 50 mm x 50 mm timber, the inside of which two layers of 13 mm fire-rated gypsum plasterboard are screwed, and the outside a 17 mm plywood encasement is nailed to.

Construction Layout

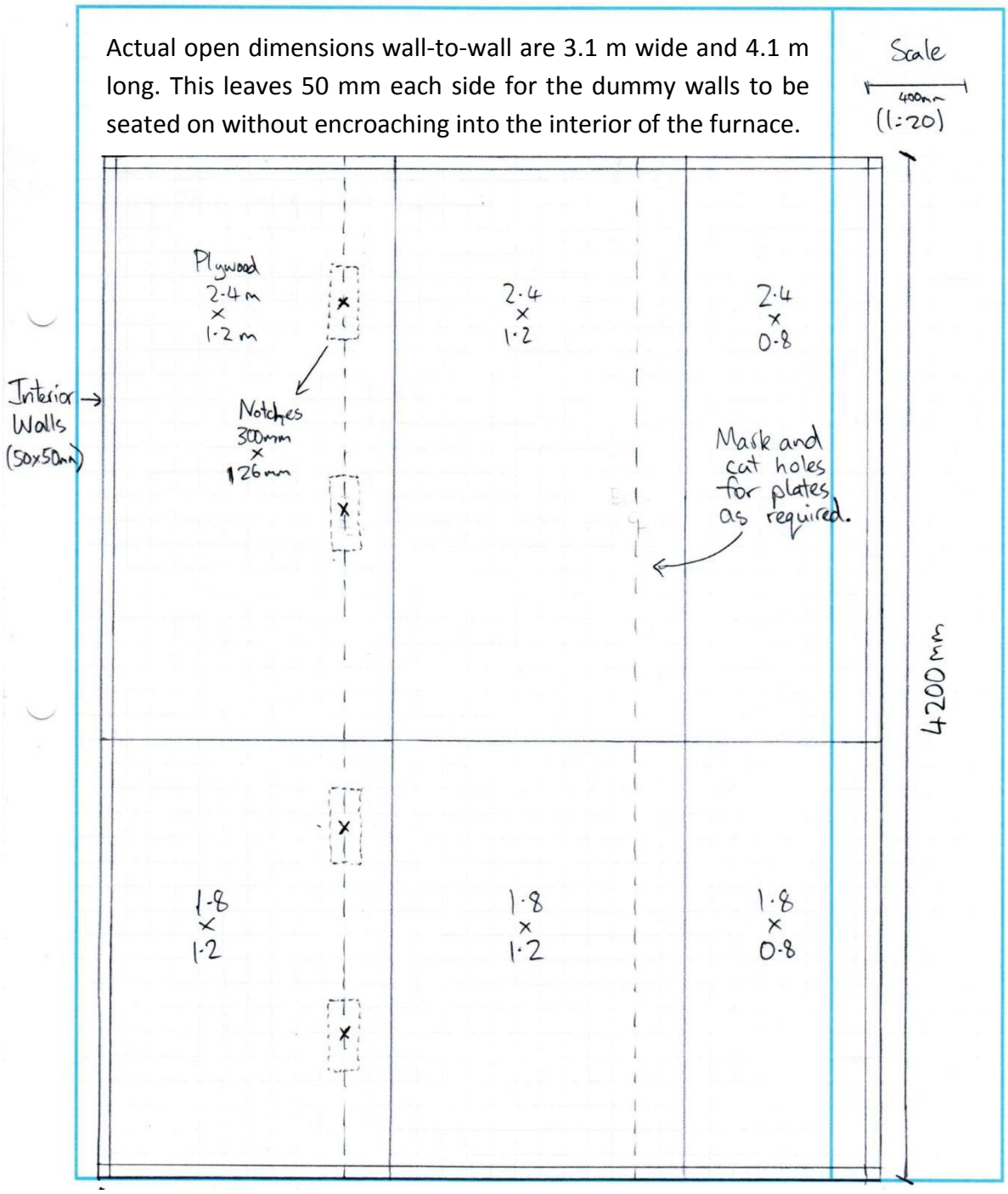

Dummy Wall Design

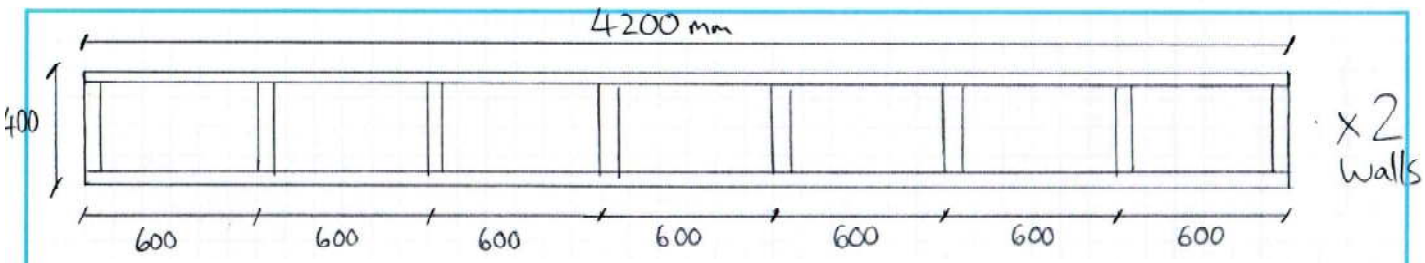

Space 300 mm studs at 600 mm centres. Note the end spacing will be 550 mm.

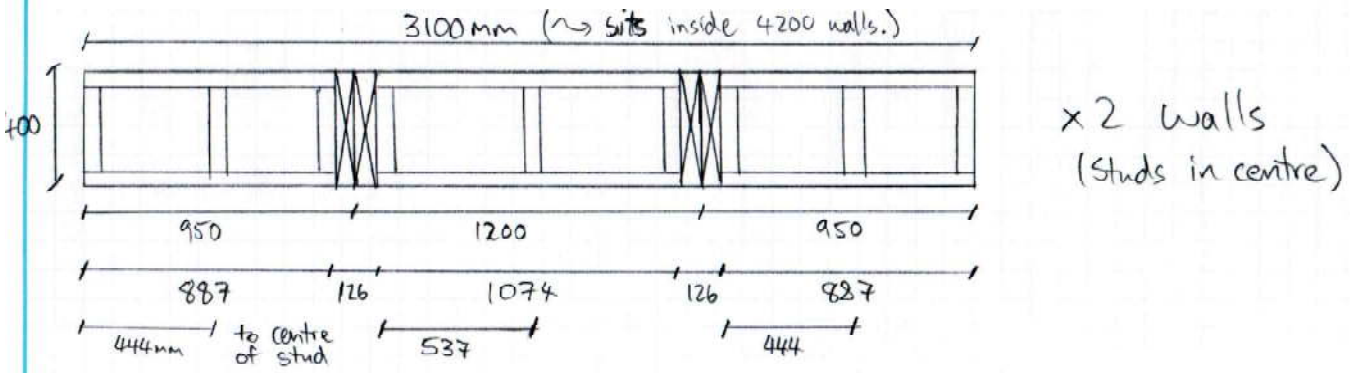

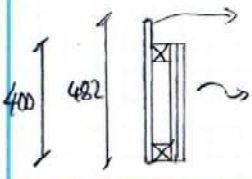

Plywood encasement protrudes 82 mm over top of wall.

2 layers of 13 mm Gib Fyreline fixed to inside.

Nail wall together with 100 mm nails, fix plywood with 50 mm clouts, screw Gib-board with 40 mm gib fixers.

Note that this entire process is repeated for the 300 mm deep floor, the only changes being 200 mm deep studs and corresponding plywood and gypsum plasterboard heights.

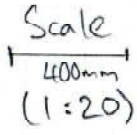

Thermocouple Placement

Place at one end of beams near the closest notch so that the full length inside the unit is not greater than 2.5 m. Use a stapler or tape to hold in place.

Scale
200mm
(1:40)

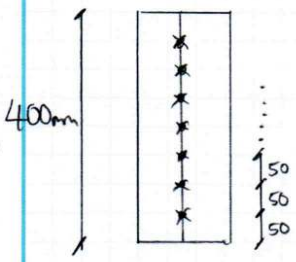

Place at 50 mm centres down the beams centreline in both plate and notch beams. Run out the ends.

First notch in from an end.

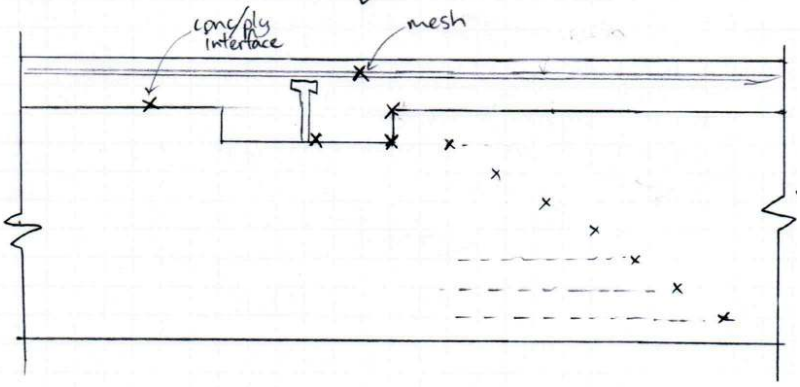

Steel Plates: Put one on a plate and keep two for the mesh and conc/ply interface.

- Ensure a staggered formation of 100 mm lengthwise is used between each thermocouple as shown above.
- Total number for 400 mm beams: Notch (12) + Plate (10) = 22
- Total number for 300 mm beams: Notch (10) + Plate (8) = 18
- 40 thermocouples required minimum

Appendix B: Full Scale Testing Thermocouple Measurements

Concrete Slab Surface: 300 mm Floor

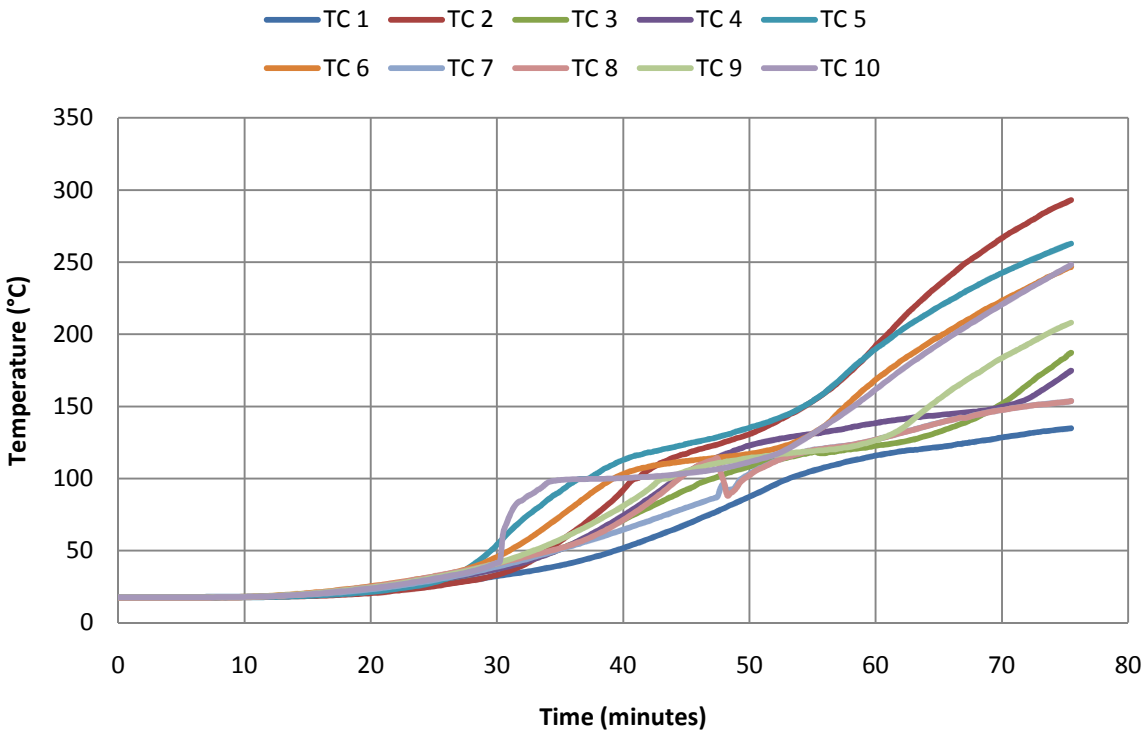

Concrete Slab Surface: 400 mm Floor

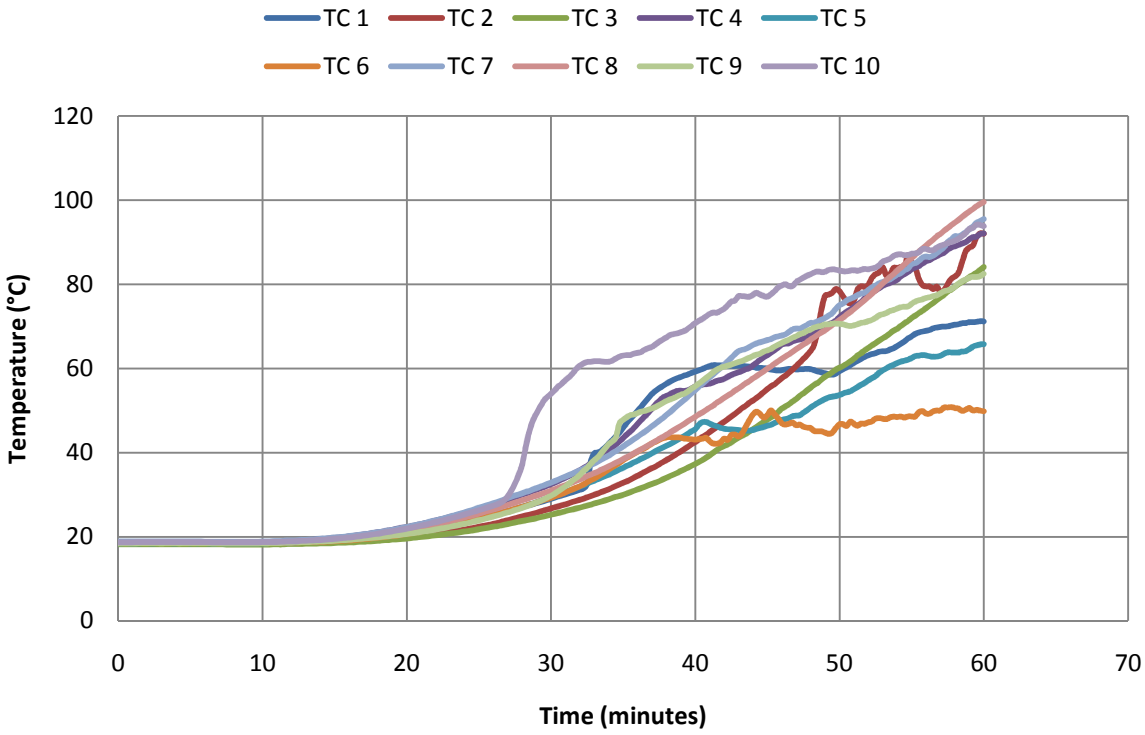

Installed Thermocouple Readings: 300 mm Floor Notch Beam

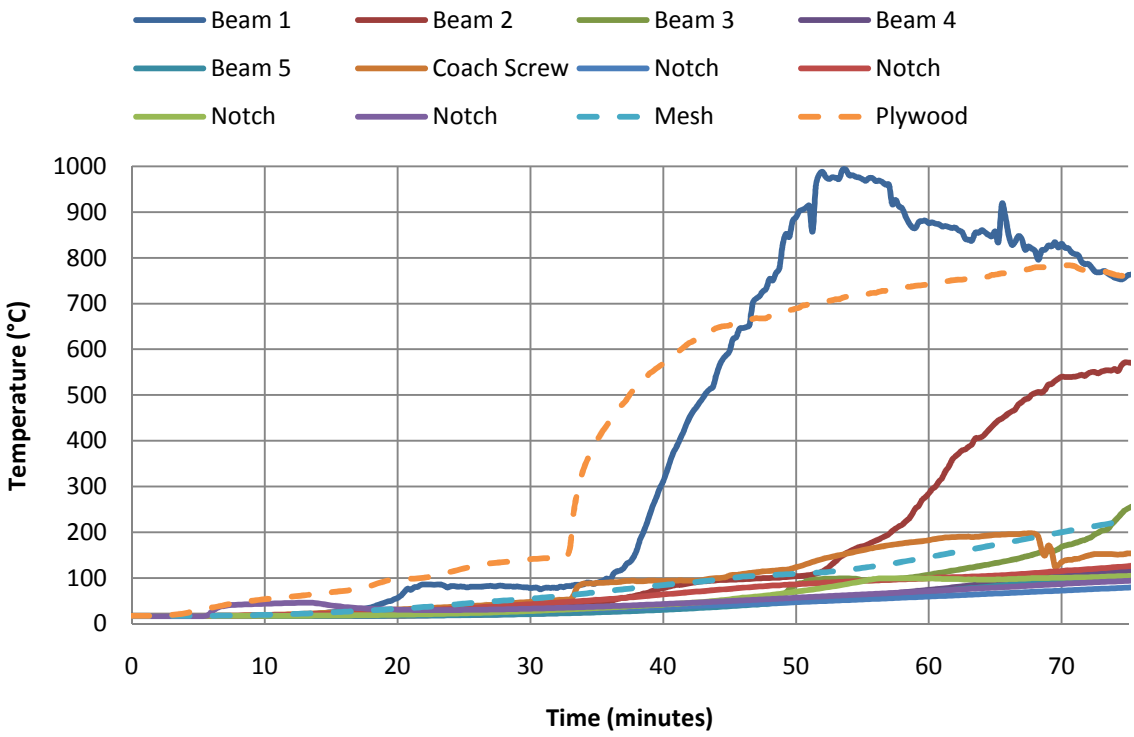

Installed Thermocouple Readings: 300 mm Floor Plate Beam

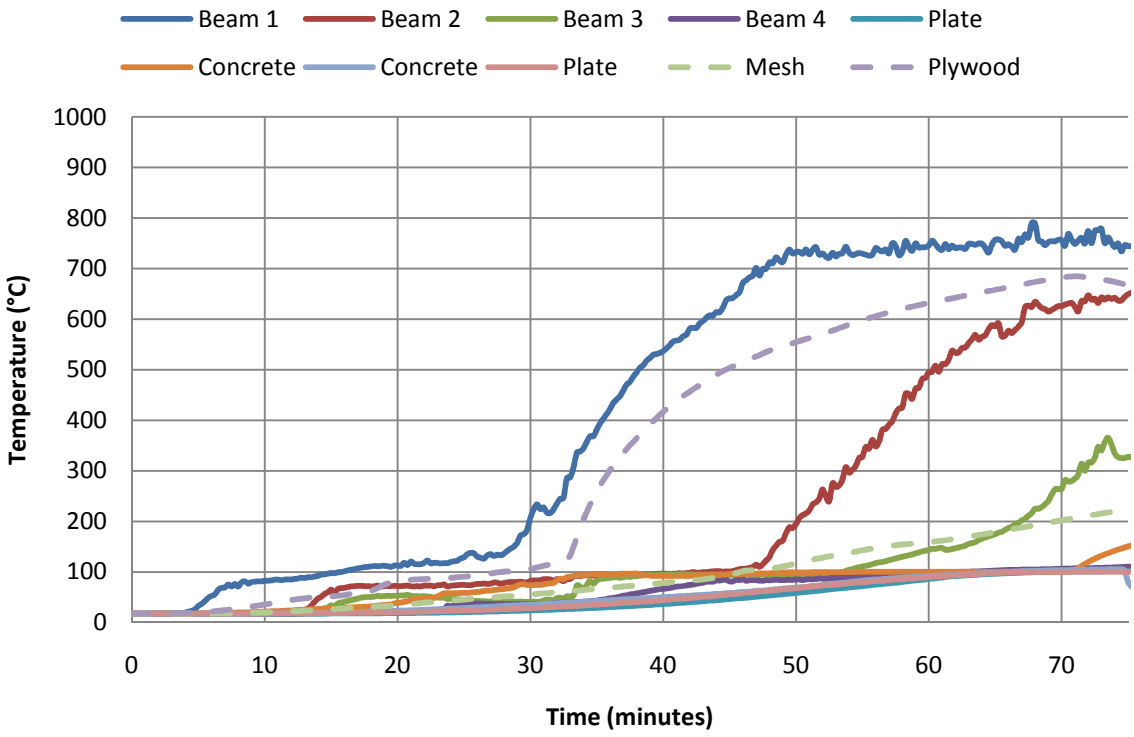

Installed Thermocouple Readings: 400 mm Floor Notch Beam

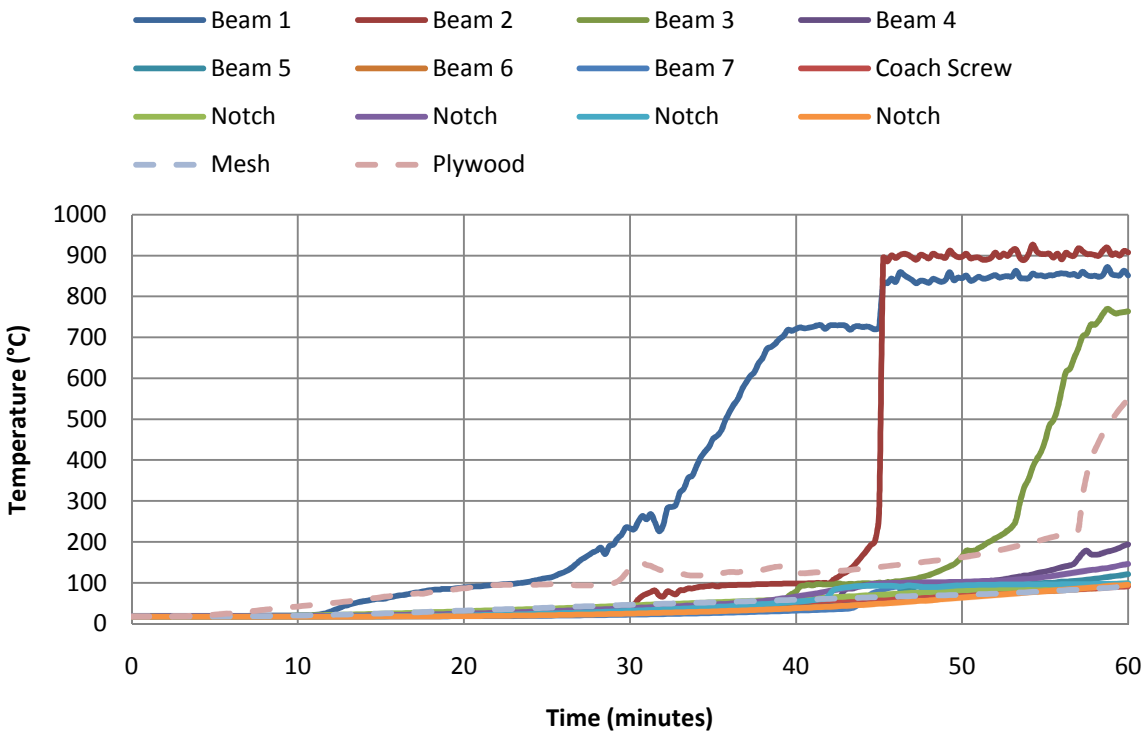

Installed Thermocouple Readings: 400 mm Floor Plate Beam

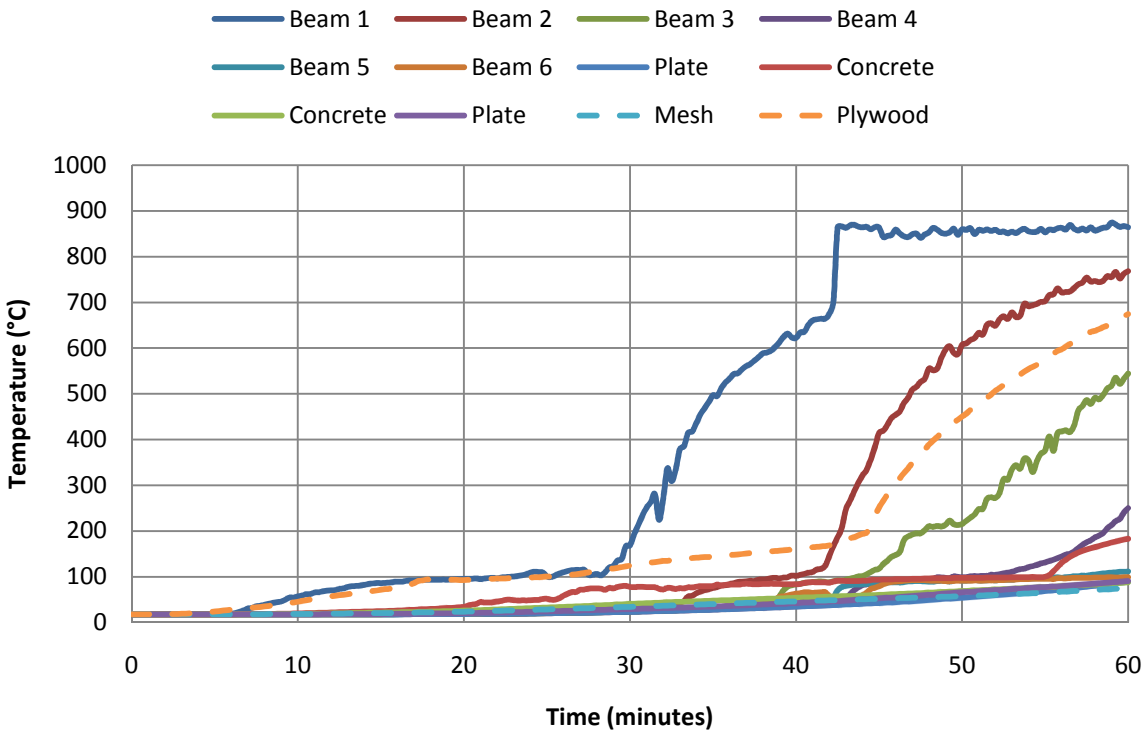

Appendix C: Full Scale Testing Displacement Measurements

Top of Slab: 300 mm Floor (Pot 2 was removed during testing at 50 minutes)

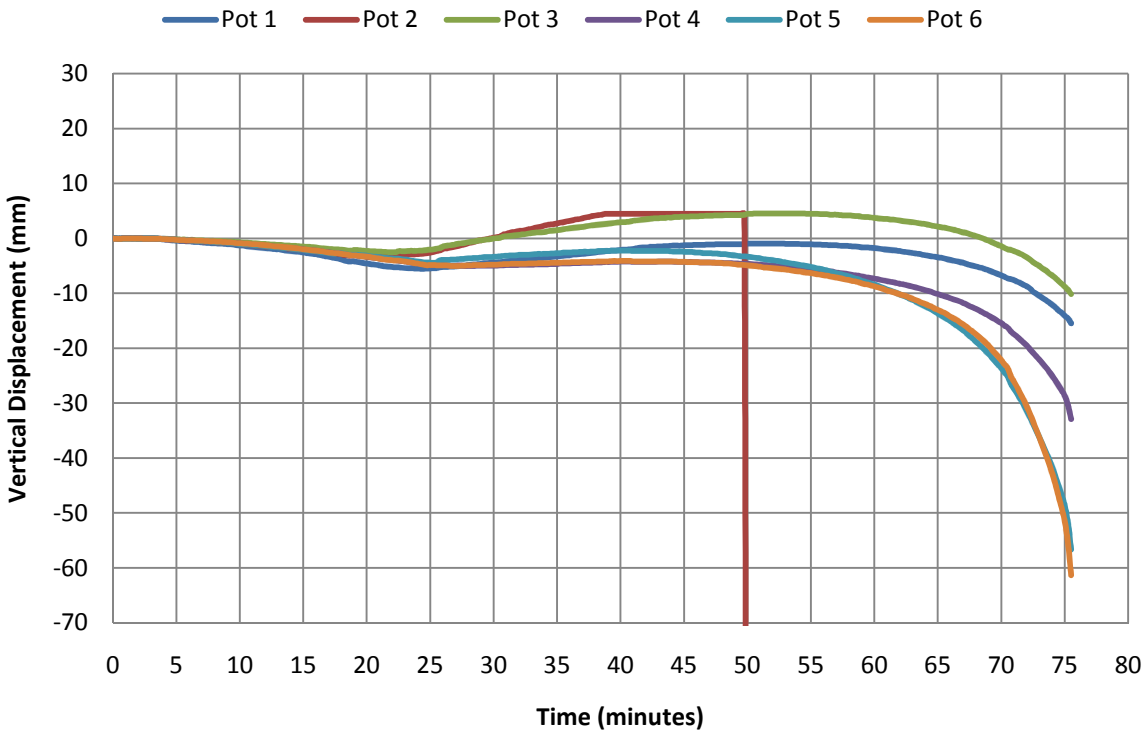

Top of Slab: 400 mm Floor

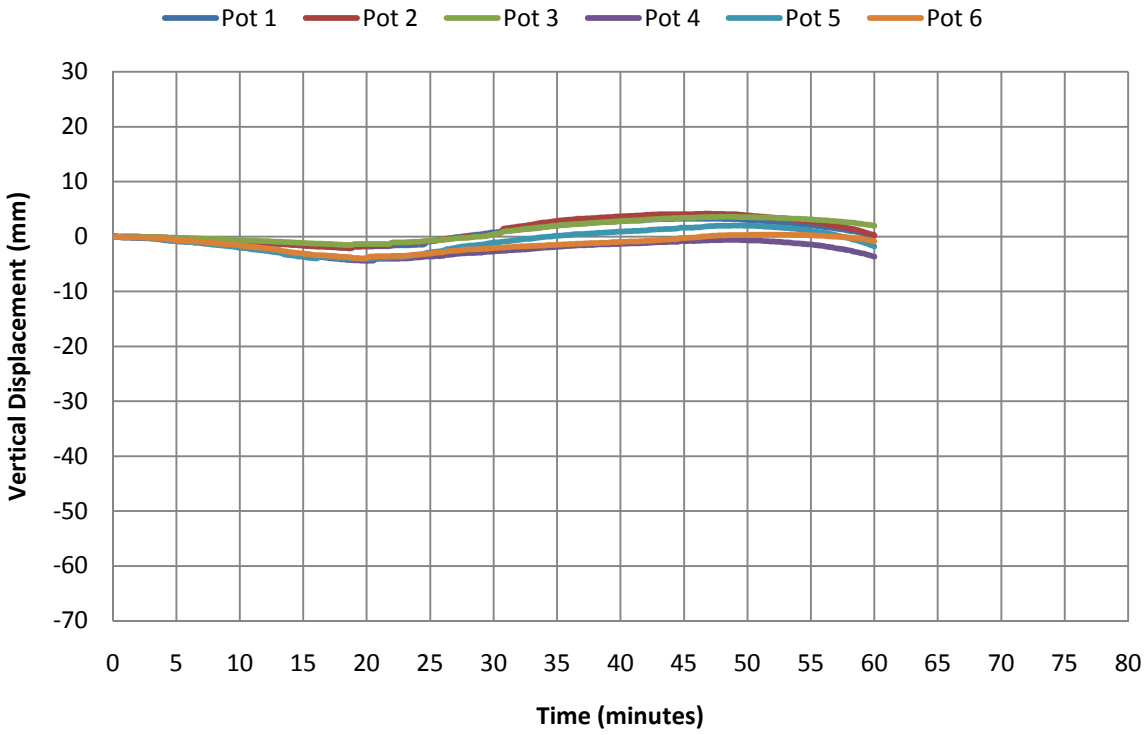

Appendix D: Full Scale Test Specimen Construction Photos

Preparing the Connections and Fixing the Beams Together:

Cutting out the notches

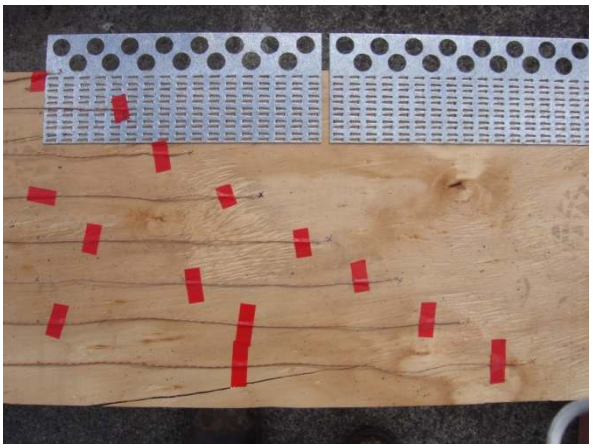

Plates and thermocouples

Fixing beams together

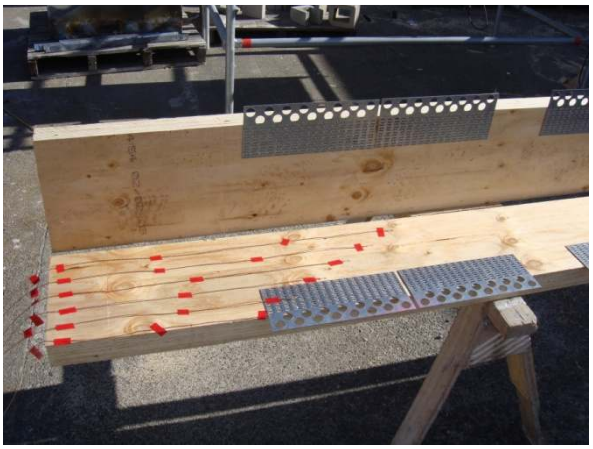

Plated beams to be fixed together

Fixing the Main Elements Together:

300 mm Floor

Corner of Unit

Installing the Plywood Sheathing and the Mesh:

Staggered Plywood Installation

Sealing the Gaps

Painting (to prevent concrete water absorption)

Separators and Mesh

Thermocouples placed

Ready to cast concrete

Appendix E: Full Scale Furnace Testing Photos

300 mm Floor: 75 minutes duration until collapse




400 mm Floor: 60 minutes duration




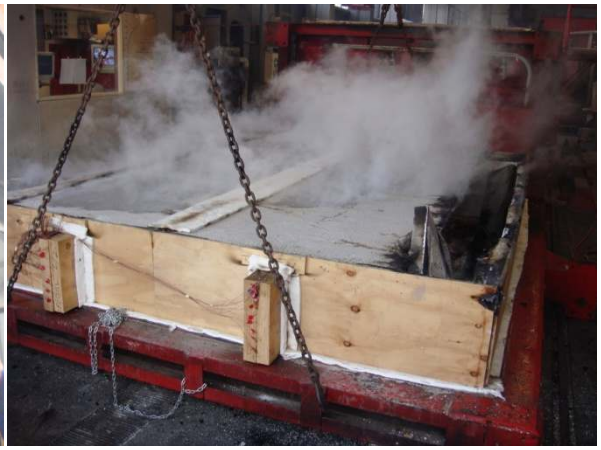

Joist Damage at the Notch Connection (400 mm Floor)


Appendix F: Small Scale Test Specimen Dimensions

Specimen No. and Type	Temperature Tested (°C)	End 1 Dimensions		End 2 Dimensions	
		Depth	Width	Depth	Width
01 Shear	20	99.0	63.7	99.3	63.6
02 Comp	20	63.0	63.9	63.2	63.9
03 Comp	50	61.8	62.8	62.4	63.0
04 Comp	50	62.1	62.9	61.8	63.1
05 Comp	50	61.9	62.5	61.7	62.8
06 Shear	50	99.3	62.8	99.4	62.6
07 Shear	50	98.4	61.7	98.3	61.9
08 Shear	50	99.4	62.8	99.2	62.3
09 Comp	100	63.3	63.6	63.1	63.7
10 Comp	100	63.1	63.4	63.1	63.2
11 Comp	100	62.8	63.6	62.9	63.8
12 Shear	100	100.0	64.1	99.5	63.7
13 Shear	100	100.5	62.7	100.3	63.7
14 Shear	100	99.1	63.3	99.3	63.8
15 Shear	200	99.3	62.8	99.4	62.7
16 Shear	200	96.1	58.1	96.5	58.1
17 Shear	200	99.9	62.7	98.6	63.0
18 Comp	200	63.4	62.5	61.6	62.1
19 Comp	200	61.8	62.5	61.5	62.5
20 Comp	200	61.7	62.6	61.6	62.2
21 Comp	150	62.2	62.7	62.0	62.8
22 Comp	150	62.6	63.0	62.4	62.9
23 Comp	150	62.5	63.1	62.2	63.0
24 Shear	150	98.8	62.6	100.5	62.9
25 Shear	150	100.3	62.9	99.9	62.7
26 Shear	150	100.1	62.5	100.7	62.8
27 Shear	20	99.4	64.6	99.8	63.9
28 Shear	20	99.6	64.0	99.7	64.3
29 Shear	20	99.3	64.4	98.5	64.1
30 Shear	20	99.4	64.1	99.3	64.2
31 Shear	20	99.4	64.2	99.4	64.0
32 Shear	20	99.5	64.1	99.6	64.6
33 Comp	20	63.6	64.2	63.7	63.9
34 Comp	20	63.7	64.4	63.7	64.1
35 Comp	20	63.1	64.4	63.4	64.2
36 Comp	20	63.5	64.3	63.3	64.1
37 Comp	20	63.0	64.0	62.7	64.1
38 Comp	20	63.8	64.2	63.4	64.3
39 Comp	50	62.9	63.6	63.2	63.8
40 Comp	50	62.3	63.7	62.9	64.0
41 Comp	50	63.2	64.1	62.7	63.1
42 Shear	50	99.3	63.6	99.6	64.3
43 Shear	50	99.1	63.4	99.4	64.4
44 Shear	50	99.8	63.6	99.5	64.0
45 Shear	150	98.9	62.1	99.2	62.9
46 Shear	150	99.0	62.5	99.6	62.7
47 Comp	20	62.3	64.0	62.1	63.0
48 Comp	20	62.5	62.9	62.2	62.9

Appendix G: Small Scale Testing Load Displacement Measurements

Compression Testing:

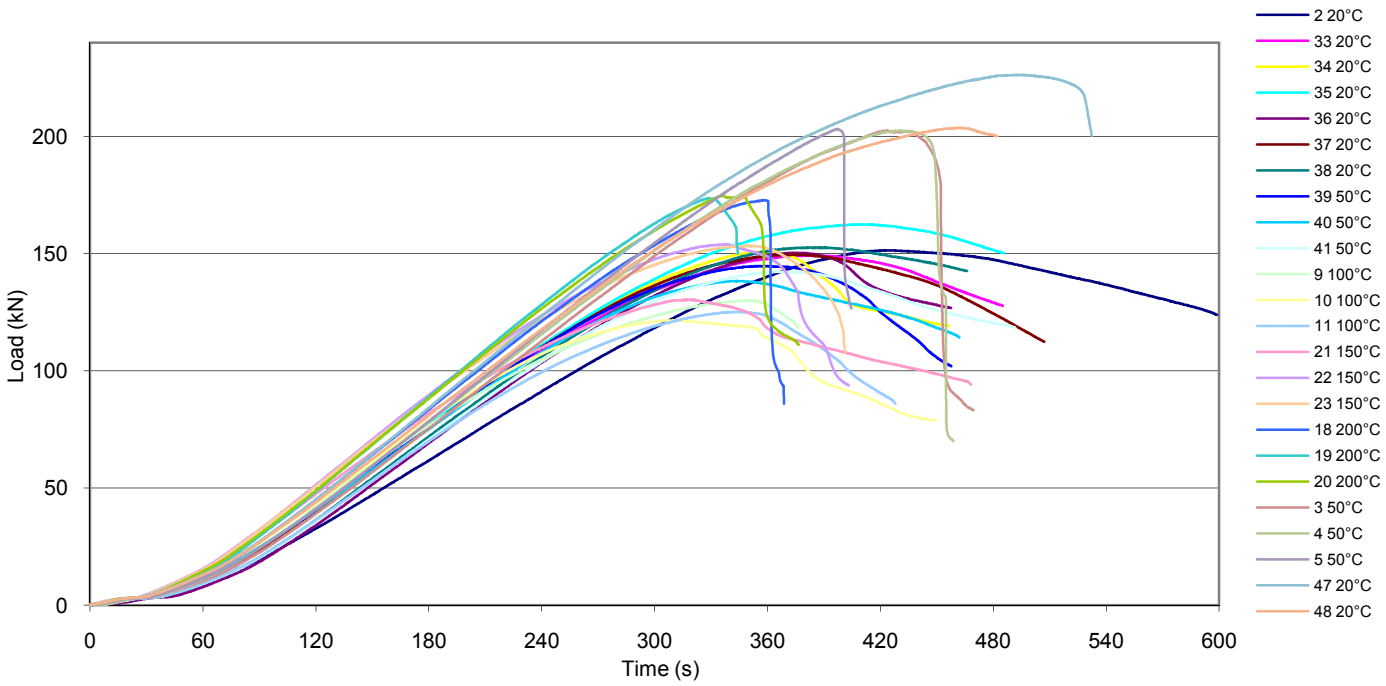

Shear Testing:

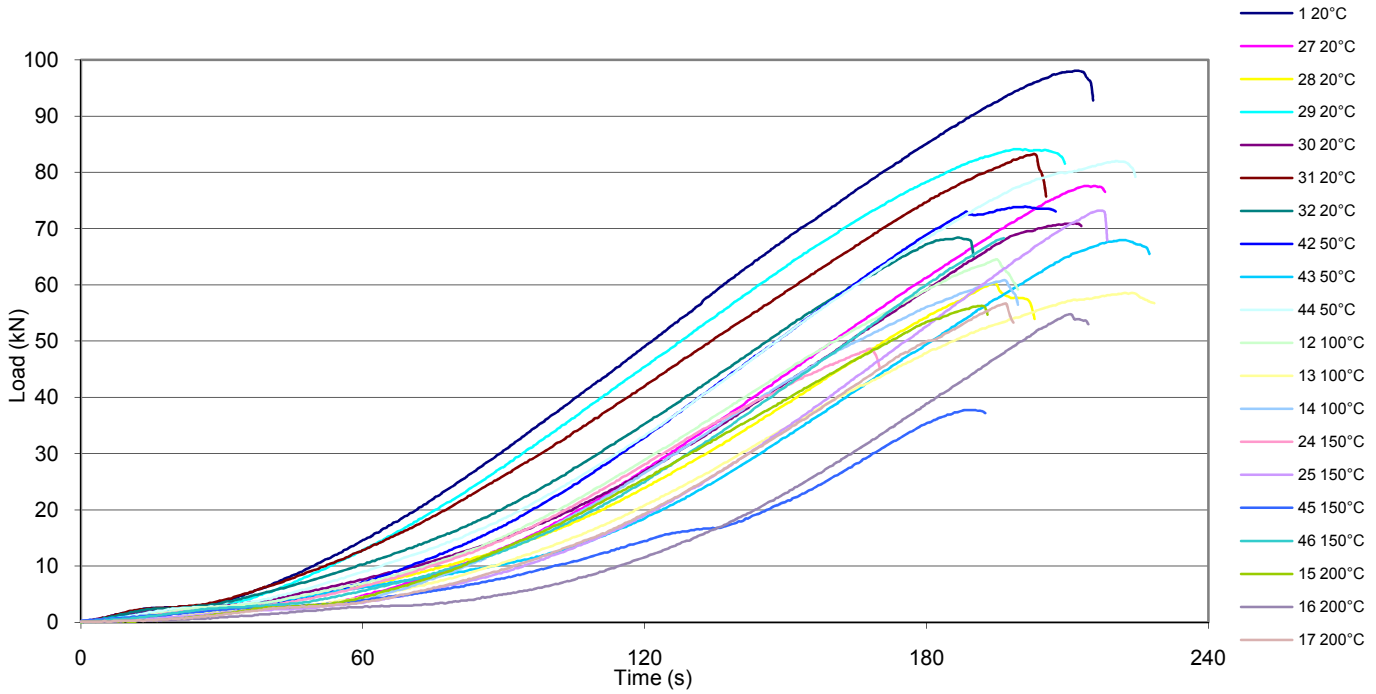

Appendix H: Small Scale Testing Modulus of Elasticity Calculations

Table of Calculated Values:

Temperature (°C)	**20**							**50**			**100**		
Force (kN)	144	142	143	154	143	142	145	137	131	135	124	115	119
A_o (mm^2)	4032	4070	4083	4045	4058	3994	4096	4020	3956	3982	4032	4007	3994
ΔL (mm)	0.52	0.60	0.58	0.63	0.66	0.63	0.69	0.68	0.64	0.77	0.94	0.62	0.73
E (GPa)	13.73	11.62	12.18	12.08	10.73	11.32	10.29	10.05	10.39	8.83	6.54	9.23	8.17
E_{av} (GPa)	11.7							9.8			8.0		

Temp (°C)	**150**			**200**			**20 (Dried)**		**50 (Dried)**		
F (kN)	124	146	146	164	165	166	215	193	192	192	193
A_o (mm^2)	3894	3919	3906	3844	3856	3869	3969	3919	3894	3906	3856
ΔL (mm)	0.71	0.74	0.70	0.72	0.63	0.70	0.81	0.79	0.82	0.87	0.79
E (GPa)	8.93	10.14	10.72	11.86	13.55	12.19	13.40	12.46	11.99	11.29	12.64
E_{av} (GPa)	9.9			12.5			12.9		12.0		

$$E = \frac{\sigma}{\varepsilon} = \frac{F/A_o}{\Delta L/L_o} = \frac{FL_o}{\Delta LA_o}$$

Appendix I: Small Scale Testing Specimen Photos

Compression Tests: 20 °C (Pre-dried)


Compression Tests: 50 °C


Compression Tests: 100 °C

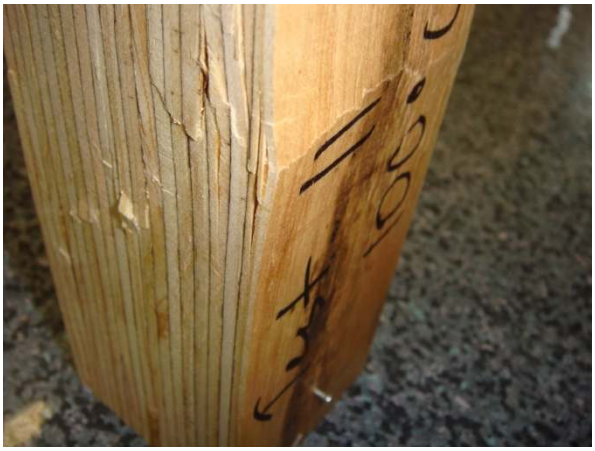
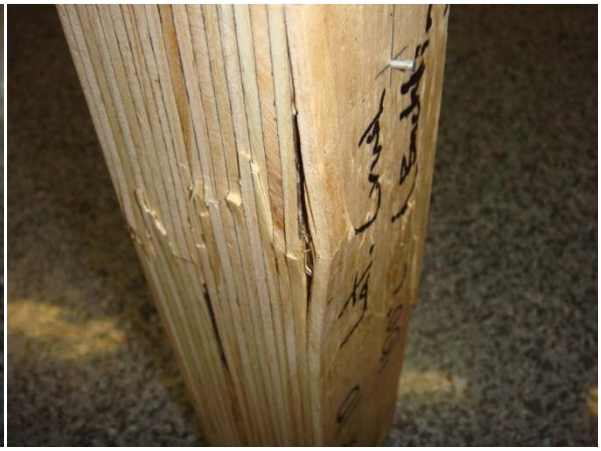

Compression Tests: 200 °C

Shear Tests: 20 °C

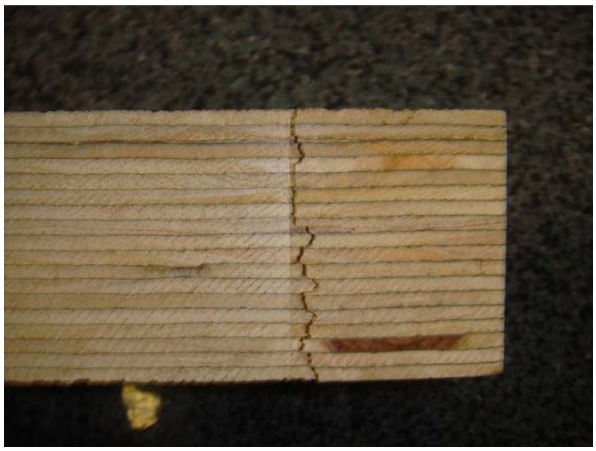

Shear Tests: 150 °C

Appendix J: Spreadsheet Design

Spreadsheet Layout:

SPREADSHEET TO DESIGN A TIMBER-CONCRETE COMPOSITE BEAM FOR FIRE (SIMPLY SUPPORTED)

Note: Macro calls on specific cells in this worksheet hence do not insert or delete rows or columns.

Δt	1	minutes	Timestep
β_1	0.55	mm/minute	Rate of Charring
$F\beta_{incr}$	15		Bottom Charring Factor
b	63	mm	Width of Joist
d	300	mm	Depth of Joist

Run FRR Calculation

t_{frr} **67** minutes Fire Resistance Time

Floor Geometry

Beams

b_t	26.15	mm	Residual Breadth
d_t	201.55	mm	Residual Depth
L	7	m	Beam Length
n	2		Number of Beams (M Panels are double)
A_t	0.011	m^2	Initial Cross Sectional Area
Z_t	3.54E+05	mm^3	Section Modulus
I_t	3.57E+07	mm^4	Moment of Inertia

Slab

t_p	17	mm	Plywood Thickness
d_c	65	mm	Concrete Thickness
b_c	1.2	m	Tributary Width between Beams (1.2 for M Panels)
A_c	0.078	m^2	Cross Sectional Area
I_c	2.75E+07	mm^4	Moment of Inertia

Notch Connection

d_n	50	mm	Depth
L_n	300	mm	Length
s_{max}	1250	mm	Maximum Spacing of Connections (midspan)
s_{min}	650	mm	Minimum Spacing of Connections (ends)
s_{ef}	800	mm	Effective Spacing
K_{ULS}	270	kN/mm	Connection Stiffness for ULS
K_{SLS}	248	kN/mm	Connection Stiffness for SLS
Q_M	139	kN	Mean Strength of Connection
Q_K	123	kN	Characteristic Strength of Connection

Material Properties

LVL

Brand	CHH Truform		Material Type
f_b	48	MPa	Characteristic Bending Strength
f_t	30	MPa	Characteristic Tensile Strength
f_s	5.3	MPa	Characteristic Shear Strength
f_c	45	MPa	Characteristic Compression Strength
MoE	10.7	GPa	Modulus of Elasticity
MoR	0.66	GPa	Modulus of Rigidity
ρ	5.7	kN/m^3	Density of Wood

Concrete

f_c	23.5	MPa	Characteristic Compression Strength
f_t	2.9	MPa	Characteristic Tensile Strength
MoE	33	GPa	Modulus of Elasticity
ρ	24	kN/m^3	Density of Concrete

Floor Design

Loads

DL	1.9	kN/m	Self Weight of Floor
SDL	0.5	kPa	Superimposed Dead Load
LL	1.5	kPa	Imposed Live Load
G	2.5	kN/m	Dead Load
Q	1.8	kN/m	Live Load
P	0.455	m	Beam Perimeter
k_f	0.7840		Reduction Factor
k_1	1.0		Load Duration Factor
k_{20}	1.15		Conversion Factor (5% to 20%)
γ_m	1.2		Material Properties Factor
W_f	3.3	kN/m	Factored Design Load
M*	19.9	kNm	Design Bending Moment at Midspan
Φ	1.0		Strength Reduction Factor
Q_d	123	kN	Design Strength of Fastener
Φ	0.7		Strength Reduction Factor
A_c	39000	mm^2	Slab Area
A_t	5270.5325	mm^2	Joist Area
I_c	13731250	mm^4	Slab Second Moment of Area
I_t	17841807.72	mm^4	Joist Second Moment of Area
γ_c	0.545		Concrete Gamma Coefficient (annex B EC5)
γ_t	1.0		Timber Gamma Coefficient (annex B

			EC5)
a_c	11	mm	a_c Distance (annex B EC5)
a_t	139	mm	a_t Distance (annex B EC5)
H	150	mm	H Distance
$(EI)_{ef}$	1.82E+12	Nmm^2	Effective Flexural Stiffness (annex B EC5)
V_{max}	9268	N	Design Shear Force for ULS
$V_{L/4}$	7317	N	Design Shear Force at L/4 from Edge
F_{max}	25.9	kN	Maximum Shear in Fastener
$F_{L/4}$	39.4	kN	Maximum Shear in Fastener at L/4

Bending

σ_t	16.3	MPa	Timber Stress due to Axial Force
N_t^*	85.7	kN	Timber Axial Force
M_t^*	2.1	kNm	Timber Bending Moment
ΦN_R	103.3	kN	Timber Tensile Strength
ΦM_R	11.1	kNm	Timber Bending Strength
CTR	1.02		Combined Tension Ratio ($N_t^*/\Phi N_R + M_t^*/\Phi M_R$)
CTR < 1	FAIL		Design Check

Shear

V*	11.4	kN	Design Shear Force at Support
V_{sf}	18.6	kNm	Nominal Strength
ΦV_{sf}	18.6	kNm	Design Shear Strength
$\Phi V_{sf} > V^*$	PASS		Design Check

Connection

ΦQ_d	86.1	kN	Design Connection Strength
$\Phi Q_d > F_{max}$	PASS		Design Check
$\Phi Q_d > F_{L/4}$	PASS		Design Check

Cold Design Check: (Same as above but for initial beam size only with revised factors)

W_c	5.9	kN/m	Factored Design Load
M*	36.3	kNm	Design Bending Moment at Midspan
Φ	0.9		Strength Reduction Factor
k_1	0.8		Load Duration Factor
V_{max}	16867	N	Design Shear Force for ULS
$V_{L/4}$	13316	N	Design Shear Force at L/4 from Edge
F_{max}	47.2	kN	Maximum Shear in Fastener
$F_{L/4}$	71.6	kN	Maximum Shear in Fastener at L/4

Bending

σ_t	29.6	MPa	Timber Stress due to Axial Force
N_t^*	156.0	kN	Timber Axial Force
M_t^*	3.8	kNm	Timber Bending Moment
ΦN_R	74.4	kN	Timber Tensile Strength
ΦM_R	8.0	kNm	Timber Bending Strength
CTR	2.57		Combined Tension Ratio ($N_t^*/\Phi N_R + M_t^*/\Phi M_R$)
CTR < 1	FAIL		Design Check

Shear

V^*	20.7	kN	Design Shear Force at Support
V_{sf}	14.9	kNm	Nominal Strength
ΦV_{sf}	13.4	kNm	Design Shear Strength
$\Phi V_{sf} > V^*$	FAIL		Design Check

Connection

ΦQ_d	68.88	kN	Design Connection Strength
$\Phi Q_d > F_{max}$	PASS		Design Check
$\Phi Q_d > F_{L/4}$	FAIL		Design Check

Time (min)	Residual Section Width	Depth	Timber Bending	Timber Shear	Connection Max Shear	Connection Shear L/4	Failure Time	Combined Tension Ratio (Nt*/ΦNR + Mt*/ΦMR)
Cold Design	63.0	300.0	PASS	PASS	PASS	PASS	Not Failed	0.60
0	63.0	300.0	PASS	PASS	PASS	PASS	Not Failed	0.24
1	62.5	299.5	PASS	PASS	PASS	PASS	Not Failed	0.25
2	61.9	298.9	PASS	PASS	PASS	PASS	Not Failed	0.25
3	61.4	298.4	PASS	PASS	PASS	PASS	Not Failed	0.25
4	60.8	297.8	PASS	PASS	PASS	PASS	Not Failed	0.25
5	60.3	297.3	PASS	PASS	PASS	PASS	Not Failed	0.26
6	59.7	296.7	PASS	PASS	PASS	PASS	Not Failed	0.26
7	59.2	296.2	PASS	PASS	PASS	PASS	Not Failed	0.26
8	58.6	295.6	PASS	PASS	PASS	PASS	Not Failed	0.27
9	58.1	295.1	PASS	PASS	PASS	PASS	Not Failed	0.27
10	57.5	294.5	PASS	PASS	PASS	PASS	Not Failed	0.27
11	57.0	294.0	PASS	PASS	PASS	PASS	Not Failed	0.28
12	56.4	293.4	PASS	PASS	PASS	PASS	Not Failed	0.28
13	55.9	292.9	PASS	PASS	PASS	PASS	Not Failed	0.28
14	55.3	292.3	PASS	PASS	PASS	PASS	Not Failed	0.29
15	54.8	291.8	PASS	PASS	PASS	PASS	Not Failed	0.29
16	54.2	291.2	PASS	PASS	PASS	PASS	Not Failed	0.29
17	53.7	290.7	PASS	PASS	PASS	PASS	Not Failed	0.30
18	53.1	290.1	PASS	PASS	PASS	PASS	Not Failed	0.30
19	52.6	289.6	PASS	PASS	PASS	PASS	Not Failed	0.31
20	52.0	289.0	PASS	PASS	PASS	PASS	Not Failed	0.31

21	51.5	288.5		PASS	PASS	PASS	PASS	Not Failed	0.31
22	50.9	287.9		PASS	PASS	PASS	PASS	Not Failed	0.32
23	50.4	287.4		PASS	PASS	PASS	PASS	Not Failed	0.32
24	49.8	286.8		PASS	PASS	PASS	PASS	Not Failed	0.33
25	49.3	286.3		PASS	PASS	PASS	PASS	Not Failed	0.33
26	48.7	285.7		PASS	PASS	PASS	PASS	Not Failed	0.34
27	48.2	285.2		PASS	PASS	PASS	PASS	Not Failed	0.34
28	47.6	284.6		PASS	PASS	PASS	PASS	Not Failed	0.35
29	47.1	284.1		PASS	PASS	PASS	PASS	Not Failed	0.35
30	46.5	283.5		PASS	PASS	PASS	PASS	Not Failed	0.36
31	46.0	283.0		PASS	PASS	PASS	PASS	Not Failed	0.36
32	45.4	282.4		PASS	PASS	PASS	PASS	Not Failed	0.37
33	44.9	281.9		PASS	PASS	PASS	PASS	Not Failed	0.37
34	44.3	281.3		PASS	PASS	PASS	PASS	Not Failed	0.38
35	43.8	280.8		PASS	PASS	PASS	PASS	Not Failed	0.39
36	43.2	280.2		PASS	PASS	PASS	PASS	Not Failed	0.39
37	42.7	279.7		PASS	PASS	PASS	PASS	Not Failed	0.40
38	42.1	279.1		PASS	PASS	PASS	PASS	Not Failed	0.41
39	41.6	278.6		PASS	PASS	PASS	PASS	Not Failed	0.41
40	41.0	278.0		PASS	PASS	PASS	PASS	Not Failed	0.42
41	40.5	277.5		PASS	PASS	PASS	PASS	Not Failed	0.43
42	39.9	276.9		PASS	PASS	PASS	PASS	Not Failed	0.43
43	39.4	276.4		PASS	PASS	PASS	PASS	Not Failed	0.44
44	38.8	275.8		PASS	PASS	PASS	PASS	Not Failed	0.45
45	38.3	275.2		PASS	PASS	PASS	PASS	Not Failed	0.46
46	37.7	274.7		PASS	PASS	PASS	PASS	Not Failed	0.46
47	37.2	274.1		PASS	PASS	PASS	PASS	Not Failed	0.47
48	36.6	273.6		PASS	PASS	PASS	PASS	Not Failed	0.48
49	36.1	273.0		PASS	PASS	PASS	PASS	Not Failed	0.49
50	35.5	272.5		PASS	PASS	PASS	PASS	Not Failed	0.50
51	35.0	271.9		PASS	PASS	PASS	PASS	Not Failed	0.51
52	34.4	271.4		PASS	PASS	PASS	PASS	Not Failed	0.52
53	33.9	270.8		PASS	PASS	PASS	PASS	Not Failed	0.53
54	33.3	270.3		PASS	PASS	PASS	PASS	Not Failed	0.54
55	32.8	269.7		PASS	PASS	PASS	PASS	Not Failed	0.55
56	32.2	269.2		PASS	PASS	PASS	PASS	Not Failed	0.56
57	31.7	268.6		PASS	PASS	PASS	PASS	Not Failed	0.58
58	31.1	268.1		PASS	PASS	PASS	PASS	Not Failed	0.59
59	30.6	267.5		PASS	PASS	PASS	PASS	Not Failed	0.60
60	30.0	259.3		PASS	PASS	PASS	PASS	Not Failed	0.64
61	29.5	251.0		PASS	PASS	PASS	PASS	Not Failed	0.68
62	28.9	242.8		PASS	PASS	PASS	PASS	Not Failed	0.73
63	28.4	234.5		PASS	PASS	PASS	PASS	Not Failed	0.78
64	27.8	226.3		PASS	PASS	PASS	PASS	Not Failed	0.83
65	27.3	218.0		PASS	PASS	PASS	PASS	Not Failed	0.89
66	26.7	209.8		PASS	PASS	PASS	PASS	Not Failed	0.95
67	26.2	201.5		FAIL	PASS	PASS	PASS	67	1.02